Departamento de Ingeniería Mecánica

Simulative and experimental investigations of a 3-Way catalyst exhaust system for a SI-Engine with a disengageable crankshaft

- Máster en Ingeniería Industrial -

Alberto Luis Mariscal Rivas

Director: Sebastian Rösler

Madrid, junio de 2018

AUTHORIZATION FOR DIGITALIZATION, STORAGE AND DISSEMINATION IN THE NETWORK OF END-OF-DEGREE PROJECTS, MASTER PROJECTS, DISSERTATIONS OR BACHILLERATO REPORTS

1. Declaration of authorship and accreditation thereof.

The author Mr. /Ms. Alberto Luis Mariscal Rivas

HEREBY DECLARES that he/she owns the intellectual property rights regarding the piece of work: Simulative and experimental investigations of a 3-Way catalyst exhaust system for a SI-Engine with a disengageable crankshaft

that this is an original piece of work, and that he/she holds the status of author, in the sense granted by the Intellectual Property Law.

2. Subject matter and purpose of this assignment.

With the aim of disseminating the aforementioned piece of work as widely as possible using the University's Institutional Repository the author hereby **GRANTS** Comillas Pontifical University, on a royalty-free and non-exclusive basis, for the maximum legal term and with universal scope, the digitization, archiving, reproduction, distribution and public communication rights, including the right to make it electronically available, as described in the Intellectual Property Law. Transformation rights are assigned solely for the purposes described in a) of the following section.

3. Transfer and access terms

Without prejudice to the ownership of the work, which remains with its author, the transfer of rights covered by this license enables:

a) Transform it in order to adapt it to any technology suitable for sharing it online, as well as including metadata to register the piece of work and include "watermarks" or any other security or protection system.

b) Reproduce it in any digital medium in order to be included on an electronic database, including the right to reproduce and store the work on servers for the purposes of guaranteeing its security, maintaining it and preserving its format.

c) Communicate it, by default, by means of an institutional open archive, which has open and cost-free online access.

d) Any other way of access (restricted, embargoed, closed) shall be explicitly requested and requires that good cause be demonstrated.

e) Assign these pieces of work a Creative Commons license by default.

f) Assign these pieces of work a HANDLE (*persistent* URL). by default.

4. Copyright.

The author, as the owner of a piece of work, has the right to:

a) Have his/her name clearly identified by the University as the author

b) Communicate and publish the work in the version assigned and in other subsequent versions using any medium.

c) Request that the work be withdrawn from the repository for just cause.

d) Receive reliable communication of any claims third parties may make in relation to the work and, in particular, any claims relating to its intellectual property rights.

5. Duties of the author.

The author agrees to:

a) Guarantee that the commitment undertaken by means of this official document does not infringe any third party rights, regardless of whether they relate to industrial or intellectual property or any other type.

b) Guarantee that the content of the work does not infringe any third party honor, privacy or image rights.
c) Take responsibility for all claims and liability, including compensation for any damages, which may be brought against the University by third parties who believe that their rights and interests have been infringed by the assignment.
d) Take responsibility in the event that the institutions are found guilty of a rights infringement regarding the work subject to assignment.

6. Institutional Repository purposes and functioning.

The work shall be made available to the users so that they may use it in a fair and respectful way with regards to the copyright, according to the allowances given in the relevant legislation, and for study or research purposes, or any other legal use. With this aim in mind, the University undertakes the following duties and reserves the following powers:

a) The University shall inform the archive users of the permitted uses; however, it shall not guarantee or take any responsibility for any other subsequent ways the work may be used by users, which are non-compliant with the legislation in force. Any subsequent use, beyond private copying, shall require the source to be cited and authorship to be recognized, as well as the guarantee not to use it to gain commercial profit or carry out any derivative works.
b) The University shall not review the content of the works, which shall at all times fall under the exclusive responsibility of the author and it shall not be obligated to take part in lawsuits on behalf of the author in the event of any infringement of intellectual property rights deriving from storing and archiving the works. The author hereby waives any claim against the University due to any way the users may use the works that is not in keeping with the legislation in force.
c) The University shall adopt the necessary measures to safeguard the work in the future.
d) The University reserves the right to withdraw the work, after notifying the author, in sufficiently justified cases, or in the event of third party claims.

Madrid, on 27th..... of June....., 2018.

HEREBY ACCEPTS

Signed.....

Reasons for requesting the restricted, closed or embargoed access to the work in the Institution's Repository

Declaro, bajo mi responsabilidad, que el Proyecto presentado con el título Simulative and Experimental Investigations of a 3-Way Catalyst Exhaust System for a SI-Engine with a Disengageable Crakshaft en la ETS de Ingeniería - ICAI de la Universidad Pontificia Comillas en el curso académico 2017/2018 es de mi autoría, original e inédito y no ha sido presentado con anterioridad a otros efectos. El Proyecto no es plagio de otro, ni total ni parcialmente y la información que ha sido tomada de otros documentos está debidamente referenciada.

Fdo.: Alberto Luis Mariscal Rivas Fecha: 28/05/2018

Autorizada la entrega del proyecto

EL DIRECTOR DEL PROYECTO

Fdo.: Sebastian Rösler Fecha: 28/05/2018

Simulative and Experimental Investigations of a 3-Way Catalyst Exhaust System for a SI-Engine with a Disengageable Crakshaft

Author: Alberto Luis Mariscal Rivas
Director: Sebastian Rösler

Summary of the project

Introduction

The Split-Crankshaft Engine (SCE) is a project developed by the Institute of Internal Combustion Engines (LVK) of the Technical University of Munich (TUM), together with the Gear Research Centre (FZG). The concept consists in two bycilynder engines which are attached at their crankshafts by the Split-Clutch Unit (SCU). Figure 1 shows a schema of the concept where it can be seen that the SCU is joining both engines. The system is able to run with both engines coupled or only with the primary engine. The main purpose of this concept is the reduction of emissions and fuel consumption. The technology is similar to the cylinder deactivation engines but has the advantage of the lower friction losses due to the not fired cylinders as the secondary engine is not moving. The primary engine is turbocharged while the secondary engine is a naturally aspirated engine.

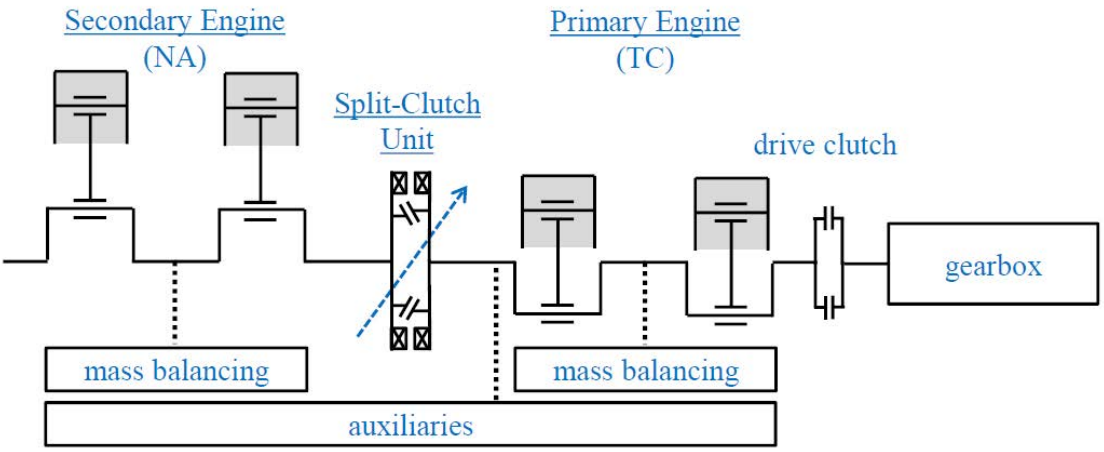

Figure 1 Schematic model of the system [1]

The main purpose of this study is the investigation and simulation of the exhaust system of the SCE. The primary engine has been tested at the test bench with the V1 exhaust system which is composed by a precatalyst located near the engine and a main catalyst after it. Emissions are measured before the precatalyst and after the main catalyst while the main

temperature measuring points are before and after both catalytic converters.

Primary engine application and engine emissions maps

The first part of this study consisted on the application of the primary engine and the measurement and building of the emissions maps.

Regarding the engine application, it was found that the throttle valve made almost no difference in the amount of aspirated air when it was opened more than 45° and almost did not increment the output torque. Thus, the torque has been decided to be regulated with the throttle valve until it is opened 45° and with the waste gate until the maximum torque is produced. Figure 2 shows the chosen application strategy for the primary engine.

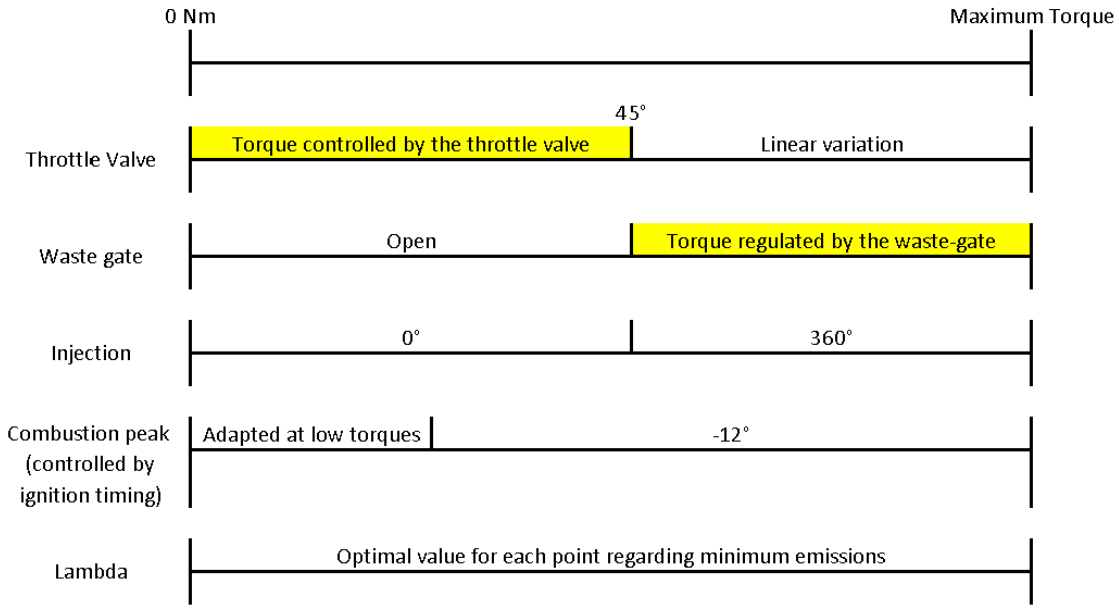

Figure 2 Application strategy of the primary engine

Once the application strategy was chosen, the emissions maps were built for NOx, HC, CO and CO2. A total of 66 points were measured from 1000 to 6000 rpm in 1000 rpm steps and from 0Nm to maximum torque at each engine speed in steps of 10% of the maximum torque. The maximum torque was found to be limited by the maximum temperature of the precatalyst which was damaged during the experiments due to the high temperatures. The emissions maps are 3D plots of the emissions [ppm or %-Vol] produced by the engine as a function of engine speed (rpm) and torque (Nm) or the mean indicated pressure (pmi). For each pollutant, two different maps were built, one of the raw emissions produced by the engine and another of the emissions after the main catalyst. To end with, a map of the exhaust mass flow was built, representing the mass flow of the exhaust system in kg/h. The exhaust mass flow is used, together with the emissions maps, to calculate the pollutants emitted at a certain running point in g/h or g/km.

Experimental investigations

After the emissions maps were built, the transient behaviour of the system was studied to find how long does the system need to reach high conversion rates and its working temperature and also to find if the precatalyst could convert all the emissions without the main catalyst.

To investigate the transient response of the system, the engine was ran from cold start to 2000 rpm and 30 Nm. For example, figure 3 shows the raw emissions of the engine and the emissions after the main catalyst for NOx. In general, for all the different pollutants, it was found that the exhaust system reaches its working temperature after 40 seconds and produces no conversion before 15 seconds.

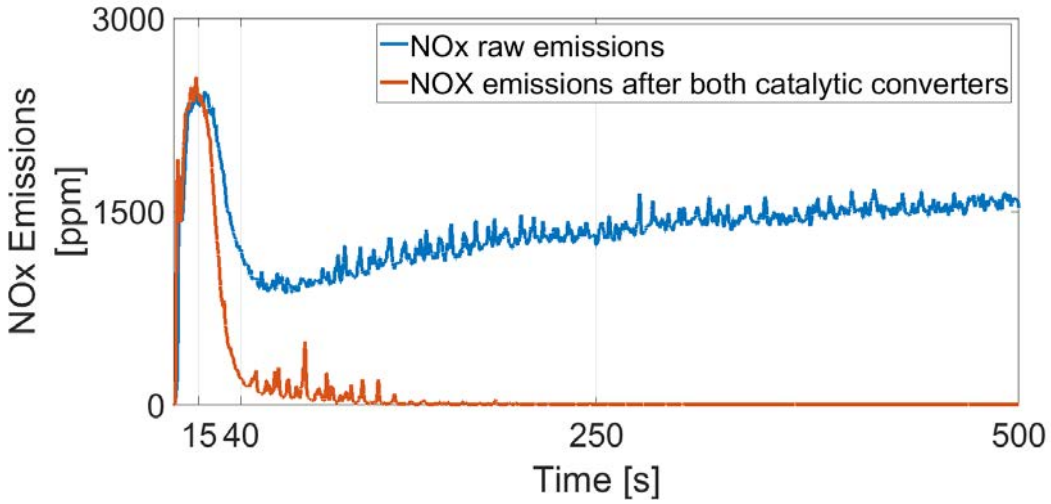

Figure 3 NOx emissions of the transient test before the precatalyst and after the main catalyst

When running the same transient curve and measuring emissions after the precatalyst, it was found that it cannot convert enough pollutants alone to fulfill the emissions standards, meaning that it is necessary to install a main catalyst after the precatalyst.

Full vehicle simulation

Sylvain Garnier [2] had previously carried out a full vehicle simulation including the SCE but without considering emissions, with which he simulated the World Harmonized Light Vehicles Test Cycle (WLTC). The result of that simulation is a pmi and engine speed profile for the primary and secondary engines of the SCE. These profiles have been joined with the previously calculated engine emissions maps to estimate the total pollutants emitted by the SCE.

To evalute the improvement of the SCE with regard to a not downsized engine, Sylvain Garnier [2] purposed a comparison with two fictive engines, a Complete Engine (CE) and a Cylinder Deactivation Engine (CDA). These two engines only exist in the simulation but allow a comparison with the SCE as they are both composed by the same primary and secondary engines of the SCE. The CE is simulated by considering that the PE and SE are joined

together through their crankshaft and running like a normal engine, while in the CDA both engines are always running but the cylinders of the SE are not always being fired.

As a result of the full vehicle simulation with the emissions maps, it was found that the SCE fulfills the CO and HC emissions limits but produces higher NOx than allowed.

The SCE presents a 10% fuel saving when compared to the CE and a 5% saving to the CDA. However, the SCE produces more NOx than the CE. This is caused because more NOx are produced when the PE of the SCE is running alone with a high pmi than when both engines of the CE are running with a lower pmi.

Exhaust system simulation

To end with, a model of the exhaust system was developed in GT-Suite. The aim of this model is to simulate the exhaust system and then be included in the full vehicle simulation developed by Sylvain Garnier [2] and other previous students. First, a model of the exhaust system alone was built, beginning after the turbine of the PE and including the precatalyst and main catalyst. Then, this model was coupled with an engine state model of the PE, which is a simple model of the engine which includes the emissions maps previously calculated.

The model was calibrated using a total error function which compares the emissions produced by the model to the known amount of pollutants measured in the test bench. To reduce the gap between the simulation and reality, GT optimizes the pre-exponent multipliers of the chosen equations.

The best calibration achieved presented a good thermal response but the simulation showed a quicker transient response, reaching earlier the steady state conversion rates. However, when the model was coupled with the engine state model and some steady state points were simulated, the system presented a good thermal adaptation but failed to estimate properly the final emissions.

Results

The main conclusions which can be drawn from this study are:

- Using a precatalyst close to the engine to reduce the time needed to reach the light-off temperature suffers from the high temperatures of the exhaust system when running at lambda = 1 and limits the maximum torque.
- The precatalyst is not capable of converting all the pollutants and needs from a main catalyst after it to fully convert all the emissions.
- The SCE presents a 10% fuel saving when compared with a complete engine but produces higher NOx emissions. The SCE also has higher NOx emissions than the legislation allows. However, it is possible to run with a different lambda value, increasing HC and CO

but reducing NOx.

[1] RÖSLER, Sebastian ; FISCHER, Patrick ; PFLAUM, Herman ; WACHTMEISTER, Georg ; STAHL, Karsten: Experimental implementation of an internal combustion engine with a disengageable crankshaft - The Split-Crankshaft Engine. Munich, Technische Universität München, Diss.

[2] SYLVAIN GARNIER: Fuel Saving Potential Determination and Optimization of the Split-Crankshaft Engine via Full Vehicle Simulation: Master Thesis (Simulative). Munich, Technische Universität München, Masterarbeit

Simulative and Experimental Investigations of a 3-Way Catalyst Exhaust System for a SI-Engine with a Disengageable Crakshaft

Autor: Alberto Luis Mariscal Rivas
Director: Sebastian Rösler

Resumen del proyecto

Introducción

El motor de cigüeñal divisible, en inglés Split-Crankshaft-Engine (SCE) es un proyecto desarrollado por el Instituto de motores de combustión interna (LVK) de la Universidad Técnica de Múnich (TUM) junto con el Centro de Investigación de Engranajes (FZG). El concepto consiste en dos motores bicilíndricos unidos por los cigüeñales a través de un embrague (Split-Clutch Unit o SCU). La figura 1 muestra un esquema del concepto, dónde se puede ver que el embrague (SCU) está uniendo ambos motores. El sistema es capaz de funcionar con los dos motores unidos o únicamente con el motor principal (PE). El objetivo fundamental de este concepto es la reducción de emisiones y de consumo de combustible. La tecnología es similar a la de los motores con cilindros desactivables (Cylinder Deactivation) pero posee la ventaja de unas menores pérdidas por rozamiento en los cilindros desactivados ya que en este caso no continúan girando. En el caso del motor primario se trata de un motor turboalimentado mientras que el secundario es un motor atmosférico.

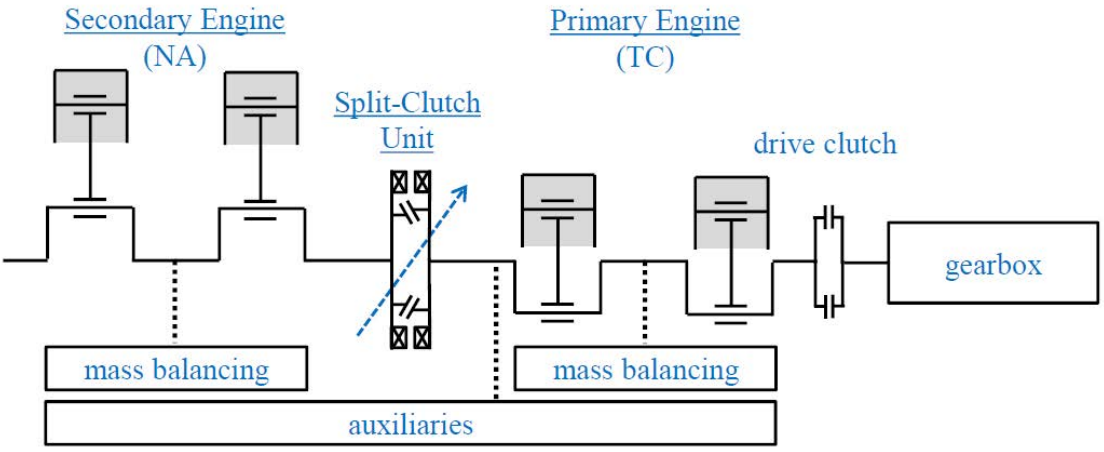

Figure 1 Esquema del sistema [1]

El objetivo principal de este estudio es la investigación y simulación del sistema de escape del SCE. El motor primario ha sido probado en el banco de ensayos junto con la configuración V1

del sistema de escape, compuesta por un precatalizador y un catalizador principal después de éste. Las emisiones han sido medidas antes del precatalizador y después del catalizador principal.

Aplicación del motor principal y mapas de emisiones

La primera parte de este estudio consiste en la aplicación del motor principal y la creación de los diferentes mapas de emisiones.

El término aplicación del motor, se refiere a la decisión de los diferentes parámetros posibles para el control del mismo. En el caso del motor primario, se demostró que la mariposa de admisión no produce variación en la cantidad de aire aspirado a partir de 45°. Por ello, se ha decidido controlar el par mediante la apertura de la mariposa hasta que ésta se halla en la posición de 45° y luego controlarlo mediante la válvula de descarga del turbocompresor hasta que se alcanza el máximo par, limitado por la temperatura antes del precatalizador. La figura 2 muestra la estrategia seguida para el motor principal.

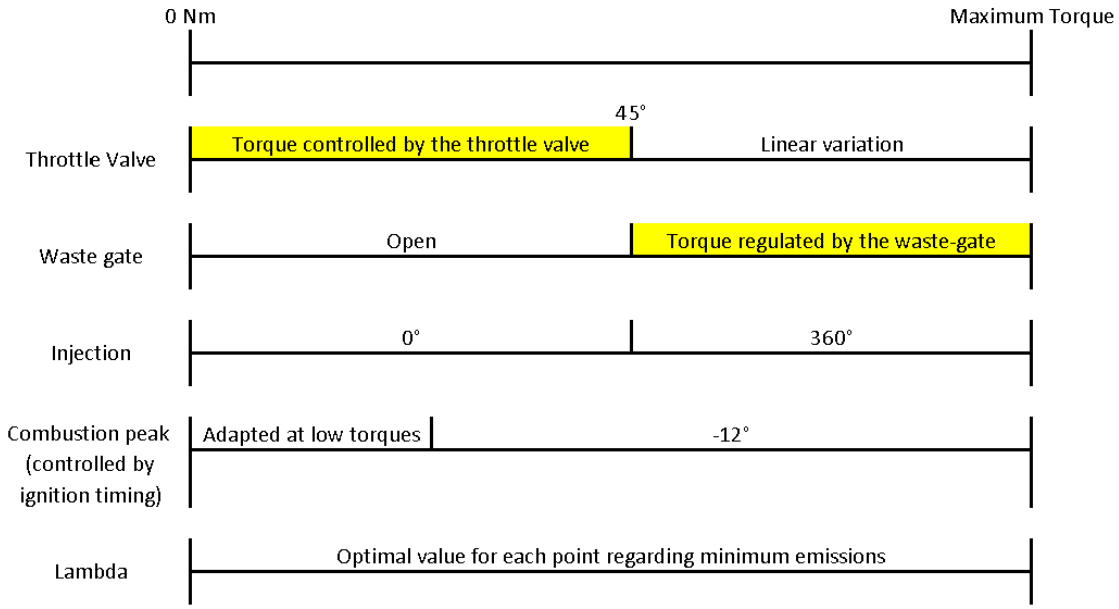

Figure 2 Estrategia seguida para el motor principal

Después de elegir la estrategia adecuada para el motor principal, se procedió a la construcción los mapas de emisiones para NOx, HC, CO y CO2, tanto de emisiones del motor como emisiones después de ambos catalizadores. Se midieron un total de 66 puntos desde 1000 hasta 6000 rpm en escalones de 1000 rpm, con 11 pares diferentes para cada velocidad desde 0Nm hasta par máximo. Los mapas de emisiones son funciones tridimensionales que permiten obtener las emisiones en ppm o %-Vol producidas en función de la velocidad del motor (rpm) y el par efectivo (Nm) o la presión media indicada (pmi). Por último, se ha calculado también un mapa de flujo másico de escape, el cual, junto a los mapas de emisiones, permite calcular la cantidad de cada especie por unidad de tiempo en g/h o g/km.

Resultados experimentales

Después de construir los distintos mapas de emisiones, se procedió a estudiar el comportamiento del sistema desde un comienzo en frío hasta alcanzar la temperatura final de funcionamiento. También se ha estudiado si el precatalizador es capaz de convertir por él mismo todas las emisiones del motor o, si por el contrario, el sistema requiere del uso del catalizador principal.

Para investigar la respuesta transitoria del sistema, se arrancó el motor desde frío hasta 2000 rpm y 30 Nm mediante un escalón, observando la evolución de las emisiones y la temperatura del sistema en función del tiempo. Por ejemplo, la figura 3 muestra las emisiones de óxidos de nitrógeno antes del precatalizador y después del catalizador principal. Se puede observar que el sistema necesita de al menos 40 segundos para alcanzar unos niveles de conversión adecuados y que no disminuye las emisiones durante los 15 primeros segundos.

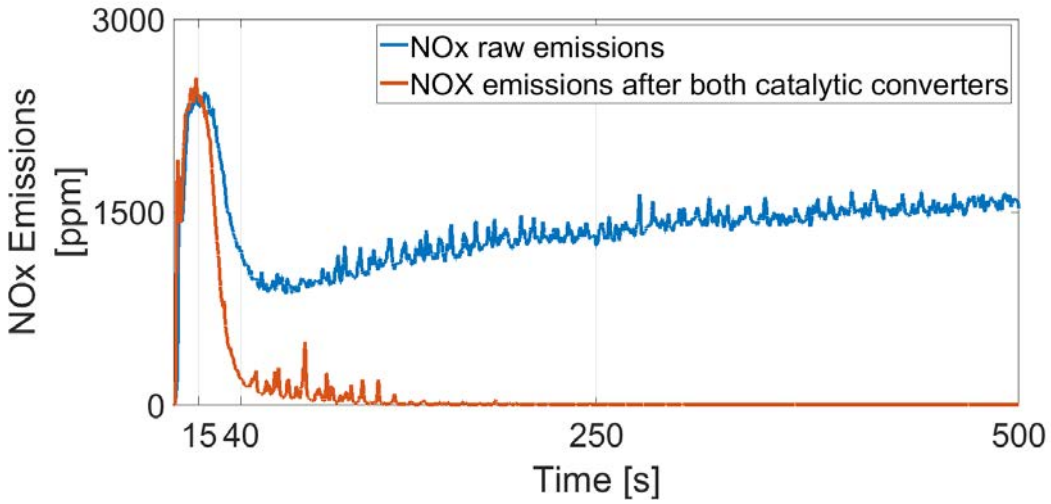

Figure 3 Emisiones de NOx producidas en el estudio de la respuesta transitoria

Después del estudio de la respuesta transitoria del sistema, se midieron también las emisiones después del precatalizador para concretar si es necesario el uso del catalizador principal. Se dedujo que el precatalizador no es capaz, por sí solo, de convertir todas las emisiones y el uso del catalizador principal es necesario.

Simulación del vehículo completo

Sylvain Garnier [2] desarrolló, previamente a este estudio, un modelo completo del vehículo, incluyendo el SCE pero sin considerar las emisiones ni el sistema de escape. Con este modelo, simuló el World Harmonized Light Vehicles Test Cycle (WLTC) y, como resultado, obtuvo el perfil a lo largo del tiempo de la velocidad y de la presión media indicada (pmi) de cada motor. Con estos perfiles, junto con los mapas de emisiones previamente medidos, se ha podido calcular las emisiones producidas por el SCE en el ciclo.

Para evaluar la mejora que el SCE representa respecto a un motor convencional, Sylvain Garnier [2] propone compararlo con dos motores ficticios: un motor completo (CE) y un motor con desactivación de cilindros (CDA). Estos dos motores no existen en la realidad, únicamente en la simulación, pero permiten la comparación con el SCE ya que ambos están compuestos por los mismos motores primario y secundario. En el caso del CE, se simula considerando que ambos motores están siempre unidos fijamente y funcionando como un motor normal de 4 cilindros. En el caso del CDA, se considera que ambos motores giran continuamente pero en algunos casos el motor secundario aunque gira, no produce par al no inyectar combustible.

Como resultado de la simulación del vehículo completo, se ha podido concluir que el SCE produce más óxidos de nitrógeno de los permitidos aunque está por debajo de los límites máximos de HC y CO.

El SCE presenta una reducción del 10% del gasto de combustible en comparacion con el CE y del 5% con el CDA. Sin embargo, el SCE produce más óxidos de nitrógeno que el CE ya que resulta menos eficiente el uso del motor primario con un pmi alto que ambos motores juntos con un pmi menor.

Simulación del sistema de escape

Para concluir, se ha construido un modelo del sistema de escape con el programa GT-Suite. El objetivo principal de este modelo es la simulación del sistema de escape V1 e incluirlo en el el modelo del vehículo completo desarrollado por Sylvain Garnier [2] y otros estudiantes anteriores. Primero se ha desarrollado un modelo del sistema de escape exclusivamente y, después, se ha unido a un modelo sencillo del motor primario, el cual incluye los mapas de emisiones previamente expuestos.

El modelo se ha calibrado mediante el uso de una función de error total, la cual compara las emisiones producidas en la simulación con las emisiones reales medidas en el banco de ensayos. Para reducir la diferencia entre modelo y realidad, GT optimiza los factores pre-exponenciales de las ecuaciones seleccionadas.

La mejor calibración alcanzada presenta una buena respuesta térmica pero comienza a tener una tasa alta de conversión de emisiones antes de lo medido en el banco de ensayos. Sin embargo, cuando se procedió a unir el modelo del sistema de escape y del motor y se simularon diferentes puntos, se obtuvo que aunque la respuesta térmica del sistema era adecuada, éste no era capaz de estimar correctamente las emisiones finales.

Conclusiones

Las conclusiones principales que se pueden extraer de este estudio son:

- El uso de un precatalizador cerca del motor para reducir el tiempo hasta alcanzar la

temperatura de funcionamiento limita la máxima potencia del motor debido a las altas temperaturas del precatalizador.

- El precatalizador no es capaz de convertir todas las emisiones y necesita de un catalizador principal después de mayor tamaño.
- El SCE presenta una reducción del 10% del consumo de combustible en comparación con un motor convencional aunque presenta mayores emisiones de óxidos de nitrógeno, además de emitir más de lo permitido. Sin embargo, es posible controlar el motor con valores distintos de lambda, sacrificando unas mayores emisiones de HC y CO para reducir los NOx ya que éstos compuestos tienen margen hasta el máximo permitido.

[1] RÖSLER, Sebastian ; FISCHER, Patrick ; PFLAUM, Herman ; WACHTMEISTER, Georg ; STAHL, Karsten: Experimental implementation of an internal combustion engine with a disengageable crankshaft - The Split-Crankshaft Engine. Munich, Technische Universität München, Diss.

[2] SYLVAIN GARNIER: Fuel Saving Potential Determination and Optimization of the Split-Crankshaft Engine via Full Vehicle Simulation: Master Thesis (Simulative). Munich, Technische Universität München, Masterarbeit

Departamento de Ingeniería Mecánica

Simulative and experimental investigations of a 3-Way catalyst exhaust system for a SI-Engine with a disengageable crankshaft

- Máster en Ingeniería Industrial -

Alberto Luis Mariscal Rivas

Director: Sebastian Rösler

Madrid, junio de 2018

A mis padres, por haberme permitido
tener esta formacion tan maravillosa y a Celia,
por estar lo suficientemente loca como para creer
en mi y seguirme hasta Alemania

Contents

List of Tables vii
List of Figures viii
Abbreviations xii
1 Introduction 1
1.1 The Split-crankshaft Engine Project 1
1.2 Objective of the study 2
1.3 Structure of the study 2
2 State of the art 4
2.1 Motivation and history overview 4
2.2 Main pollutants in the exhaust gases 5
2.2.1 Water vapour 6
2.2.2 Carbon dioxide 6
2.2.3 Nitrogen 7
2.2.4 Carbon monoxide 7
2.2.5 Hydrocarbon 8
2.2.6 Nitrogen oxides 9
2.3 Exhaust gases aftertreatment for Lambda controlled Otto engines 10
2.3.1 The lambda value and its calculation 10
2.3.2 Lambda Sensors 10
2.4 Catalytic converters 13
2.4.1 Catalytic configurations 14
2.4.2 Heating up strategies 16
2.4.3 Three-Way Catalysts Internal composition 18
2.4.4 Lambda regulation loop 21
2.5 Exhaust gas systems of current production in series vehicles 24
2.6 The consequent challenge derivated from close-coupled catalysts and retarded ignition 28
3 Legislation for light-vehicles with combustion engines 34
3.1 The old cycle: New European Driving Cycle (NEDC) 34
3.2 The new cycles: Worldwide harmonized Light Vehicles Test Procedure and Real Driving Emissions 35
3.2.1 Worldwide harmonized Light Vehicles Test Procedure (WLTP) 35
3.2.2 Real Driving Emissions (RDE) 37
3.2.3 Comparing the WLTP and the NEDC 42
4 Measurements and calculation methodology 52
4.1 The Mexa Measuring System 52
4.1.1 The Non-Dispersive Infrared Detection method (NDIR) 52
4.1.2 The Flame Ionisation Detection Method (FID) 53
4.1.3 The Chemi-luminiscence detector (CLD) Method 55
4.2 Humidity calculation and conversion 55

4.3 Dry-wet Emissions conversion 57
4.4 Emissions rate calculation 58
5 Emissions experimental analysis with the V1 Exhaust System of the SCE 62
5.1 The V1 Exhaust System 62
5.2 Application of the Primary Engine 63
5.3 Measured Emission maps and torque grid 65
5.4 Transient analysis of the catalytic conversion 70
5.4.1 The Light-Off and Light-Out Temperatures 70
5.4.2 Experimental analysis of the transient behaviour of the aftertreatment system 71
5.4.3 Experimental analysis of the conversion rate of the precatalyst 75
5.5 Experimental analysis of the stationary conversion rates of the system without the precatalytic converter 81
6 Simulation of a real test cycle considering a complete vehicle simulation and the tested engines 83
6.1 Objective of the simulation 83
6.2 Methodology, approximations and assumptions 84
6.3 World Harmonized Light-vehicles Test Cycle Simulation 86
6.3.1 Analysis of the emissions 86
6.3.2 Analysis of the influence of the cold start for each pollutant 89
6.3.3 Conclusions of the WLTC simulation 90
7 Building a model and simulation of the aftertreatment system to optimize and develop the concept 91
7.1 Objective of the GT-Simulation 91
7.2 Simulation models of catalytic converters 92
7.3 Model overview 94
7.3.1 Tests, modelling theory and strategy 97
7.3.2 Thermal model 97
7.3.3 Transient curve simulation 98
7.3.4 Snapshot simulation 102
7.4 Conclusions and optimization potential of the model 105
8 Conclusions, summary and outlook 107
Bibliography 108
A Annex A 111
A.1 DVD Content 111

List of Tables

Table 1 Thermal deactivation phaenomena as a function of catalyst operating temperature [19] 29

Table 2 Driving characteristics of the different WTLC classes [28] 36

Table 3 RDE test main speeds and requirements presented by Donateo u. Giovinazzi [7] 38

Table 4 Test parameters and their source as determined by European Commission [12] 40

Table 5 Basic characteristics of NEDC and WLTC class 3 [27] 43

Table 6 MEXA-7170HEGR Characteristics [15] 52

Table 7 Main common hydrocarbons and their uses [22] 54

Table 8 Constants for the water vapour saturation calculation [29] 56

Table 9 Raw exhaust gas u values depicting the ratio between the densities of exhaust component or pollutant [km/m^3] and the density of the exhaust gas [kg/m^3]. Extracted from [12] 61

Table 10 Points measured to analyse the steady state conversion rate of the precatalyst 81

Table 11 Emissions for the analysis of the precatalyst's conversion rate 82

Table 12 Emissions and fuel consumption from the simulation of the WLTC 86

Table 13 Average pmi and engine speed during the cold start or the total WLTC 87

Table 14 Percentage of emissions which correspond to the cold start with regard to the total cycle 90

Table 15 Main reactions in Three Way Catalysts [23] 94

List of Figures

Figure 1 Schematic model of the system [24] 1

Figure 2 Petrol consumption and emissions from 1999 to 2009 between Otto and Diesel engines [18] 5

Figure 3 Influence of the Air-to-Fuel ratio and ignition timing in degrees before top dead centre in the CO Emissions produced by the engine[18] 8

Figure 4 Influence of the Air-to-Fuel ratio and ignition timing (degrees before top dead centre) in the HC Emissions produced by the engine[18] 9

Figure 5 Composition of a binary lambda sensor [21] 11

Figure 6 Characteristic lambda-voltage curve of a binary lambda sensor [21] 12

Figure 7 Schematic composition of a Wide-Band lambda sensor [21] 12

Figure 8 Characteristic lambda-pumping intensity curve of a Wide-Band lambda sensor [21] 13

Figure 9 Standard configuration for a TWC. 1) Engine 2) Wide-Band Lambda sensor 3) TWC 4) Binary lambda sensor [18] 14

Figure 10 Different possible configurations for catalytic converters. 1)Pre-catalyst 2)Main catalyst 3) First pipes join 4) Second pipes join [18] 16

Figure 11 Schema of the secondary air pump system [18] 1) Secondary air pump 2) Relay for the aspirated air 3) Relay 4) ECU 5) Secondary air valve 6) Control valve 7) Battery 8) Inlet point in exhaust system 9) Exhaust valve 10) Connection to intaxe pipe 18

Figure 12 Composition of a catalyst converter [21] 19

Figure 13 Conversion capacity of the TWC with regard to the lambda value [30] 20

Figure 14 Catalytic converter system with a 3 cylinder engines with unequal lambda values [21] 21

Figure 15 Example of the binary lambda control. Upper figures are the voltage produced by the lambda sensor while lower figures are the controlled variable. a) Case where the system is displaced in the rich direction b) Case where the system is displaced in the lean direction[18] 22

Figure 16 Control schema using two or three lambda sensors. 1) Binary or wide band sensor 2)Binary lambda sensor 3) Pre-catalytic converter 4) Main catalytic converter 24
Figure 17 Mercedes-Benz exhaust gas system for a cylinder deactivation engine in the year 2000 [8] 25
Figure 18 Schema of the exhaust system in the Split engine control system patent by Haruhiko Iizuka u. Fukashi Sugasawa [14] 27
Figure 19 Schematic diagram of the experimental set-up used by Lee u. a. [19] 29
Figure 20 Relationship between catalyst inlet gas temperature and catalyst temperature at 2500 rpm. CCC refers to close-coupled-catalyst and UCC to under floor catalytic converter [19] 30
Figure 21 Effect of the lambda value on the catalyst inlet and catalyt temperatures for different engine speeds [19] 31
Figure 22 Effect of ignition timing on catalyst inlet gas temperature [19] 31
Figure 23 Effect of the misfire rate on catalyst temperature and inlet temperature [19] 32
Figure 24 Influence of ignition timing on catalyst light-off [19] 33
Figure 25 New European Driving Cycle sped profile [26] 34
Figure 26 WLTC class 3 speed profile 36
Figure 27 RDE cycle procedure [10] 37
Figure 28 Schema of the CVS system with a critical flow venturi [16] 41
Figure 29 Parameters which may affect CO2 emissions and change between NEDC and WLTC [20] 45
Figure 30 Impact of engine starting temperature on CO2 emissiosn related to 23C [20] .. 46
Figure 31 Different tests and results obtained in the NEDC-WLTC comparison with Ricardo DVT [20] 47
Figure 32 Different tests and results obtained in the NEDC-WLTC comparison with Ricardo DVT [20] 48
Figure 33 Different tests and results obtained in the NEDC-WLTC comparison with AVL carried out by Mock u. a. [20] 49
Figure 34 ADAC Test results averages where error bars represent 95% confidence intervals [20] 50

Figure 35 (1) Deviations in the CO2 emissions tests for 7 different cars between NEDC and WLTC. (2) Scatterplot NEDC-WLTC. [1] 50
Figure 36 Basic schema of the NDIR Emissions measuring method [2] 53
Figure 37 Basic schema of the FID Emissions measuring method [3] 54
Figure 38 Basic schema of the CLD Emissions measuring method [4] 55
Figure 39 The V1 Exhaust System. 1) Inlet 2) Precatalyst 3) Main Catalyst 4) Outlet 62
Figure 40 Photograph of the test bench 63
Figure 41 Influence of the throttle valve in the aspirated air mass flow 64
Figure 42 Application strategy for the primary engine 65
Figure 43 Points measured to build the engine emissions maps 66
Figure 44 Damages in the pre-catalytic converter due to the high temperatures 67
Figure 45 NOx Emissions in the different simulated cases 68
Figure 46 Exhaust mass flow map 70
Figure 47 Complete light-off curve with both light-off and light-out points [25] 71
Figure 48 Temperatures before and after each catalytic converter 72
Figure 49 Wide-Band lambda value and effective torque for both tests 72
Figure 50 HC Emissions raw and after both catalytic converters 73
Figure 51 NOx Emissions raw and after both catalytic converters 74
Figure 52 CO Emissions raw and after both catalytic converters 74
Figure 53 CO2 Emissions raw and after both catalytic converters 75
Figure 54 Temperatures before and after each catalytic converter when measuring raw emissions and after the precatalyst 76
Figure 55 Relative humidity in the tests measuring raw emissions and after the precatalyst 76
Figure 56 MFB 50% 77
Figure 57 Sum of the pmi of both cylinders 77
Figure 58 Effective torque 78
Figure 59 HC emissions in the three points 78
Figure 60 NOx emissions in the three points 79
Figure 61 CO emissions measured in the three points 80
Figure 62 CO2 emissions measured in the three points 80

Figure 63 pmi-Time profile for the simulation carried out by Sylvain Garnier [26] in the case of the SCE running the WLTC 84
Figure 64 Engine speed-Time profile for the simulation carried out by Sylvain Garnier [26] in the case of the SCE running the WLTC 85
Figure 65 Fuel consumption map measured in the test bench 88
Figure 66 NOx raw emissions map 88
Figure 67 Optimization process of the SCE [24] 91
Figure 68 View of the catalyst block together with the surface reactions one in the GT-Suite simulation software 93
Figure 69 Screenshot from the exhaust system model 95
Figure 70 Screenshot engine state model plus the exhaust system 96
Figure 71 Temperature before main catalytic converter when simulating a point where the engine is running aspiratedly 98
Figure 72 Temperatures of the simulation and at the test bench when simulating a transient curve 99
Figure 73 NOx emissions simulation and measurement at the test bench 100
Figure 74 CO emissions simulation and measurement at the test bench 100
Figure 75 CO2 emissions simulation and measurement at the test bench 101
Figure 76 HC emissions simulation and measurement at the test bench 101
Figure 77 Engine speed and torque when simulating the points which composed the emissions maps 102
Figure 78 Temperature after the precatalyst 103
Figure 79 Temperature before the main catalyst 103
Figure 80 Temperature after the main catalyst 104
Figure 81 NOx and CO emissions after main catalyst 104
Figure 82 CO and O2 emissions 105

Abbreviations

Symbol	Units	Designation
CCC	-	Close-Coupled Catalyst
$CSER$	-	Cold Start Emissions Reduction
DEM	-	Detailed Engine Model
EGR	-	Exhaust Gas Recirculation
FRM	-	Fast-Running Model
LVK	-	Lehrstuhl für Verbrennungskraftmaschinen/Institute of Internal Combustion Engines
$NEDC$	-	New European Driving Cycle
PE	-	Primary Engine
PMR	-	Power to Mass Ratio
RDE	-	Real Driving Emissions
SCE	-	Split-Crankshaft Engine
SCU	-	Split-Clutch Unit
SE	-	Secondary Engine
$SULEV$	-	Super Ultra Low Emissions Vehicle
TDC	-	Top Dead Centre
$UNECE$	-	United Nations Economic Commission for Europe

1. Introduction

1.1 The Split-crankshaft Engine Project

The Institute of Internal Combustion Engines (LVK) of the Technical University of Munich (TUM), together with the Gear Research Centre (FZG), have rescued an engine concept which was discarded decades ago, due to costs and technical difficulties. The increasing concern of emissions and fuel saving are pushing new developments like this [24].

The concept consists of two bicylindrer engines attached at their crankshafts by the Split-Clutch Unit (SCU). The primary engine (turbo engine) will always be running while the secondary one (naturally aspirated) may be working or not, depending on the needs. Figure 1 shows the schematic setup of the SCE. The primary engine (TC) is connected on one side to the drive clutch and on the other side to the Split-Clutch Unit (SCU). The SCU is then connected on its other side to the secondary engine (NA).

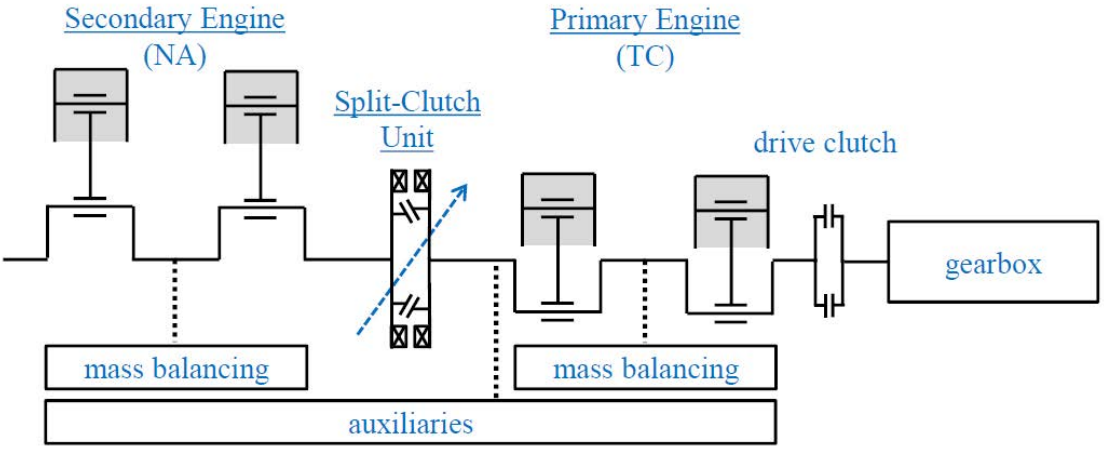

Figure 1 Schematic model of the system [24]

The main advantage of this engine with respect to the cylinder deactivation technology which is currently on the market is the absence of friction losses from the not fired cylinders as they are disengaged and not running instead of just not being fired.

At the moment of the beginning of this thesis, the actual state of the SCE (Split-Crankshaft Engine) project is:

- A complete model of the whole vehicle with both engines as Fast-Running Models in GT-Power and the SCU (Split-Clutch Unit) modelled in Simulink and also the activation and deactivation logic of the SE (Secondary Engine) [26]
- A Detailed Engine Model of the PE (Primary Engine) and SE in GT-Suite

- The test bench and the data adquisition system are built with both engines mounted and the first configuration of the exhaust system with the catalyst but without the SCU. Possibility of running individually each engine or both with a fixed coupling.
- A first simulative analysis of the exhaust system was carried out by Christoph Eger [5] where he studies different possible configurations to improve the efficiency.

1.2 Objective of the study

The true emission rates of the Split-crankshaft engine are still unknown and so is the feasibility of the project in the real world. It is important to simulate the new test cycles and estimate the emissions of the system. The main purposes and objectives of this project are:

- Analysing the behaviour of the V1 configuration of the exhaust system
- Analysing the conversion rates of both catalytic converters
- Studying the transient response of the system from the cold start
- Building the emissions maps of the engine and running a full vehicle simulation of a test cycle
- Measuring the emissions of the primary engine within the full operating range
- Adapting a model of the exhaust system, allowing a further improvement and simulation of the system
- Analysing the alternatives found in the market in the exhaust systems from similar engines
- Studying the possible problems and challenges which have to be faced when designing these types of exhaust systems
- Analysing the new emissions legislation

1.3 Structure of the study

The project is basically divided into four different parts. The first one is a summary of the state of the art, presenting how some car manufacturers have designed their exhaust systems. The main pollutants and the basic components of an exhaust system will also be explained. The second part is an analysis of the new emissions legislation implemented in Europe and a comparison with the old one, understanding the results which different authors have found within their investigations. The third part concerns different engine tests which have been carried out at the test bench in order to analyse the behaviour of the engine and exhaust system and collect the data needed for further simulations. The last one is composed by two different simulations and models. The first one is a full vehicle simulation of a test cycle to see how many pollutants the SCE produces and calculate how efficient it is when compared to a regular engine. To end with, a simulation model of the catalyst will be presented, which

is built to run in the future simulations which can lead to an improvement of the system.

2. State of the art

2.1 Motivation and history overview

Emissions, global warming, pollution... these are terms we become more familiar with every day. As governments have been really concerned during the last years with the environment, the introduction of new regulations for environmental emissions has forced car manufacturers to improve and develop their technologies to fulfill the requirements and imposed standards.

Downsizing is one of the most spread solutions to reduce pollutant emissions . The idea of downsizing consists in reducing the engine's size and has backgrounds back in the 1960s [6], where different patents showed the idead although it was not successfully implemented. With the need to reduce emissions, the concept was brought up and succesfully carried out. Probably, the most known variants are the static downsizing (where the engine is just built smaller but keeping the same power by increasing the mean indicated pressure) and the cylinder deactivation strategy, where depending on the power demands of the driver not all the cylinders may be fired but still kept moving. However, the introduction in the market of engine dynamic downsizing is taking part slowly as just the 12.8% of the vehicles in 2015 were equipped with a cylinder deactivation system [17].

Engine downsizing is nothing but the last of a series of technologies developed to reduce emissions. The first changes to engines were driven in the 1960s and 1970, when the exhaust gases recirculation (EGR) was introduced to reduce NOx emissions on both diesel and otto engines. Some time later, when microprocessors were improved, rudimentary computers were introduced to enhance the control of the fuel delivery and the reduction of HC and CO emissions. Later on, the oxygen sensor (lambda sensor) was implemented, a sensor which was needed to improve the air and fuel control in order to optimize the three-way catalysts efficiency. General Motors and Honda project cylinder deactivation to grow in market share in the following years. It was estimated that approximately te 27.4% of the light trucks fleetwide are equipped with this technology in 2015, although only 2.7% of cars use this system. This may be caused because conventional cylinder deactivation is easier to be implemented on cam-in-block (valvetrain layout where the camshaft is placed within the cylinder block) V6 a V8 engines, widely used on light trucks, than on the four-cylinder engines that dominate car sales [17].

One of the first models which implemented cylinder deactivation was the Cadillac L62 V8-6-4 of 1981 which could switch off 2 or 4 from its 8 cylinders. The industry has been focusing on engines which are capable of not firing certain cylinders but no differing from standard engine configurations, including may times standard exhaust gas systems [8].

2.2 Main pollutants in the exhaust gases

Nowadays, vehicles are one of the main causes of pollution [18]. At vehicles equiped with an internal combustion engines, it can be distinguished between three types of emission sources:

- The emissions deriving from the internal combustion which is the biggest pollutants source.
- The emitted gases due to the crankcase ventilation which are, by law, obligued to be redirected to the engine's inlet.
- The emissions due to the petrol evaporation.

In our case, only the emissions due to the combustion will be considered and reduced by the catalyst.

In the last years, the amount of pollutants emitted by combustion vehicles has been considerably reduced due to technical improvements. On the one hand, the engine's raw emissions have been improved with better motor controlling concepts or better engine designs. On the other hand, also the final emissions have been reduced thanks to more efficient exhaust aftertreatment systems. This can be clearly confirmed in the graphic 2 from Konrad [18], which shows how the emissions have diminished from year 1999 to 2009 in Germany.

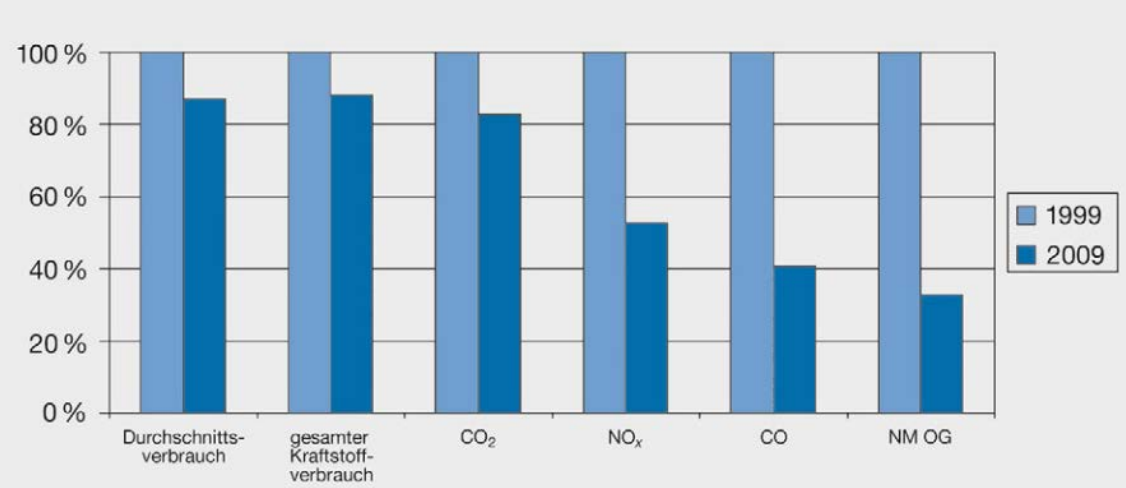

Figure 2 Petrol consumption and emissions from 1999 to 2009 between Otto and Diesel engines [18]

The introduction in year 2000 of the Euro 3 normative and Euro 4 in 2005 have impulsed this reduction in the emissions. There is also a general trend in the market in the direction of vehicles which consume less petrol. The percentage of emissions regarding vehicles and road transport in general with regard to the global amount of pollutants (considering also industry, other transport ways, electricity generation plants and houses) are ([18]):

- 41% of the total NOx
- 37% of CO
- 18% of CO_2
- 9% of HCs

At a perfect full and ideal combustion, the only resultant products would be CO_2 and H_2O. However, as this ideal combustion never takes place and the fuel has other components such as sulfur, the resultant products contain also NOx and HCs, as well as toxic minor products. These minor products can be reduced by improving the combustion and the fuel's quality. However, the amount of CO_2 is only dependant, under ideal conditions, from the carbon (C) content present in the fuel and cannot be changed. The CO_2 emissions are, therefore, proportional to the fuel consumption and cannot be reduced unless fewer petrol is burnt [18].

It is possible to distinguish between main components of the exhaust gases and harmful side products of the combustion:

- Main combustion components
  - H_2O
  - CO_2
  - N_2
- Harmful side products
  - CO
  - HC
  - NOx

2.2.1 Water vapour

The amount of hydrogen present in the fuel (CmHn) is burnt with atmospherical oxygen to form water vapor (H2O). It can be seen on cold day as steam going out of the exhaust gas. It represents around a 13% of the totat exhaust gases [18].

2.2.2 Carbon dioxide

The carbon contained in the fuel produces CO2 after the combustion with a usual percentage of about 14%. It is an uncoloured and non-toxic gas which is naturally present in the atmospherical air. It is not considered as a pollutant gas for vehicle emissions. However, it is one of the main causants of the greenhouse effect and therefore the related climatic change. Since the beginning of the industrial era, the amount of CO2 present in the air has been increased around a 30% to today's 400 ppm. The reduction of CO2 emissions through the fuel saving

is always an urgent measure [18].

2.2.3 Nitrogen

Nytrogen or N2 is the main component of the atmospherical air with a rate of the 78%. It remains almost unchanged during the combustion and represents around the 71% of the exhaust gases [18].

2.2.4 Carbon monoxide

The CO or Carbonmonoxide appears when incomplete combustions take place with a lack of air in the fuel-air mixture ($\lambda < 1$). However, also at rates of lambda greater than one (air excess) some CO emissions are produced as there are some regions in the combustion chamber which present a lack of air and, therefore, have a rich local composition [18].

In order to understand the influence of different parameters in the CO emissios, it is necessary to understand the formation process of the element. In the case where the combustion is incomplete, not all the CO have time to be burned and oxydized into CO2 and the emissions levels will arise. On the other hand, in the case where the combustion has a good mixture preparation, allowing a combustion that is more similar to the ideal one (complete combustion), more CO will be oxydized and therefore less emissions will be released. The most important external conditions which can influence the CO emissions are [18]

- Torque: at high torque points, the engine's working temperature increases, improving the combustion conditions and reducing the CO emissions.
- Engine speed: at high engine speeds the mixture has less time to be prepared and to be burned, leading to an incomplete combustion, increasing the CO emissions
- Lambda value: in the zone of rich lambda values (lambda less than 1, meaning that more fuel than necessary is injected), CO emissions increase considerably. On the other hand, by lean air-to-fuel ratios, there are theoretically no CO emissions. The resulting emissions are produced due to an imperfect air-fuel mixture which may lead to regions in the combustion chamber which have a rich composition.

Figure 3 shows the influence of the air-to-fuel ratio and the ignition timin (measured in degrees before top dead centre). Interesting is the small influence of the ignition timing at all lambda value, having only a small influence at rich air to fuel ratios.

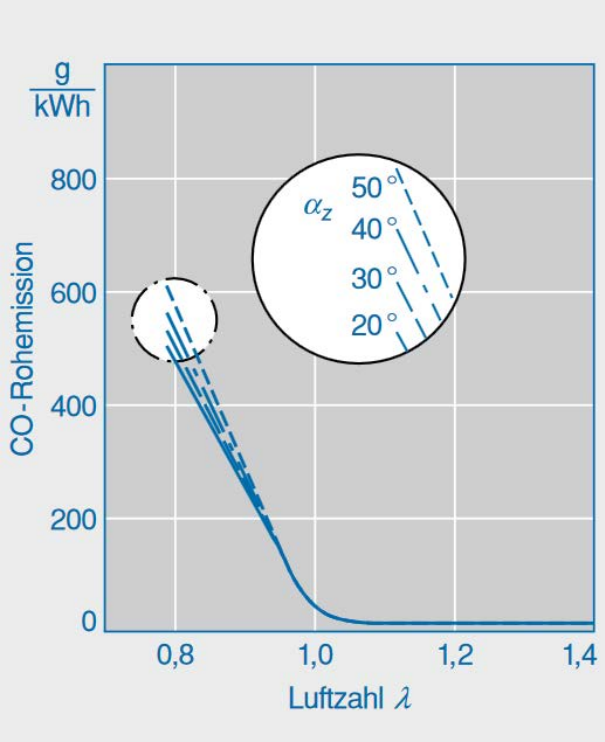

Figure 3 Influence of the Air-to-Fuel ratio and ignition timing in degrees before top dead centre in the CO Emissions produced by the engine[18]

2.2.5 Hydrocarbon

The abbreviation HC refers to a big family of elements combinating hydrogen and carbon. They appear as a secondary product due to an incomplete combustion with lack of oxygen or time. It is important to remember that HC is the main structure of all fuels used in internal combustion engines. Therefore, when fuel is not burned and gets directly into the exhaust system, HC components will appear. However, the molecule form may vary as some of the molecular bonds may be destroyed.

Some of the main parameters which influence HC engine emissions are [18]:

- Torque: increasing the output torque means increasing the temperature in the combustion chamber. This improves the combustion reaction, burning more fuel and decreasing the emitted HC. Also, the high temperatures make the reactions continue even after the combustion has ended. For this reason, the exhaust gases may continue reacting, converting HC into CO2 and water and decreasing even more the HC emissions.
- Engine speed: increasing the engine speed reduces the time for the combustion, decreasing the burned fuel and emitting more HC molecules.

Figure 4 shows the influence of the air to fuel ratio and the ignition timing on HC emissions. Both extreme low and high lambda values result in an increment of HC emissions while values of lambda around 1.1 present the minimum ones. Except for extreme lean points, the ignition

timing has a big influence on HC emissions almost constant at all lambda values.

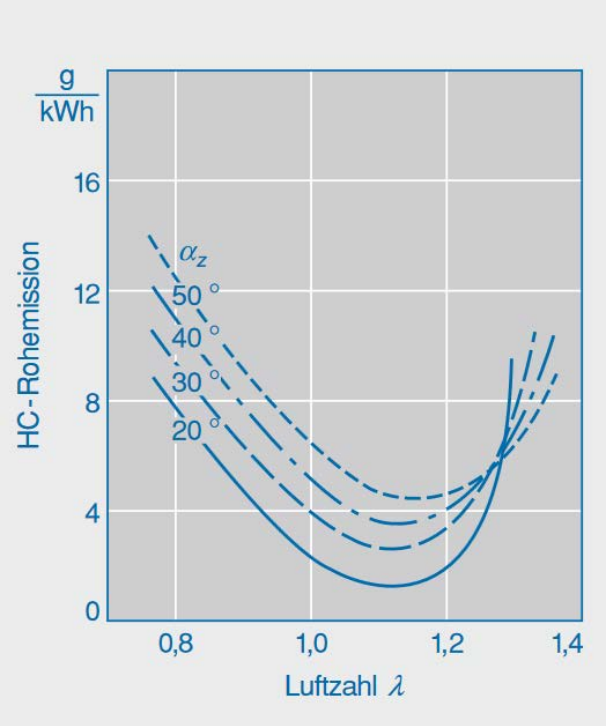

Figure 4 Influence of the Air-to-Fuel ratio and ignition timing (degrees before top dead centre) in the HC Emissions produced by the engine[18]

2.2.6 Nitrogen oxides

The NOx emissions are increased with higher temperatures of the combustion chamber. This means that the main parameters which influence the NOx emissions of the engine are:

- Engine speed: when increasing the engine speed, reactions have less time to be produced and the NOx emissions decrease. Additionally, the gases which remain in the combustion chamber decrease the maximum temperature. These gases decrease with higher engine speeds, meaning that there is also a counter effect of the rest gases in the NOx emissions [18].
- Torque: higher torques produce higher temperatures in the combustion chamber which increase the NOx formation reactions.
- Air-fuel ratio: the maximum amount of NOx emissions are produced with lambda values from 1.05 to 1.1. When going leaner or richer, the NOx decrease.
- Ignition timing: no matter at which lambda value the engine is running, the NOx increase with earlier ignition timings due to the higher peak pressures.

2.3 Exhaust gases aftertreatment for Lambda controlled Otto engines

2.3.1 The lambda value and its calculation

When the combustion process takes place with an stoichiometric composition, there will generally be in Otto engines 14.7 kilogrammes of aspirated air for every kilogramme of injected fuel. The lambda value represents the ratio between the amount of air which is actually aspirated in the operating point with regard to the ideal needed aspirated air [21]. In our case, for the SCE, the ideal stoichiometric value is 14.52 instead of the usual 14.7, calculated by the composition of the used RON 95 fuel.

The lambda value is defined as:

$$\lambda = \frac{(Actually)\ aspirated\, air\ mass}{Necessary\ aspirated\, air\ mass} = \frac{(Actually)\ aspirated\, air\ mass}{(Actually)\ injected\ fuel \cdot 14.7} \tag{2.1}$$

When the value of lambda is greater than one, it means that more air than necessary is used and it is called a lean combustion. On the other hand, when lambda is smaller than one, it means that less air is being used and the combustion will be called as rich.

Three Way Catalysts need values of lambda = one in order to work properly. However, when running at high engine speed and high loads, the increasing temperatures may lead to reaching the temperature limits of the components. For this reason, it is normal to work intermittently with periods of rich lambda values to reduce exhaust system temperatures. However, this periods will also lead to high emissions as three way catalysts can only convert the different species properly with lambda one. The new legislations, which are much stricter, will force manufacturers develop a new way to cool down the exhaust systems.

It is also possible to calculate the lambda value from the exhaust gases mole fraction as follows [21]:

$$\lambda = \frac{2 \cdot y_{O2} + 2 \cdot y_{CO2} + y_{H2O} + y_{CO} + y_{NO} + 2 \cdot y_{NO2}}{2 \cdot y_{CO} + y_{H2} + 9 \cdot y_{C3H6} + 10 \cdot y_{C3H8} + 2 \cdot y_{CO2} + y_{H2O}} \tag{2.2}$$

2.3.2 Lambda Sensors

In order to control the injected amount of fuel, it is necessary to have a good control of the lambda value. A normal controlling system will be composed of a controller unit as processing unit and two lambda sensors as information collectors. The typical configuration consists on a Wide-Band lambda sensor before the catalyst and a two-step-lambda sensor after it [21].

The binary lambda sensor

As previously mentioned, the binary lambda sensor will be positioned after the catalyst and its composition can be found in figure 5

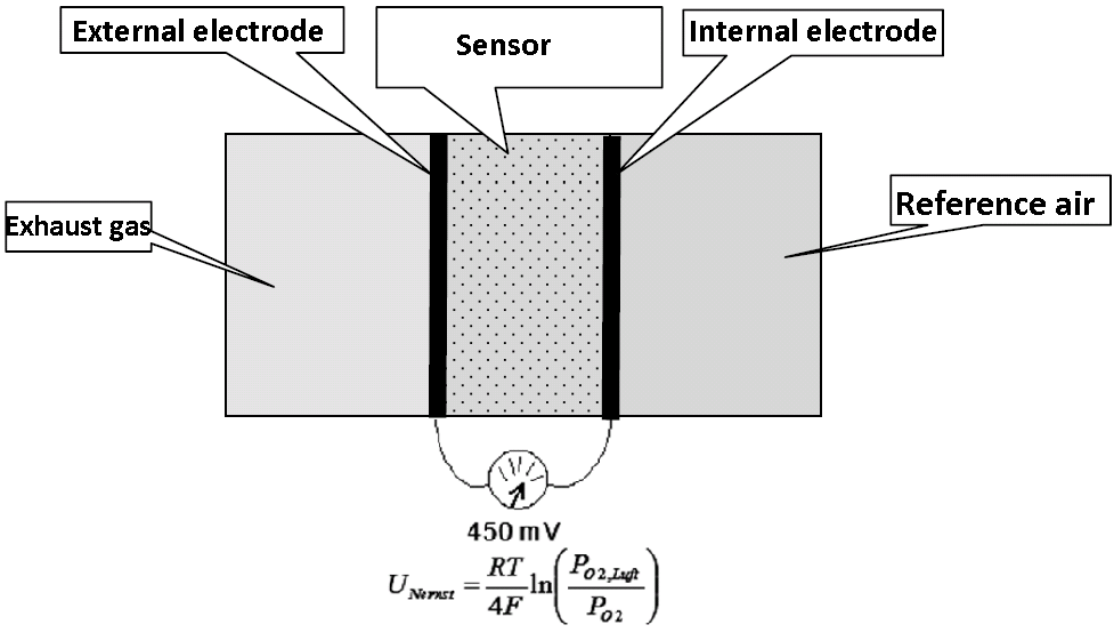

Figure 5 Composition of a binary lambda sensor [21]

The sensor is composed of two different electrodes. The external one will be in contact with the exhaust gases which are being measured, while the inner one will take ambients air as reference. Due to the difference of oxygen partial pressure between both electrodes, the sensor will produce the Nernst Voltage. The voltage's characteristic curve represents a jump around values of lambda one, which is the desired controlling value in our case. As after the middle spring the voltage curve is flat, this sensor only allows the controller to distinguish between lean and rich lambda values but prevents from knowing the actual lambda value. The lambda-voltage curve is shown in 6

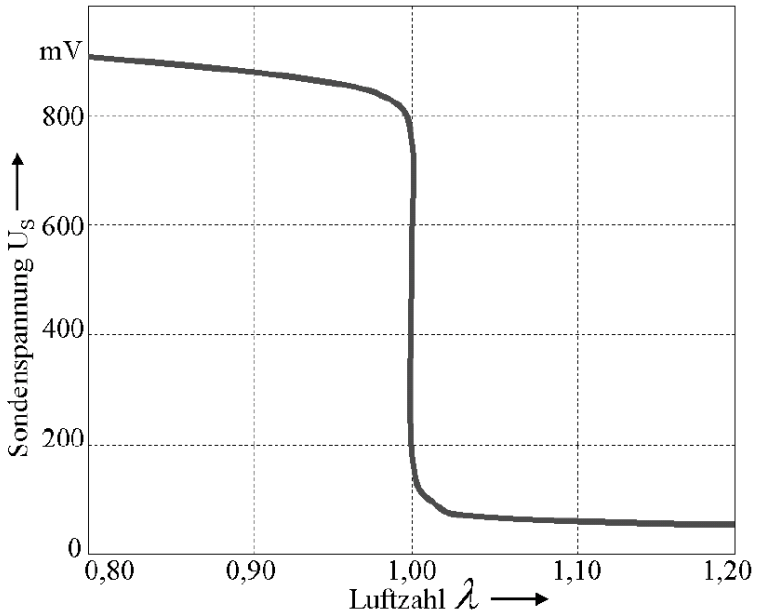

Figure 6 Characteristic lambda-voltage curve of a binary lambda sensor [21]

However, although the curve is almost vertical at the lambda = 1 value, with the available technology it is possible to regulate to a 680 mV value [21].

The Wide-Band lambda sensor

The second type of sensors, the wide-band sensor, is composed of two different cells. It covers, in contrast to the binary lambda sensor, a much wider lambda zone. Figure 7 shows an schematic composition of this type of sensors.

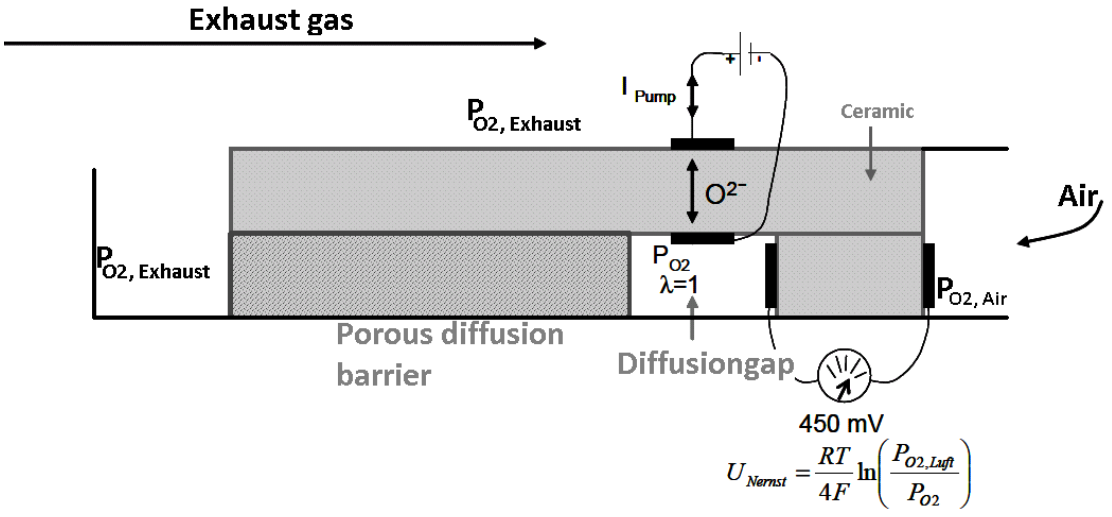

Figure 7 Schematic composition of a Wide-Band lambda sensor [21]

The Wide-Band lambda sensor is composed by a Nernst-Concentration cell and an oxygen pumping cell. The system is built so that between both cells there is a diffusion gap of 10 to 50 μm. The diffusion gap is connected to the exhaust gases through a diffusion barrier. The Nernst-Concentration cell is connected by one side to the ambient air and through the other to the exhaust gases' diffusion gap. By applying a pumping voltage in the pumping cell's electrode, it is possible to pump oxygen ions into or out of the diffusion gap. An electronic circuit in the control unit regulates the voltage applied at the pumping cell so that the composition of the gases measured using the Nernst concentration cell in the diffusion gap is constant at lambda = 1. With lean gases, the pumping cell pumps the oxygen from the exhaust gases in the gap to the outside (positive pumping direction). On the other hand, with rich mixtures oxygen will be pumped in the diffusion gap (negative pumping direction). When the mixture is lambda = 1, no oxygen hast to be transported and therefore the pumping electrical intensity will be 0 [21].

Figure 8 shows the sensor's behaviour. As it can be seen, at lambda = 1, the pumping intensity is 0. The sensor is capable of measuring values of lambda between 0.7 to 3.

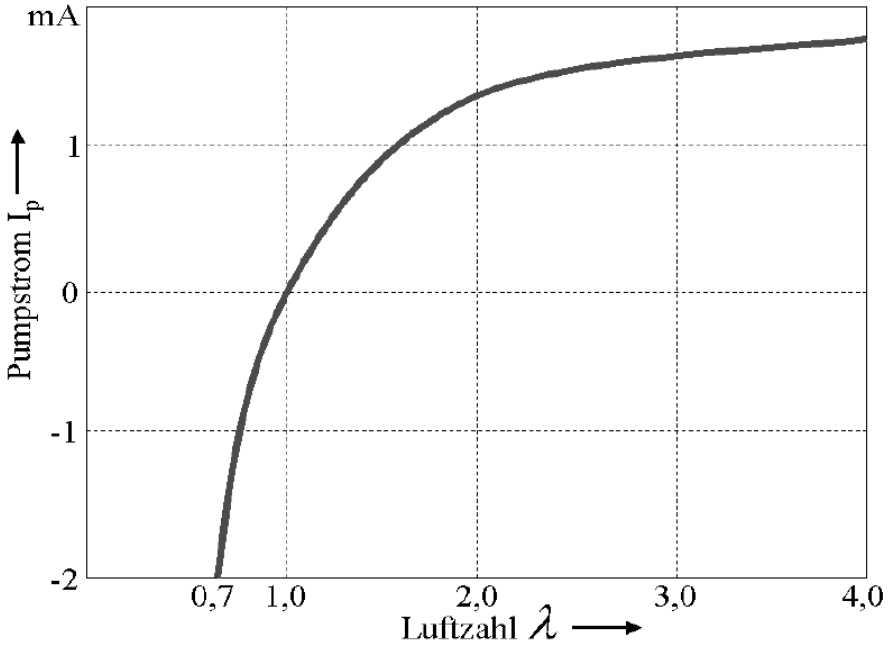

Figure 8 Characteristic lambda-pumping intensity curve of a Wide-Band lambda sensor [21]

2.4 Catalytic converters

One of the greatest improvements in the automotive industry is the catalyst converter, a component which can considerably reduce the CO, NOx and HC emissions. Catalytic reactors have high conversion rates, maintaining low pressure drops while they convert at high flow rates.

The Three Way Catalyst converter (often shortened as TWC) is, at the moment, the most effective system to reduce emissions in Otto engines. The TWC can be used for both Direct and Indirect injection engines. When working with mixtures of lambda = 1, the three way catalyst is able to convert almost all the CO, HC and NOx emissions. However, the necessity of working in such an small lambda region forces the usage of electronically controlled fuel injection. Although the ideal conditions cannot always be present, in average more than 98% of the pollutants can be converted by running an ICE with a three-way catalyst and lambda = 1 controlled by a lambda sensor and electronic fuel injection [18]. A standard catalytic converter configuration can be found in figure 9, where the catalytic converter is located after the exhaust manifolds and has a lambda sensor before and after it.

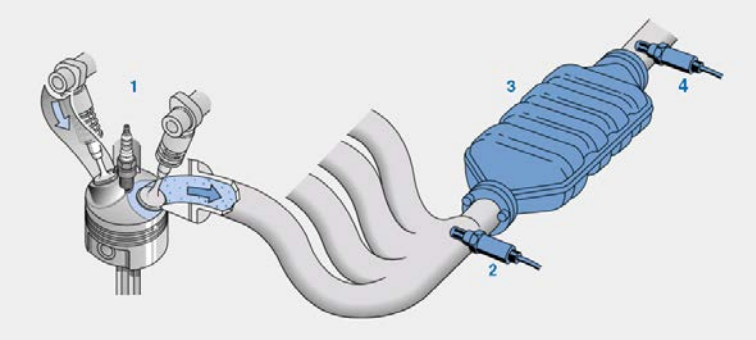

Figure 9 Standard configuration for a TWC. 1) Engine 2) Wide-Band Lambda sensor 3) TWC 4) Binary lambda sensor [18]

When running with rich mixtures, the TWC cannot properly convert NOx emissions. To prevent from high NOx emissions, the system may also have an additional NOx-Storage catalytic converter.

Catalytic converters can be divided into two different classes: continue and discontinue converters. The first ones convert the different gases without any interruption and without any active intervention of the engine. In this group would be the TWC, the Oxidation Catalytic converter and the Selective Catalytic Reactor (SCR) which is only used with Diesel engines. The discontinue catalytic converters go through different phases, changing actively the converting conditions through different engine operating points. For example, the NOx-Storage catalytic converter will store NOx for some time and needs from a short period of rich mixture to complete the reaction cycle [18].

2.4.1 Catalytic configurations

As engines are normally composed of more than one cylinder, it is necessary to join the exhaust systems together in order to have one common catalytic converter for the whole engine and not one for each cylinder. Engines with four cylinders will normally have two different possibilities to locate the catalytics. The first option is joining the four exhaust pipes through the exhaust manifolds and displacing the catalytic converter after them in a common pipe for the four cylinders. This configuration allows building the catalytic near the engine,

which will considerably reduce the heating time periods and the consequent periods of low conversion rates and high emissions. However, in order to improve the engine's power, it may be more favorable to use two exhaust manifolds of two cylinders, reducing the pressure in the exhaust site of the engine and increasing power. In this case, locating the catalytic converter after the second pipes joint is too unfavorable for the heating up periods. For this reason, it is normal installing two pre-catalytic converterter in the first section and a common main catalyst in the common pipe for the four cylinders. Engines with more than four cylinders may also use this configuration [18]. Different possible configurations are shown in figure 10, for a 4 or 6 cylinders engine with a precatalyst and a main catalyst.

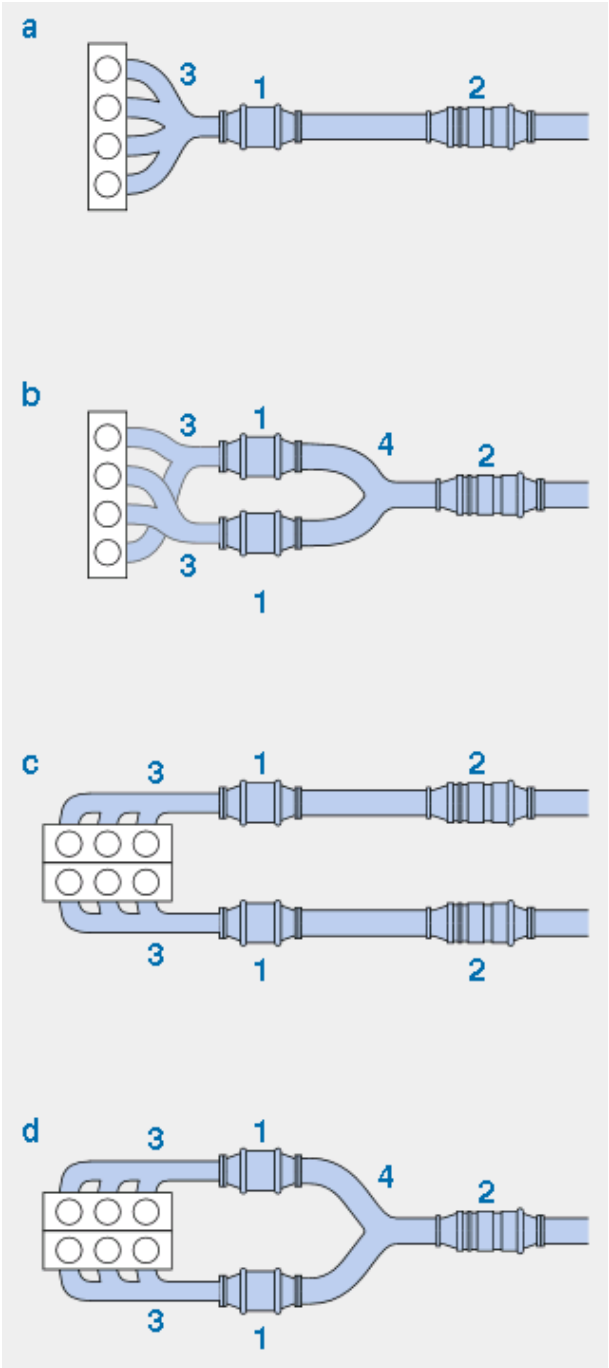

Figure 10 Different possible configurations for catalytic converters. 1)Pre-catalyst 2)Main catalyst 3) First pipes join 4) Second pipes join [18]

2.4.2 Heating up strategies

A proper design of the system, together with a good heating up strategy, may help the catalyst reaching earlier its optimum temperature, reducing the emissions during the cold start. With the new legislation and tests, every emission's gramme counts and it is important to reduce the emissions in the first moments of the test and getting the catalyst's temperature high while the engine speed and load are low.

Now, the main methods to rise the temperature fast explained by Konrad [18] are presented. On the first hand it is possible to use methods which only need from the engine, without any additional systems being built in the car. In order to increase the catalyst's temperature, there are two different options: increasing the exhaust gases temperature or increasing the exhaust mass flow. Both things can be reached only by changing some combustion parameters, reducing the combustion's efficiency and, therefore, increasing the exhaust gases enthalpy.

- Changes in the ignition timing: delaying the ignition moment is the main method to increase the exhaust gases' enthalpy. This means that the combustion will take place in the expansion phase and the exhaust gases will maintain higher temperatures. However, the overall efficiency will fall.
- Idle speed: increasing the idle speed means also increasing the exhaust gases mass flow. It also allows delaying the ignition time in order to ensure a good combustion. This method, however, is not so effective with modern cars provided with start-stop systems.
- Changes in the exhaust times: it is possible to increase the exhaust gases enthalpy by opening earlier the exhaust valves. However, this methods needs from an adjustable camshaft, which increases the engine costs.
- Homogeneous-split: this option is only possible with direct injection engines. These engines are capable of injecting the fuel in multiple short period of times. This allows increasing the enthalpy by injecting in the intake phase to obtain a homogeneous lean mixture. At the end, a short injection in the compression phase or near the ignition after TDC (around 20° or 30° after TDC) increases the enthalpy.

On the other hand to all the previously mentioned alternatives, the secondary-air-system method is a much more sotisficated way to increase the catalyst's temperature. This system has the disadvantage of requiring being exclusively built for this purpose. As it has been shown, delaying the ignition time increases the exhaust temperature. A rich mixture with a lambda value between 0.9 and 0.6 will be used. A secondary system will pump air to the exhaust system, creating an exhaust mixture with a lean composition.

When the mixture is really rich (lambda = 0.6), the unburned fuel components above a certain temperature threshold oxidize exothermically. To reach these temperatures, it is necessary to delay the ignition time to increase the temperature and the secondary air is introduced as close as possible to the exhaust valves. The exothermal reaction in the exhaust system increases the enthalpy in the catalyst converter and diminishes the time to reach the light-off. Moreover, the HC and CO emissions, in comparison to pure engine methods, will be reduced at the catalyst's entrance. When the mixture is not so rich (lambda = 0.9), no reactions take place before the catalyst. The unburned species oxidize in the catalyst and heat it up from inside.

An schema of the secondary-air-system is represented in figure 10

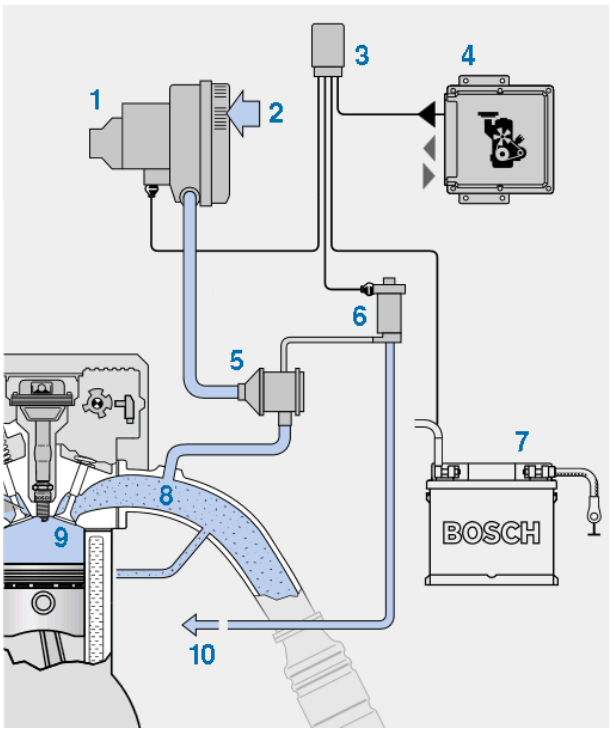

Figure 11 Schema of the secondary air pump system [18] 1) Secondary air pump 2) Relay for the aspirated air 3) Relay 4) ECU 5) Secondary air valve 6) Control valve 7) Battery 8) Inlet point in exhaust system 9) Exhaust valve 10) Connection to intaxe pipe

2.4.3 Three-Way Catalysts Internal composition

The TWCs are regulated with lambda = 1 and are used in Otto engines. This type of catalyst converters allows the conversion of HC, CO and NOx pollutants.

Figure 12 shows the different components of the internal channels which compose a catalytic converter. The monolith reactor inside the catalyst is a structure which is, in general, built from a ceramic material. The structure is divided into many parallel flow channels with a thin and narrow wall as can be seen in the left image in figure 12. All these parallel flows make up the substrate. The catalyst is applied on the walls of the narrow channels either as a thin layer or as a porous washcoat, which is supported on the monolith substrate. The fluid (gas) will be carried by convection and diffusion through the parallel channels and the reactions will occur on the active catalytic surface in the washcoat [23].

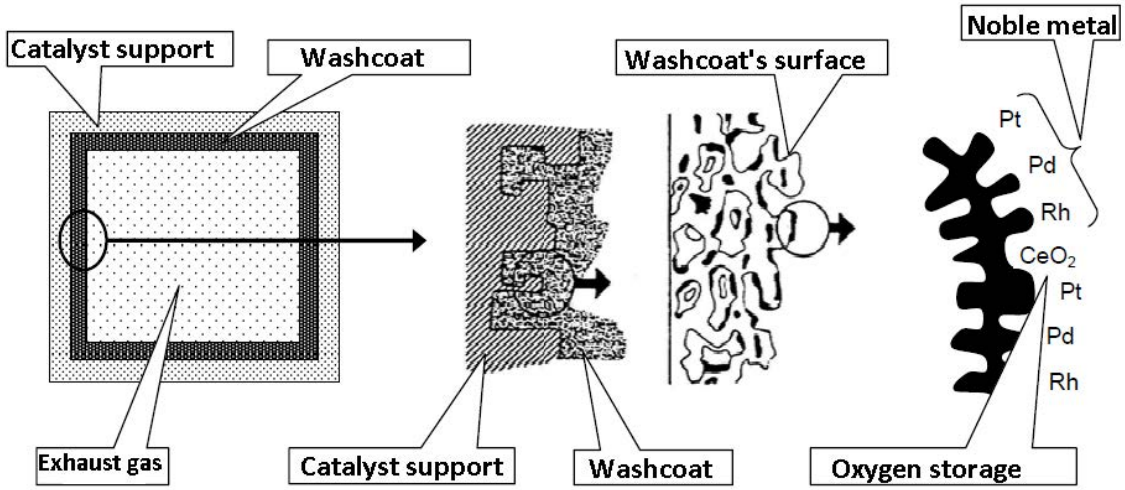

Figure 12 Composition of a catalyst converter [21]

The different reactions which take place inside the catalytic converter are fully dependent on the lambda value. These reactions can be divided into three types: oxidation, reduction and Water-Shifting reactions [21].

Oxidation reactions

$$CO + \frac{1}{2}O_2 \rightarrow CO_2 \tag{2.3}$$

$$H_2 + \frac{1}{2}O_2 \rightleftharpoons H_2O \tag{2.4}$$

$$C_nH_m + (n + m/4)O_2 \rightarrow nCO_2 + m/2H_2O \tag{2.5}$$

Reduction reactions

$$NO_2 \rightleftharpoons NO + \frac{1}{2}O_2 \tag{2.6}$$

$$NO + H_2 \rightarrow \frac{1}{2}N_2 + H_2O \tag{2.7}$$

$$NO + CO \rightarrow \frac{1}{2}N_2 + CO_2 \tag{2.8}$$

Water-Shifting reactions

$$CO + H_2O \rightleftharpoons CO_2 + H_2 \tag{2.9}$$

$$C_nH_m + nH_2O \rightarrow nCO + (m/2 + n)H_2 \tag{2.10}$$

Figure 13 shows the conversion capacity of a three-way catalyst with regard to the lambda value. It can be seen how only in a small zone around lambda = 1 a good conversion of all the pollutants can be achieved. When leaving this narrow zone, some emissions are reduced while other are increased drastically.

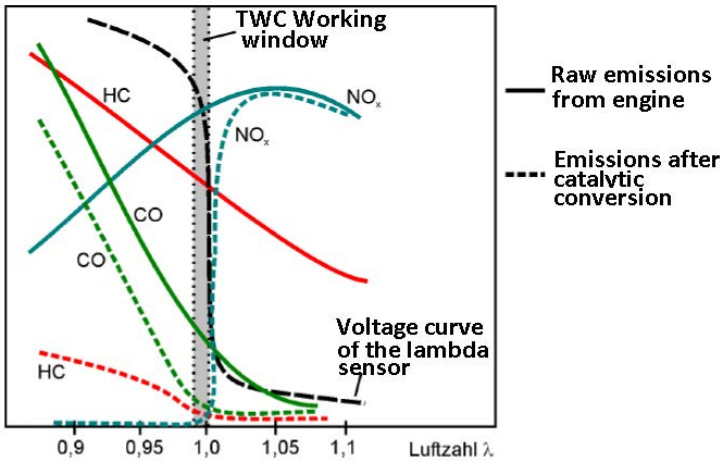

Figure 13 Conversion capacity of the TWC with regard to the lambda value [30]

However, it is necessary to emphasize that it is impossible for the control loop to have in each cylinder in every ignition a perfect lambda = 1 value. Odendall [21] shows as an example, illustrated in figure 14, imagining a three cylinder engine, one cylinder working a little bit rich and two cylinders working lean. In this case, the catalyst will convert the emissions in "packets" as the exhaust gases from the different cylinders reach the converter. Although in this case the average lambda value may be one, the HC, NOx and CO emissions would remain high.

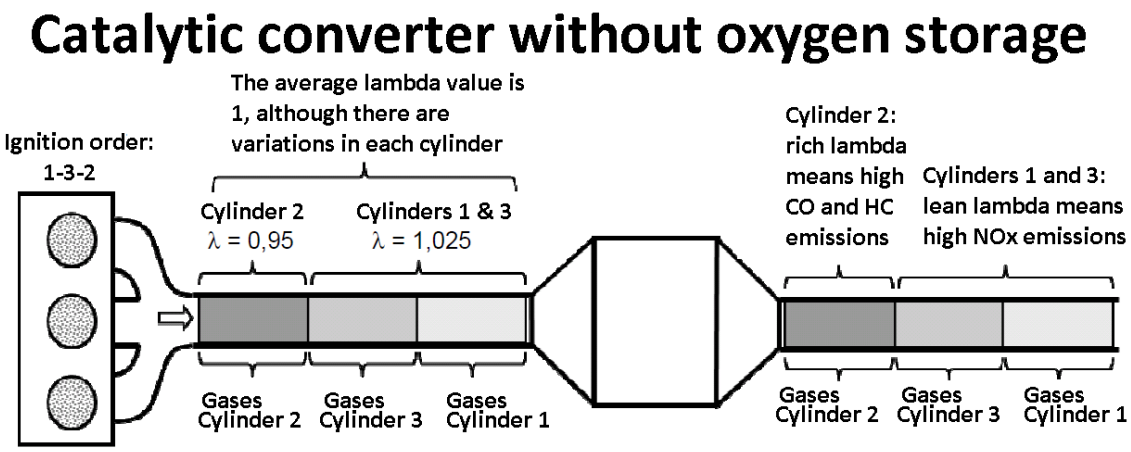

Figure 14 Catalytic converter system with a 3 cylinder engines with unequal lambda values [21]

2.4.4 Lambda regulation loop

The control loop is the system in charge of regulating the lambda value, adjusting it to the desired value, which is normally lambda = 1, in order to reduce final emissions as much as possible. The deviations from the desired value are regulated through the amount of injected fuel in the cylinders as the amount of air in the intake is not a controlled variable, but it is given by the throttle valve which regulates the torque. There are two possible ways of regulating the lambda value according to the two types of lambda sensors which were already presented.

When controlling with just one lambda sensor installed, the precision will then depend on the type of sensor. With only a binary sensor, it is only possible to regulate at lambda = 1 values with a slow response, while with a wide-band sensor it is possible to regulate in a wider range.

However, in order to improve the control accuracy, it is normal to regulate with two sensors installed in the system. In this case, the control loop will consist of an internal loop with the sensor before the converter, while a second loop corrects the output with the measurements from the second sensor [18]. In the test bench at the LVK, the system is controlled by the first lambda sensor while the second is only used to check that the regulation loop is working properly. The main strategies for the lambda control are summarized by Konrad [18] and shown here.

Two-points Control

Figure 15 shows the behaviour of the two-points control which regulates the lambda to the value of 1. A binary lambda sensor located in the exhaust pipe returns continued information of the mixture, whether it is lean or rich. When transienting from rich to lean or lean to rich, the signal will report a jump in the output voltage. This means that the controlled injected fuel will be varied to correct the fluctuation.

The controlled variable's response is composed by a jump and a ramp. This means that when a jump in the sensor occurs a quick jump in the controlled variable takes place for a fast correction of the air-fuel ratio. Then, a ramp follows the jump until a new jump in the measured signal is reported.

The exhaust gases will always be in an small area around labmda = 1. However, the dynamic of the controlling loop is really limited because of the dead times in the system. The deviation from the theoretical lambda = 1 point can be compensated by manipulating assymetrically the controlling variable, this means, having a different slope in the ramp when shifting from lean to rich than from rich to lean. In the case that the system has a tendency in the rich direction, when the lambda value measured value shifts to rich mixture, the manipulated variable will remain in the rich position for a dwell time, even though the probe signal has already jumped in the direction of rich composition. However, only after a short time 'tv' the manipulated variable will jump and then make a ramp in the lean direction. However, when the measured lambda value jumps in the lean direction, the manipulated variable will directly jump without waiting a short period of time.

On the other hand, when the system has a tendency in the lean direction, the system will work on the opposite way. When the signal reads a jump in the lean direction, the system will wait the corresponding 'tv' delay time to produce a response. When measuring a jump from lean to rich, the system will produce an inmediate answer.

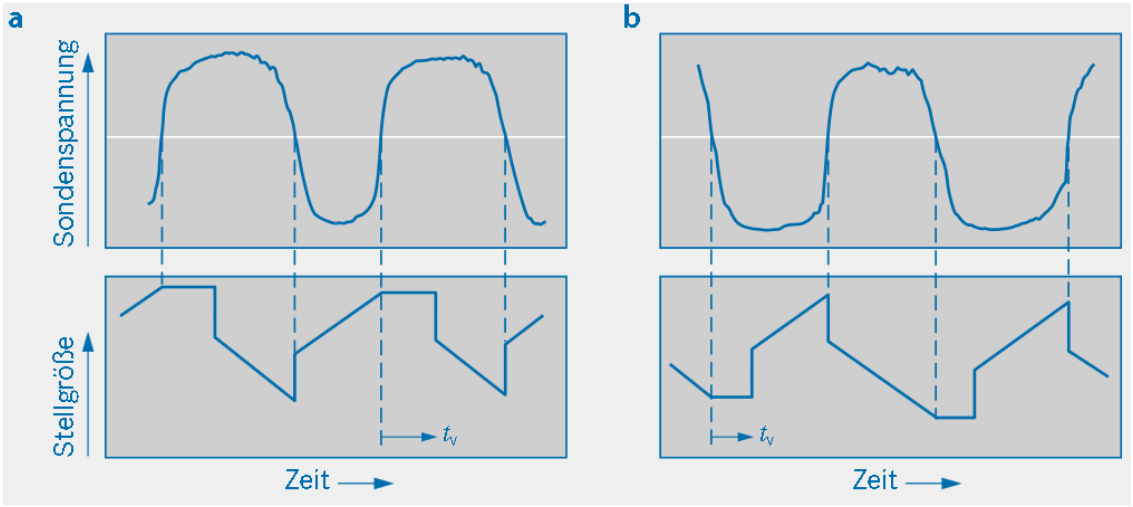

Figure 15 Example of the binary lambda control. Upper figures are the voltage produced by the lambda sensor while lower figures are the controlled variable. a) Case where the system is displaced in the rich direction b) Case where the system is displaced in the lean direction[18]

Steady lambda Control

Konrad [18] suggests that the way to improve the system's dynamic, with regard to the previously explained control method, means measuring the deviation of the lambda from lambda = 1. This can only be achieved by the use of a wide-band lambda sensor. The regulation with

this type on sensors can achieve in stationary conditions low amplitudes and good dynamic responses. The system will calculate and adapt the control parameters to the different engine working points.

In comparison to the binary control, the wide band lambda sensor also allows setting lambda points outside the typical lambda = 1. This may not be necessarily benefitial in terms of global emissions but can be used to protect components and cool them down (by short working periods with $\lambda < 1$) or a quick catalyst heating up (with $\lambda > 1$).

Two-sensors control

The previously mentioned options had the lambda sensor installed before the catalytic converter. This positioning has a limited precision as the sensors are exposed to big load conditions with dirty exhaust gases and poisoning. All these working conditions can influence the characteristic curves of the lambda sensors, influencing in a bad way the measured values.

Locating the sensors after the catalytic converters, as figure 16 shows, diminishes the influence of the "bad" raw exhaust gases from the engine. However, regulating the system with just a lambda sensor which is located after the catalyst will suffer from high control delays as the measuring point placed way too far and also will be influeced by the storage behaviour of the converter.

The disadvantages of both perspectives can be improved by using a cascade control which is composed by a fast primary loop which regulates with a wide band or binary sensor before the catalyst and is corrected by a slower secondary loop regulating with binary sensor after the catalytic converter [18].

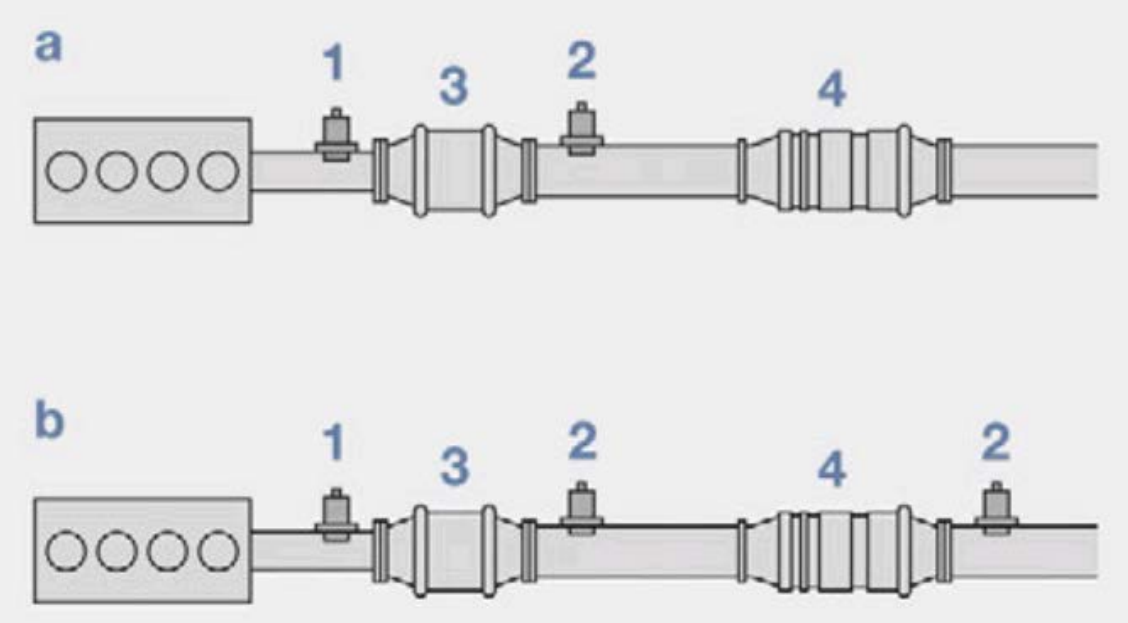

Figure 16 Control schema using two or three lambda sensors. 1) Binary or wide band sensor 2)Binary lambda sensor 3) Pre-catalytic converter 4) Main catalytic converter

Three-sensors control

The last option, the three-sensors control is variation from the previous one but introducing a lambda sensor between both catalytic converters. This improvement has been impulsed for the diagnosing and monitoring of both catalysts and also to accomplish with the US SULEV (Super Ultra Low Emissions Vehicle) category. The third sensor will take part in a third control loop, slower than the previous ones.

2.5 Exhaust gas systems of current production in series vehicles

In the early 2000s, with the increasing concern on emissions and fuel saving, the German brand Mercedes-Benz released an engine which could be considered as the perfect example of the regular cylinder deactivation in today's market [8]. It is a V12 engine capable of not firing determined cylinders. Some engines always deactivate the same cylinders, while others, in order to prevent from an irregular wear, alternate in each cycle the cylinder which is not being fired [8]. The alternation of the not fired cylinder is also an easy way to solve the catalyst heating problem, as all the catalysts will continuously have an air flow which keeps their temperature high. In this type of engines, when running in partial engine mode, depending on the configuration or the design, it may happen that the catalyst of the not fired cylinders is below optimum operating temperature and, when full operation mode is entered, the catalyst is not able to convert the emissions of the just fired cylinders [8]. This represents a big issue as it may happen the opposite as expected, increasing the emissions. In the emissions tests, such as the WLTP or RDE tests, accelerations are being taken more into consideration

as in the old NEDC, in order to have a more realistic cycle. This would mean for this type of engines an intermittent dis-/Connection of a secondary engine or the unfired cylinders, resulting in higher emissions and risking the test approval.

Interesting for this study is the investigation on how different companies have solved and designed their exhaust gases systems for engine downsizing and cylinder deactivation, facing the different issues which this systems present. The schema shown in figure 17 was used by Mercedes [8]. The german engineers decided to build a precatalyst converter for each group of three cylinders (4 pre-catalysts in total) and two main big catalysts after them. The small precatalysts located near to the engine reach converting temperatures faster due to the lower thermal intertia an the nearer location to the engine, taking more advantage of the exhaust enthalpy. However, when high conversion rates are needed, the two main catalysts are designed for higher gases volumes.

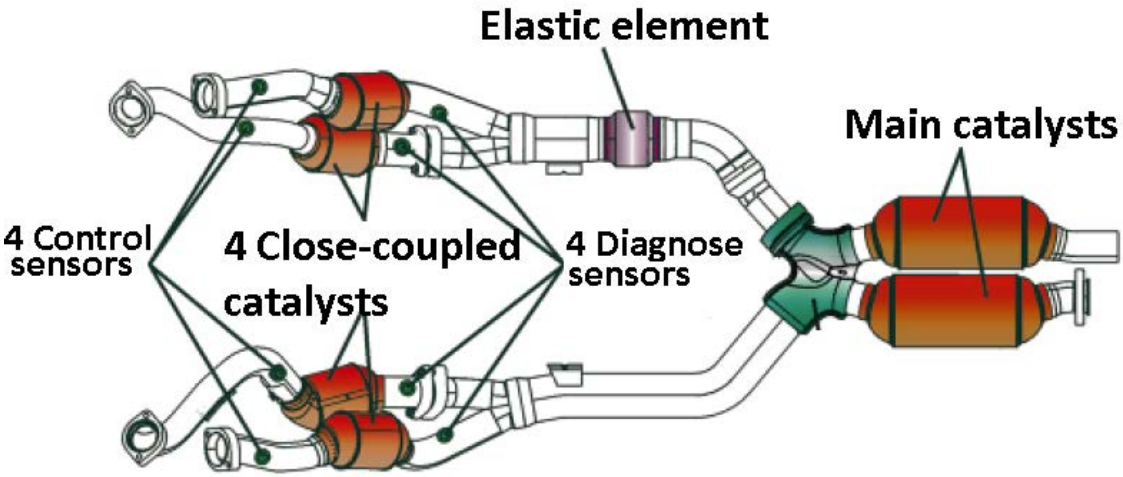

Figure 17 Mercedes-Benz exhaust gas system for a cylinder deactivation engine in the year 2000 [8]

Dr.-Ing Fortnagel u. a. [8] indicate that a possible sollution to fulfill the emissions standards is the use of a electrically heated catalyst. However, this system, which has advantages, shows also disadvantages and was discarded by the developers. The main presented disadvantages are an increment in the fuel consumption due to the energy needed, extra weight, unsatisfactory reliability and increased need for space. Instead, designers implemented the double ignition. This double ignition has a first advantage, as it reduces the HC emissions due to the unburned fuel-air mixture at the end of the cycle, which is clearly an smaller amount than with a single ignition. The second advantage of this system is the good combustion stability with extreme late ignition times at the start and heating phase, allowing higher exhaust temperatures which result in shorter times for the catalytic converter to reach the operating temperature. Dr.-Ing Fortnagel u. a. [8] also implemented a secondary air system, which consists of an electrical pump and a secondary air valve for each cylinderbank, adding oxygen to the exhaust system exactly after the exhaust valve, elevating the temperature before the catalytic converter. For this particular system, the designers expect to reach the catalyst's

working temperature after 18 seconds in the NEDC cycle.

Dr.-Ing Fortnagel u. a. [8] could not build all the catalysts near to the engine due to the lack of space. The main catalysts' volumes are the ones needed to meet the limit values for the required lifetime.

Due to the intermittent high load needs, it is not possible to fulfill the emissions tests with the engine working partially the whole time. Therefore, the engine always starts and runs in full mode until all the pre-catalysts reach the necessary temperature. When the engine is running in partial mode, the left cylindersbank is completely turned off. Dr.-Ing Fortnagel u. a. [8] afirm that the precatalysts' cooling down when the left bank is not firing is so small that the full conversion rates are almost inmediately reached when they are firing again. This conversion will then be supported by the main catalyst as it is permanently hot because of being constantly heated by the exhaust mas flow of the right cylinder bank.

In the case of the Mercedes M271KE engine, which is statically downsized, has a similar configuration to the previously exposed engine [9]. This system integrates the pre-catalysts in the exhaust manifolds in all the engine versions. These precatalysts, in order to improve the light-off behaviour and the long-term stability, with a total volume of 0.9 liters and 600 cells/in2, are composed of a triple metal coating in Europe and a Platin-Rhodium coating in the USA. Dr.-Ing Mikulic u. a. [9] affirm also that this close-coupled system ensures a much lower structure-borne noise radiation in the high frequency by the significant reduction of the gas-dinamically induced structure excitation of the entire catalyst system. This is remarkable during the startphase. Furthermore, the existing geometry, together with a perfored plate located transversaly to the exhaust flow, creates an optimal flow and temperature distribution in the monolith.

The previously mentioned systems have in common that both have been produced and sold in real cars. However, not all the interesting designs have been introduced to the market. Many others, maybe because for economical reasons, lack of technical capacity at a certain time or simply useless design, have not been produced. Between all these designs, it is interesting to remark a patent by Haruhiko Iizuka u. Fukashi Sugasawa [14]. The patent is, in fact, a control system for an split engine but shows an interesting aftertreatment configuration. The developers divided the engine into two different cylinder groups, where the second one can be deactivated under light load conditions, exactly like the SCE, where the catalyst of the not working cylinder bank becomes cold. The engine, in this case, is provided with an exhaust passage which consists of first and second upstream exhaust passages connected to the first and second cylinder group, respectively, and a common downstream exhaust passage as shown in figure 18. The system also has an exhaust gas sensor and a first catalytic converter in the first upstream exhaust passage, while there is a second catalytic converter and a temperature sensor disposed in the common downstream exhaust passage.

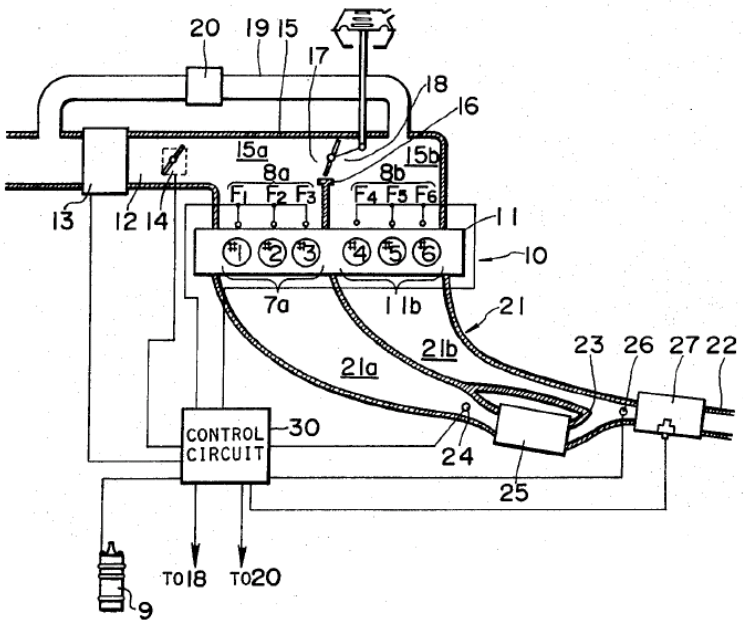

Figure 18 Schema of the exhaust system in the Split engine control system patent by Haruhiko Iizuka u. Fukashi Sugasawa [14]

When the temperature of the second catalytic converter (number 27) is above a certain threshold during the partial cylinder mode, the engine is feedback controlled by a signal from the exhaust gas sensor and the exhaust gases are purified by the first catalytic converter. In the case where the temperature is below a certain threshold during the partial cylinder mode, the air-fuel mixture is enriched with respect to the stoichiometric point so as to promote reduction of the NOx component of the exhaust gases in the first catalytic converter (number 25) and oxidation of the remaining HC and CO components in the second catalytic converter.

In order to reduce the pumping losses during the partial cylinder mode of operation, fresh air, at substantially atmospheric pressure, is introduced into the deactivated second cylinder group (7b) through a bypass passage (19) which connects the air induction passage (12) upstream of the airflow sensor (13) and the second intake passage (15b) downstream of the first stop valve (18). Valve 20 will open during the partial cylinder mode so as to introduce the fresh air into the deactivated second cylinder group.

When running in full cylinder mode, the ratio of the air-fuel mixture supplied to the engine is maintained at the stoichiometric point so that the first and second three-way catalytic converters, 25 and 27, can simultaneously reduce the NOx component and oxidize the HC and CO species of the gases exhausted from the first and second cylinder groups. On the other hand, when running in partial mode, the first stop valve 18 closes so as to shut off the flow of air through the throttle valve 14 into the deactivated second cylinder group 7b. The second stop valve 20 opens and introduces fresh air, at substantially atmospheric pressure, through the bypass passage 19 into the deactivated second cylinder group 7b in order to minimize the pumping losses.

To end with, in order to prevent the transient problem which occurs when the temperature of the second catalyst is below the reference temperature, the air-fuel mixture supplied to the first cylinder group 7a is enriched with respect to stoichiometric point. This allows the first catalytic converter 25 to promote reduction of the NOx component of the gases exhausted from the first cylinder group. The gases, which still include the HC and CO, are then mixed with the fresh air pumped from the deactivated cylinder 7b. This will allow the second catalytic converter to promote oxidation of the HC and CO species.

2.6 The consequent challenge derivated from close-coupled catalysts and retarded ignition

As it has been shown in the previous section of the chapter, close-coupled catalysts (catalysts which are located really near the engine to take advantage from the exhaust gases' enthalpy), together with ignition delay are two of the preferred options by the industry to reduce the needed time to reach the light-off temperature and maintain high catalyst temperatures. However, too high catalyst temperatures, typically above $1500°C$ may lead to the deactivation of the converter and poor conversion efficiency. Lee u. a. [19] present a study which tests the influence of the different engine operation conditions on the catalytic converter temperature.

Some years ago, high exhaust temperatures were the limiting factor for the catalytic converter designs due to the limited temperature resistance of the washcoat, where gas inlet temperatures into the converter above $850°C$ lead to an increased ageing of the coating [19]. With the further materials development, new catalysts are able to achieve temperatures of $1050°C$ without impairment of the coating. High temperature coatings are capable of holding temperatures up to $1050°C$ for 24 hours still maintaining a hydrocarbon conversion efficiency of 98%, allowing catalysts to be set nearer the engine. However, it has to be kept in mind that any misfunction may lead to temperatures above $1050°C$, which can deactivate the catalyst. Table 1 summarizes the main thermal deactivation phenomenas as a function of the catalyst operating temperature [19].

Temperature	**Thermal Deactivation**
$1900°C$	Pellet Melting
$1700°C$	High temperature ceramic melts (50% Mulite, 50% Titanate)
$1500°C$	Ceramic monolith melts
$1300°C$	Cordierite phase change to mulite
$1200°C$	θ-Alumina phase change to α-Alumina

Table 1 continued from previous page

1050°C	σ-Alumina phase change to θ-Alumina
900°C	Alumina sinters (γ-Alumina to σ-Alumina)
750°C	Pt-Pd and Pt-Rh alloy forms in reducing A/F
700°C	Pt sinters
650°C	Rh-Alumina reaction in oxidation A/F
500°C	Optimum converter operating temperature

Table 1 Thermal deactivation phaenomena as a function of catalyst operating temperature [19]

Lee u. a. [19] tested a 1.0L 4-cylinders SI engine with a similar exhaust gas configuration to the one built in the LVK to test the SCE. Figure 19 shows the schematic diagram of the set-up used by Lee u. a. [19]. The SCE V1 exhaust configuration consists also of a precatalyst and a main catalytic converter with a thermocouple type K before and after each converter. However, the precatalyst is not located directly after the exhaust manifolds but after the turbine which is located after the exhaust manifolds. This has to be taken into consideration when comparing the results. However, in the case of the secondary engine of the SCE, there is no turbine and the precatalyst may be located almost like Lee u. a. [19] did.

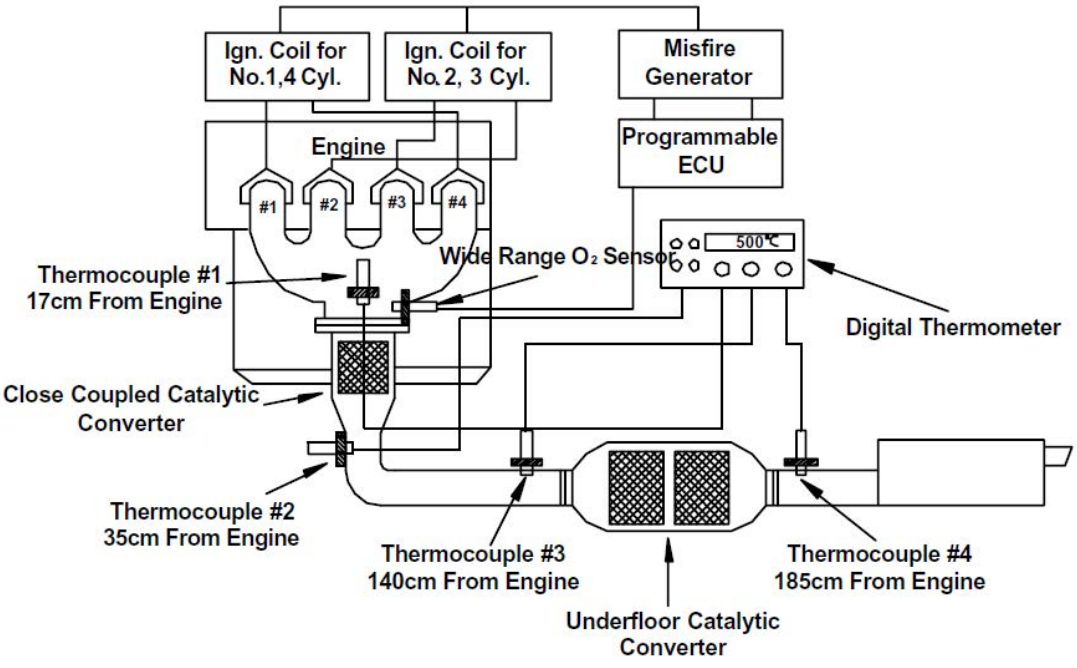

Figure 19 Schematic diagram of the experimental set-up used by Lee u. a. [19]

The first study carried out by Lee u. a. [19] shows that the catalyst temperature is higher than the exhaust gas temperature of catalyst inlet by 100 - 110°C, as seen in figure 20, which represents the temperature of the catalyst and its inlet. As the limit temperature of the catalyst was considered to be 1050°C, the maximum allowed temperature measured by the thermocouple placed directly in front of it will be 950°C. This temperature difference is caused by the exothermic reactions which take place in the catalyst when CO gas is converted into CO2 gas.

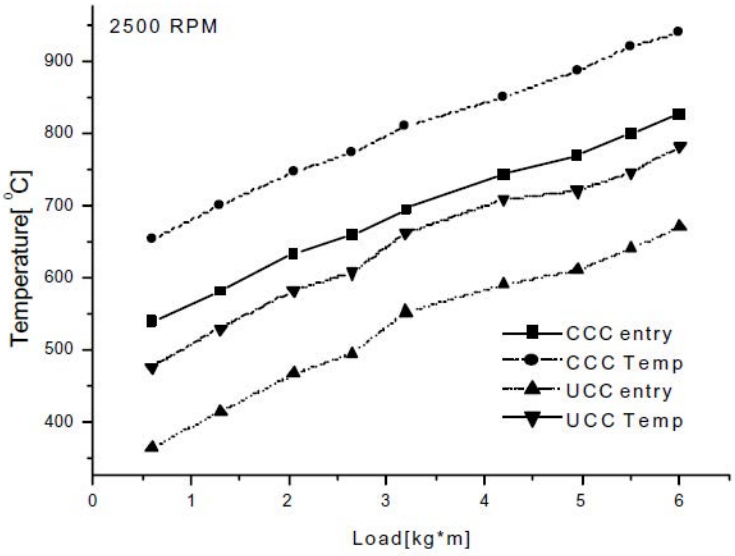

Figure 20 Relationship between catalyst inlet gas temperature and catalyst temperature at 2500 rpm. CCC refers to close-coupled-catalyst and UCC to under floor catalytic converter [19]

The second interesting result reported by [19] is shown in figure 21 and is an analysis of the exhaust gas temperature variation with regard to the lambda value. The results showed that the exhaust gas and pre-catalyst temperature were maximum at the point of lambda = 1. This point is exactly the working point of the SCE as three-way catalysts need from an stoichiometric air-fuel ratio for a proper conversion, meaning that the working point of the SCE will be the one with the highest exhaust temperatures.

Lee u. a. [19] explain the fact that lambda = 1 produces the hottest gases by two reasons. The first one is the exothermic reaction of the CO into CO2 is maximum at this point and secondly, the combustion temperature is maximum also at lambda = 1.

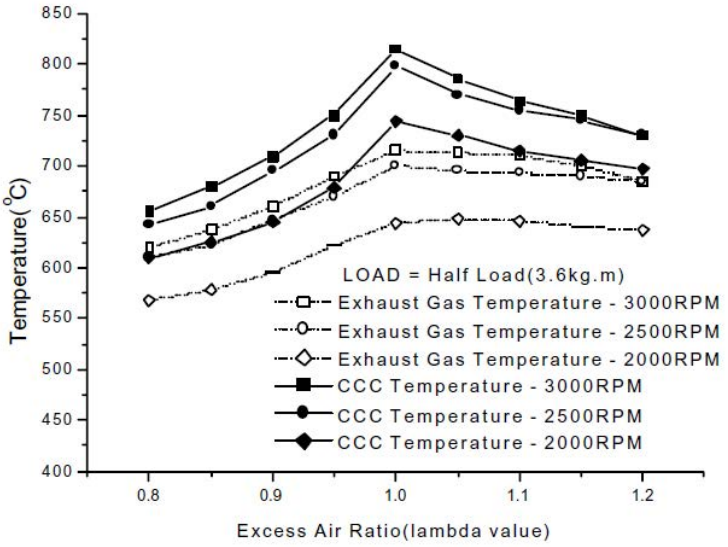

Figure 21 Effect of the lambda value on the catalyst inlet and catalyt temperatures for different engine speeds [19]

Furthermore, Lee u. a. [19] study the exhaust gas temperature with regard to the variation of the ignition timing, which is one of the applied techniques by the industry to heat up quick the catalytic converters. It was found that ignition timing retarded at 20°C crank angle relative to the TDC can cause thermal deactivation of the catalyst. Excessive retardation would lead to engine afterburn in the exhaust and, in the worst case, engine stalling which results in serious emissions problems. However, a proper retardation of the ignition timing for a short period is affirmed to be a good measure to warm up the catalytic converter fast enough [19]. Figure 22 shows the effect of the ignition timing in the catalyt inlet temperature.

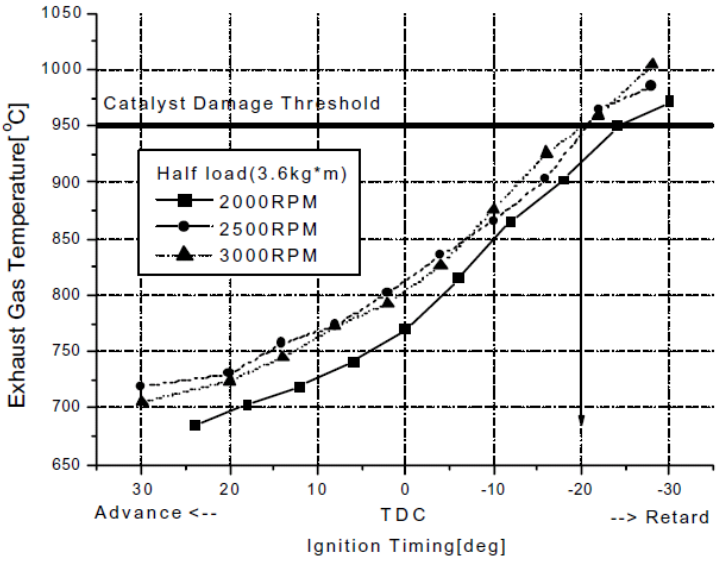

Figure 22 Effect of ignition timing on catalyst inlet gas temperature [19]

The last steady-state study presented concerns the engine misfiring. Misfiring of the SI engines may cause inmediate damage to the catalyst and increase emissions since it brings unburned fuel and oxygen into the catalyst, resulting in an increment in temperature due to subsequent combustion. It is interesting to remark the misfiring as it is an unstudied factor in the case of the SCE. Lee u. a. [19] show an interesting figure which is here presented in figure 23. As it can be seen, engine misfiring does not change (nor increase) the inlet gas temperature but highly increases the pre-catalyst temperature, which may lead to catalyst damage without being noticed in the case that the system is just equipped with one thermocouple before the pre-catalytic converter.

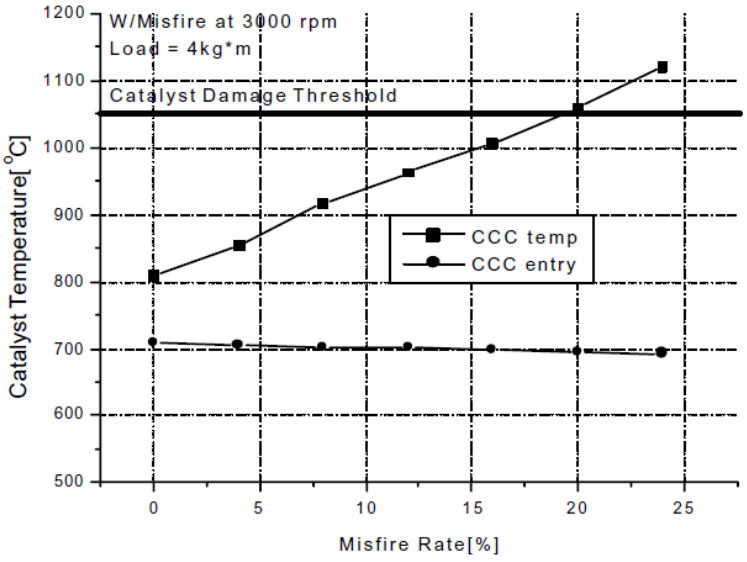

Figure 23 Effect of the misfire rate on catalyst temperature and inlet temperature [19]

To end with, it was shown that the time needed to reach the light-off temperature can be shortened by about 34 seconds with a 30° retard of ignition timing under idle state, as can be seen in figure 24.

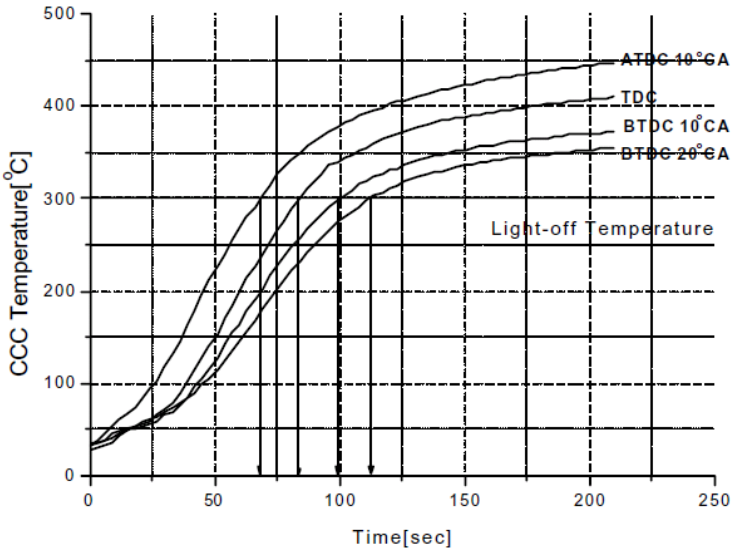

Figure 24 Influence of ignition timing on catalyst light-off [19]

3. Legislation for light-vehicles with combustion engines

In this chapter, the new and the old offical emissions testing cycles will be presented. It is important to understand how the cycles have changed, trying to be more accurate to reality. This changes make tests be more difficult to be passed, forcing car manufacturer's improve their emissions rates and fuel consumption.

3.1 The old cycle: New European Driving Cycle (NEDC)

The New European Driving Cycle was designed in the 1980 and has become outdated. The original test has suffered from few modifications, although the maximum emissions levels have been updated according to the different Euro norms (Euro 5, Euro 6...). At the moment, Europe is in a transient period from the NEDC to the WLTP and cars will have both test values, a mess for the final user. However, it is pretended that in 2019 the NEDC is finally disused and replaced by the WLTP together with the RDE [11].

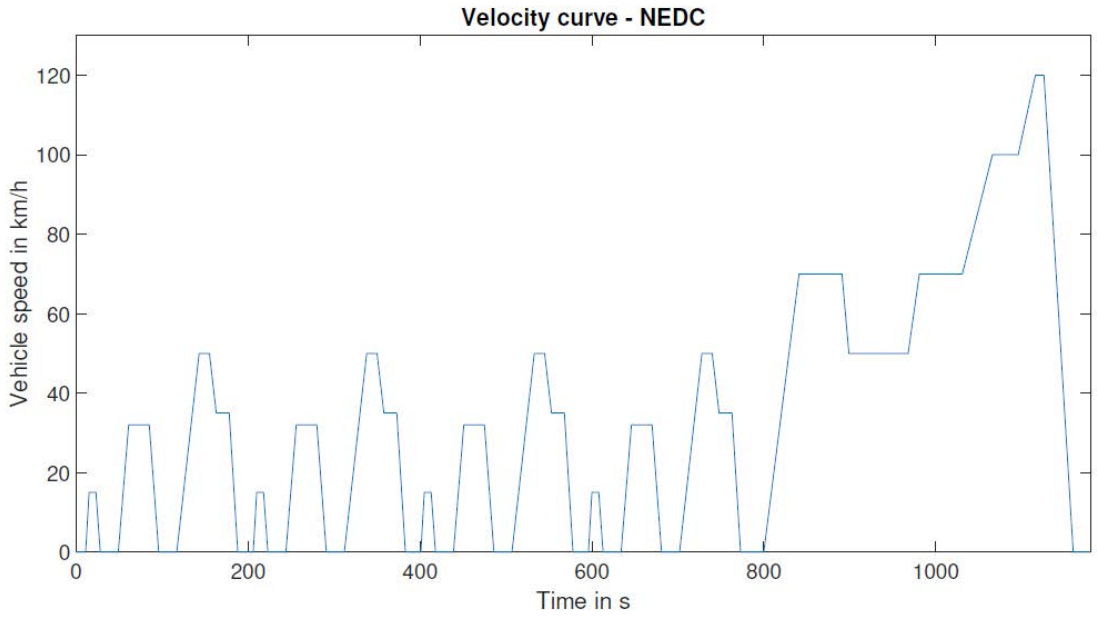

Figure 25 New European Driving Cycle sped profile [26]

The NEDC speed profile is presented in figure 25 and consists of an urban phase (ECE) and a motorway phase (EUDC). It contains accelerations, decelerations, constant speed, idle and warm up phase. The cycle starts with a warm up phase, continued by four ECE cycles and then an EUDC to conclude as shown in figure 25. The warm-up phase is 40 seconds long and was not taken into account for the measurements until year 2000. The total test duration

is 1180 seconds in a test bench, with a temperature between 20 and 30 C.

3.2 The new cycles: Worldwide harmonized Light Vehicles Test Procedure and Real Driving Emissions

3.2.1 Worldwide harmonized Light Vehicles Test Procedure (WLTP)

The need to ensure that light-duty vehicles emissions were similar in the tests and in the road, forced the development of a new cycle: the Worldwide Harmonized Light vehicles Cycle. The cycle and procedure have been developed by the United Nations Economic Commission for Europe (UNECE), although it is not the first harmonized developed test as the World Harmonized Heavy Duty Cycle or Non-road Transient Cycle already exists [28].

The automotive industry will be happy to have the same test cycle worldwide as vehicles will not have to be anymore optimized for the different markets although for the moment is has only been approved in the EU. The WLTC was developed after collecting data about light duty traffic in different regions of the world. The driving behaviour was then filtered to remove errors, noise and extreme driving behaviours and analyzed to derive the main elements for the new cycle [28]. After some iterations, the developers came with the last cycle version, which is summarized in table 26 and the speed profile is shown in figure 26. This test was found to be impossible to drive with some vehicles due to the high accelerations. For this reason, the test was adapted to three different vehicle classes (class 1, 2 and 3) of different power to mass ratio (PMR). The original WLTC cycle is class 3, while classes 2 and 1 were obtained by applying a downscaling factor to the speed profile and the acceleration profile [28]. Final WLTC class 3 applies for vehicles with a PMR > 34 kW/ton, class 2 to vehicles with a PMR between 22 and 34 kW/ton and, to end with, classe 1 to vehicles with a PMR lower than 22 kW/ton.

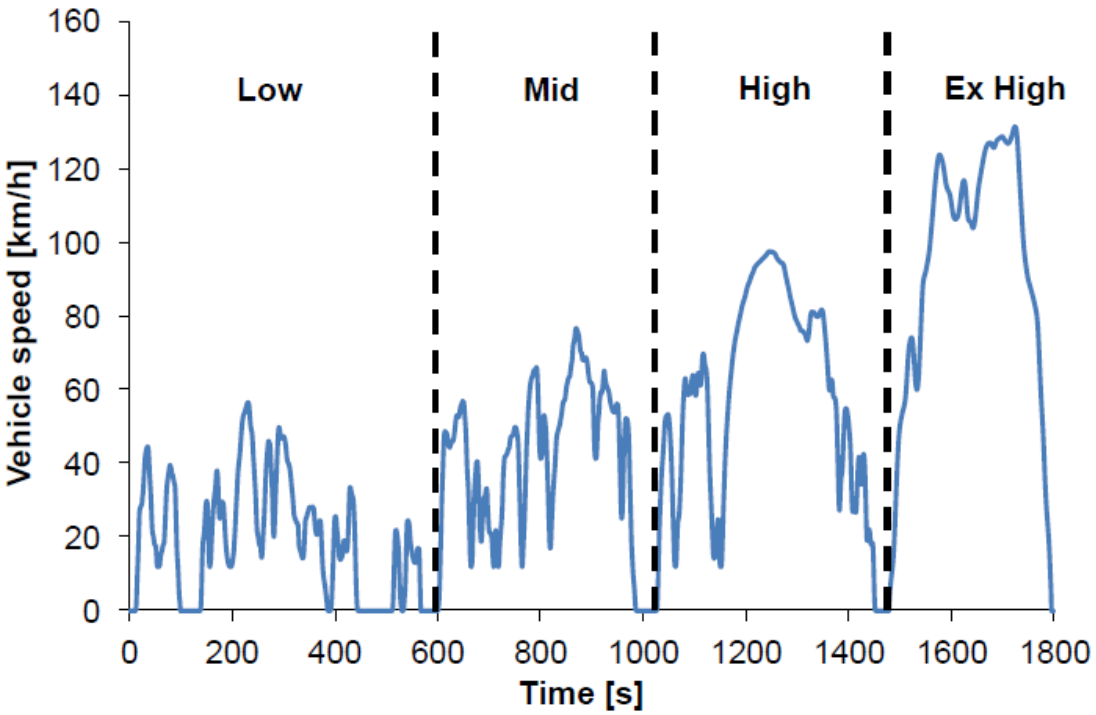

Figure 26 WLTC class 3 speed profile

WLTC	Phase	Duration	Stop duration	Distance (km)	Idling ratio	Maximum speed	Average running speed	Average total speed
Class 3	Low	589 s	156 s	3.09 km	24.8 %	56.5 km/h	25.7 km/h	18.9 km/h
	Medium	433 s	48 s	4.76 km	10.6 %	76.6 km/h	44.5 km/h	39.2 km/h
	High	455 s	31 s	7.16 km	6.4 %	97.4 km/h	60.8 km/h	56.7 km/h
	Ex-High	323 s	7 s	8.25 km	1.5 %	131.3 km/h	94.0 km/h	92.0 km/h
	WLTC	1800 s	242 s	23.27 km	12.6 %			
Class 2	Low	589 s	155 s	3.10 km	24.6 %	51.4 km/h	25.7 km/h	19.0 km/h
	Medium	433 s	48 s	4.73 km	10.6 %	74.7 km/h	44.3 km/h	39.4 km/h
	High	455 s	30 s	6.79 km	6.2 %	85.2 km/h	57.5 km/h	53.7 km/h
	Ex-High	323 s	7 s	8.01 km	1.5 %	123.1 km/h	91.4 km/h	89.4 km/h
	WLTC	1800 s	240 s	22.64 km	12.4 %			
Class 1	Low	589 s	154 s	3.33 km	24.4 %	49.1 km/h	27.6 km/h	20.4 km/h
	Medium	433 s	48 s	4.76 km	10.6 %	64.4 km/h	44.6 km/h	39.6 km/h
	WLTC	1022 s	202 s	8.09 km	18.4 %			

Table 2 Driving characteristics of the different WTLC classes [28]

Tutuianu u. a. [28] explain that when devloping the cycle it was necessary to fulfill some requirements which are contradictory like the statistical representativeness of the unified database and fulfilling the test constraints (duration, driveability and durability). With these requirements, Tutuianu u. a. [28] suggest that the WLTC has the best possible compromise as any modification of its speed profile would lead to a deterioration of any aspect.

From all the regional databases used to design the WLTC, Tutuianu u. a. [28] finds USA's database as the most dynamic one while Asia is the least dynamic, finding Europe in the middle.

3.2.2 Real Driving Emissions (RDE)

The European Comission has carried out a detailed analysis regarding emissions, based on their own and external evidences, and has deducted that the real vehicles' emissions on the road of the EURO 5 and 6 cars overcome the legal limits of the New European Driving Cycle [12]. The homologation requirements for emissions of the vehicles' engines have become harder with the introduction and revision of the Euro norms, however, the gap between homologated and real emissions is still too big and has propitiated the introduction of the RDE.

The RDE will measure emissions directly from the car while circulating on the road with a Portable Emissions Measuring System (PEMS). Then, as shown in figure 27, the test is carried out in real traffic and to end with, the data is analysed to decide whether the test has been succesfully fulfilled or not. This cycle will live together with the WLTP laboratory test and does not pretend to substitute it. It will also be the first ever introduced on-road test.

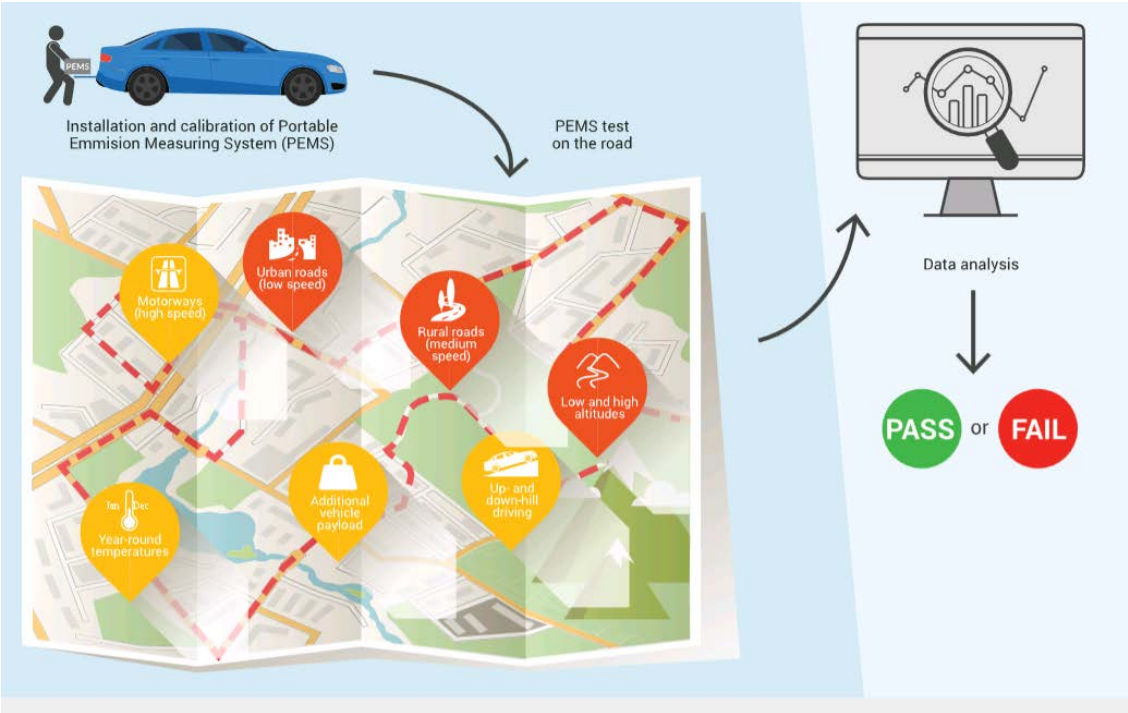

Figure 27 RDE cycle procedure [10]

The implementation will have two phases [10]

- Phase one has a conformity factor and applies from 1 September 2017 for new car models and for all from September 2019

- The second phase has no conformity factor and a lower error margin and will apply in January 2020 for new types and from January 2021 for all types

Conformity factors take into account the margin for error present in the PEMS (Portable Emissions Measuring System) as this type of systems do not present as good repeatability as emissions measuring devices located in laboratories [10].

The RDE test will be representative of the vehicles on it normal tracks and with the normal load. The test course will include approximately a 34% of the distance of urban performance, a 33% of rural and a 33% of motorway. For approximately it is understood a deviation of +/- 10% around the declared percentages. However, the urban region shall never represent less than the 29% of the total distance. The three regions are categorized according to speed:

- Urban zone v < 60 km/h
- Rural zone 60 km/h < v < 90 km/h
- Motorway v > 90 km/h

In general terms, the vehicle's speed will not be higher than 145 km/h, which may be realistic for the German "Autobahn" but is 25 km/h above the legal limits of other countries like Spain, which may be a legal conflict in the tests development. However, exceeding the legal speeds of the roads will not affect or invalidate the PEMS tests.

The average speeds for each region are also determined. For the urban sector, average speed must be between 15 and 30 km/h (including stops), which is quite a big range. Stops must be at least a 10% of the urban time and shall include some stops of 10 seconds or longer. The main speed requirements are shown in table 3

	Unit	Urban	Rural	Motorway	Notes
Speed (v)	km/h	$v \leq 60$	$60 < v$	$90 \leq v \leq 145$	$v > 100$ for at least 5 min in motorway
Distance	% of the total distance	29-44	33 ± 10	33 ± 10	
Minimum distance	km	16	16	16	
Average speed (v_{avg})	km/h	$15 \leq v_{avg} \leq 40$	-	-	
Number of stops	s	several > 10	-	-	
Maximum speed	km/h	60	90	145	
Total test time	min	Between 90 and 120			
Elevation difference	m	100			Between start and end point

Table 3 RDE test main speeds and requirements presented by Donateo u. Giovinazzi [7]

The total test time is between 90 and 120 minutes, with a minimum of 16 km in each of the three zones. This represents a huge difference against the 1180 seconds and 11.017 km of

the NEDC. The longer the test performance is, the lower is the influence in the total emissions amount of the cold-start and its share in the result. Furthermore, the RDE test limits the stops to 80 seconds.

The legislation determines that the measuring systems interfer as few as possible in the vehicle and secondary systems. For this reasons, the PEMS (Portable emissions measuring system) will have its independent battery and GPS to track the vehicle's position, altitude and speed. It is allowed to be connected to the car's ECU (Engine Control Unit) to read different values as RPM or gas throttle. Table 4 shows the different reading sources where analyser refers to the PEMS and sensors are independent devices connected to the data logger.

Parameter	**Recommended unit**	**Source**
THC Concentration	ppm	Analyser
CH4 concentration	ppm	Analyser
NMHC concentration	ppm	Analyser
CO concentration	ppm	Analyser
CO2 concentration	ppm	Analyser
NOx concentration	ppm	Analyser
PN concentration	#/m3	Analyser
Exhaust mass flow rate	kg/s	EFM
Ambient humidity	%	Sensor
Ambient temperature	K	Sensor
Ambient pressure	kPa	Sensor
Vehicle speed	km/h	Sensor, GPS or ECU
Vehicle latitude	Degree	GPS
Vehicle longitude	Degree	GPS
Vehicle altitude	M	GPS or Sensor
Exhaust gas temperature	K	Sensor

Table 4 continued from previous page

Engine coolant temperature	K	Sensor or ECU
Engine speed	rpm	Sensor or ECU
Engine torque	Nm	Sensor or ECU
Torque at driven axle	Nm	Rim torque meter
Pedal position	%	Sensor or ECU
Engine fuel flow	g/s	Sensor or ECU
Engine intake air flow	g/s	Sensor or ECU
Fault status	-	ECU
Intake air flow temperature	K	Sensor or ECU
Engine oil temperature	K	Sensor or ECU
Current gear	#	ECU
Desired gear (e.g. gear shift indicator)	#	ECU
Other vehicle data	unspecified	ECU

Table 4 Test parameters and their source as determined by European Commission [12]

The legislation does not set any PEMS as the official PEMS of the tests and each manufacturer will create their own system [10]. Against when measuring in ideal test conditions, the sampling of the representative gas at on-road tests is crucial [16]. The procedure which makes possible to withdraw a sample of the exhaust gas to measure is called Constant Volume Sampling (CVS) and a schema of the device is shown in figure 28. Iit Kanpur [16] explains that the system dilutes the exhaust gases with air which is previously filtered to reduce the possible condensation in the sampling line of hydrocarbons where the partial pressure is lower. To supply a constant flow rate to the CVS, the system is equipped with a pump or critical venturi and a heat exchanger to regulate the temperature.

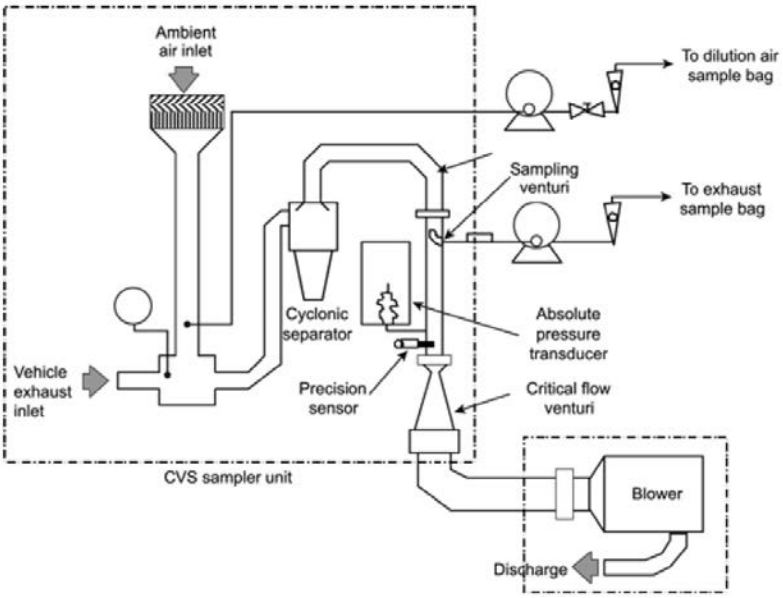

Figure 28 Schema of the CVS system with a critical flow venturi [16]

The RDE and the WLTC are not completely independent tests. When the data of the RDE test is collected, then it has to be processed in order to see if the test has been succesfully fulfilled or not. Basically, the imposed method by the european commission calculates the emissions of the RDE for the three different phases and compares the results with a tolerance window calculated from the WLTC, this means that the RDE and WLTC are coupled and not independent.

Is the RDE Test Cycle consistent?

As someone starts to think about carrying out an RDE test, many questions show up but one appears to be the main one: how can the test be repeated? Do the conditions influence the result? This is what the European Comission pursues, a real test where traffic, rain, temperature... are not controlled and are what the real final user will find on its everyday car usage. The University of Salento carried out a study to see the influence of different parameters in the final test result [7].

The RDE is a really long test which needs from a previous planning, instead of just running wherever the test driver wants. Almost a two hours test can be a waste of time when the speed ranges percentages are not met, the time paused is too long or the total paused percentage is too small. For this reason, the route has to be minutely plant. There are some computer softwares which may help institutes and organisations schedule their routes like the SUMO (Simulation of Urban Mobility), developed by the German Institute of Transportation (DLR). Users may include this script in their vehicle simulations as many other external conditions like wind or temperature.

Donateo u. Giovinazzi [7] used the SUMO software to generate routes and traffic together with openstreetmap, to simulate first the chosen routes. The routes where carefully designed and then driven as the RDE would do. After analysing all the data, the investigators reached some conclusions:

- When compared to the NEDC, the WLTC class 3 is more realistic. It covers a wider range of engine conditions and is more representative of real driving
- The RDE performed by the investigators showed higher accelerations at both lower and higher speeds when compared to the WLTC. The high accelerations at low speeds occur when the driver slows down before proceeding at intersections or stops, while at high speeds when overtaking another vehicle.
- When testing the robustness of the test with respect to traffic, lower speed values were obtained in high traffic conditions, seen during rush hours. It was seen that long idling time during rush hours clearly affects the total emissions and should be avoided. However, idling time shall be at least 10% of the total urban path time, which means that defining the urban path and test starting time are crucial in the definition of the RDE cycle.
- The investigators also tried to minimize as much as possible the distance of the test to reduce emissions. When running an optimized test route when compared to a normal one, the average speed was increased from 26.4 km/h to 28.9 km/h and the consumed fuel was decreased by a 23.5%.

Donateo u. Giovinazzi [7] determine that the RDE cycle is really sensitive to the testing route and the traffic as could be expected. The route has to be carefully designed and can make a huge impact on the final result.

3.2.3 Comparing the WLTP and the NEDC

Regarding pure technical aspects, the NEDC and WLTC differ in the cycle itself and also the way the data is aftertreated and the test is prepared. Table 5 shows the basic different characteristics of the NEDC and WLTC class 3 cycles.

	NEDC	WLTC
Distance (km)	11.023	23.262
Duration (s)	1180	1800
Idle time (s)	280	235
Phases	2	4
Average speed /w & w/o idle (km/h)	33.6 (44.7)	46.5 (53.5)
Max speed (km/h)	120.0	131.3
Max acceleration (m/s2)	1.0	1.7

Table 5 Basic characteristics of NEDC and WLTC class 3 [27]

Af first glance, it is clear that the WLTC is longer in time and length, has a higher average and maximum speed and also a higher maximal acceleration. Regarding the preparation of the vehicle for the testing and the post-test data management, both tests have also big differences. One of the main issues in the NEDC is the use of correction factors applied to the emissions measurements to account for the contribution of the different vehicle's electrical systems, a correction which is crucial nowadays due to the high penetration of micro and mild hybridization systems to modern cars [27].

Tsokolis u. a. [27] present and exhaustive comparison between both tests regarding pure technical aspects (no results comparison). The main differences will be exposed here:

- Mass, road load and driven wheels: the procedure which determines the road load (RL) or driving resistance coefficients at the NEDC presents a series of flexibilities which allow lower driving resistances to be applied. The test mass in the NEDC is determined by inertia classes are categorized into groups, which means that a quantity that is continuos in the real world is treated as discrete. On the other hand, in the WLTP, the RL coefficients are calculated from the maximum and minimum loaded masses, producing a best and worst case scenarios.
- Chassis preconditioning: Tsokolis u. a. [27] found that a preconditioning of the chassis dynamometer and the vehicle during the adjustment of the driving resistance of the dynamometer plays a non-negligible part on emissions. The resistance of the dynamometer has a component which is purely electrical, but also a component which depends on temperature (bearings, friction...). This means that a hotter dyno at the beginning may result in lower friction. Due to the longer time and distance of the WLTC, this issue has a lower impact on its results as in the NEDC.

- Gear shifting: for automatic transmissions there is no difference but for manual transmission vehicles there are differences in the procedure. In the NEDC, the gear shifting points are fixed defined without taking into account the different drivetrain configurations. In the WLTP there are some algorithms which calculate the shifting points with regard to the engine's power. The algorithms are designed to emulate the gear shifting experienced in real world driving from normal drivers.
- Temperature: in the NEDC, the soak and test temperature are set between 20 and $30°$C, while, in the WLTP, the restriction is bigger and both temperatures have to be set between 20 and $26°$C. However, the EU is planning to adopt a WLTP test with an initial test temperature of $14°$C which is closer to the European average temperature.

The improvement in measuring technologies has also been considered in he WLTC, reducing error tolerances. The NEDC allowed tolerances for some variables which have impact on emissions like, for example, the speed schedule of the driving cycle ($\pm 2km/h$ and $\pm 1second$), the dynamometer control coast-down times ($\pm 5\%$ and $\pm 10\%$), gap between measured and official CO2 values ($\pm 4\%$), temperatures, tolerances of the measurement devices... Some of these tolerances ranges have been reduced or even eliminated in some cases [20].

Comparing the WLTP with the NEDC means also studying how will the legislation change affect the fuel consumption and emissions by testing vehicles with both procedures. The International Council on Clean Transportation (ICCT) concludes that the difference between the official laboratory tests and the real-world fuel consumption and CO2 emission values was around a 7% in 2001 and has continuously increased to around 30% in 2013 [20]. As Mock u. a. [20] affirm, this huge gap between real and test emissions has many repercussions. For example, consumers spend more on fuel and vehicle manufacturers loose credibility. Also, governments are loosing taxes incomes as cars are being homologated with lower emissions than the really produce, meaning this that they pay less that would be expected (some countries include taxes to the vehicles which only depend on how much a vehicle pollutes). To end with, the world is being polluted more than we think.

The main parameters which may have impact onc the CO2 emissions and which are defined different in both cycles are shown in figure 29

Parameter	Definition in NEDC (Euro 6)	Definition in EU WLTP	To be considered for a WLTP-NEDC conversion factor?	
TEST CYCLE				
Driving cycle	NEDC	WLTC	YES	Revised driving cycle
Gear shift strategy for manual transmission vehicles	fixed gear positions	vehicle specific gear positions	YES	Part of revised driving cycle
ROAD LOAD DETERMINATION				
Tyre size and type	worst tyre (2nd worst if >3 tyres with different rolling resistances)	vehicle specific	NO	Equal demands of NEDC intention (NEDC slightly more stringent)
Tyre tread depth	>3,000 km running-in or 50%-90%	80%-100%	NO	Equal demands of NEDC intention (WLTP slightly more stringent)
Tyre pre-treatment	not defined	no heating or ageing	NO	Equal demands of NEDC intention
Tyre pressure	not defined	as specified	NO	Equal demands of NEDC intention
Wheel alignment	no definitions on adjustments of toe and camber	as production vehicle	NO	Equal demands of NEDC intention
Aerodynamics	worst bodywork, no definitions on movable parts	vehicle specific, use of movable parts as under test conditions	NO	Equal demands of NEDC intention (NEDC slightly more stringent)
Brakes	not defined	no manual adjustment	NO	Equal demands of NEDC intention
Calculation procedure	erroneous	corrected	NO	NEDC procedure deficient
Warm-up	not defined	>20 min at 118 km/h	NO	Effect on CO_2 negligible
TEST TEMPERATURES				
Soak area	20 °C-30 °C	14 °C / 23 °C	YES/NO	Effect on CO_2 negligible for 23 °C
Test cell	20 °C-30 °C	14 °C / 23 °C	YES/NO	Effect on CO_2 negligible for 23 °C
VEHICLE MASSES				
Test mass	Kerb weight + 100 kg	Kerb weight + 100 kg + extras + payload	YES	Revised definition
Inertia	discrete classes	step-less, vehicle specific	NO	On fleet average: Effect on CO_2 negligible
Rotating masses (wheels)	simulation of total inertia of the vehicle as driven on the road	+ 1.5% for 1-axle dynamometers	NO	Equal demands of NEDC intention
OTHER				
Vehicle running in	>3,000 km	3,000 km-15,000 km	NO	Effect on CO_2 negligible
Pre-conditioning cycle	diesel: 3x EUDC petrol: 1x UDC, 2x EUDC (opt., only PFI)	WLTC	NO	Effect on CO_2 negligible
Battery state of charge	not defined	no battery charging before emission test	NO	Equal demands of NEDC intention
Procedure for hybrids	not defined	not yet defined	NO	WLTP definitions to follow
Four wheel drive vehicles	1-axle dynamometer possible	2-axle dynamometer only	NO	Effect on CO_2 negligible

Figure 29 Parameters which may affect CO2 emissions and change between NEDC and WLTC [20]

The ICCT ([20]) estimates that, although there are obvious differences between both procedures, the impact on CO2 emissios results will be marginal (<1%).

From the parameters shown in figure 29, the major variations which will affect the CO2 emissions result are:

- The WLTC is a more dynamic driving cycling and includes also a more flexible gear shift strategy for manual transmissions. The fact that WLTC is longer influences how important the cold start is but not the total amount of pollutants produced as the results are studied in g/km.
- The WLTC considers a higher vehicle test mass

- At the beginning of the test, at the WLTC the engine's temperature is lower

The cold start in the WLTC is longer than in the NEDC. However, the longer the cycle is, the lower the impact of the cold start in the global test result. The ICCT [20] estimates the cold start contribution to the total emissions in the WLTC only about half of the added cold start contribution in the NEDC. The NEDC sets the test temperature between 20 and 30°, while the WLTP sets a temperature of 23 $\pm 5°$. The influence of ambient temperaure is quite important as it affects importantly the cold start transient

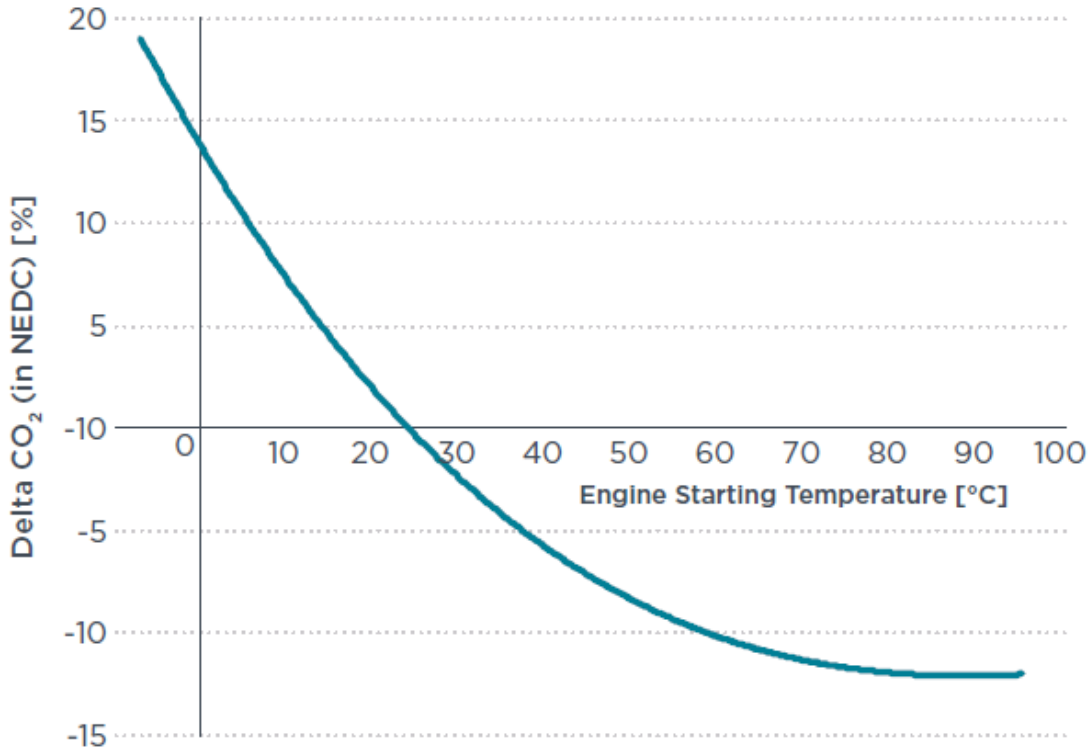

Figure 30 Impact of engine starting temperature on CO2 emissiosn related to 23C [20]

Start-stop systems, which turn off the engine when the vehicle is stopped, will produce less benefits in the WLTC as the total stop phase rate is 12% against the 23.7% in the NEDC [20].

To nummerically show the differences between both tests, four different studies will be presented, which compare the WLTC and NEDC emission results. Three of them are presented by Mock u. a. [20] while the fourth one was carried out by the BOSMAL institute in Poland [1]

- Analysis with the Ricardo DVT Vehicle Simulation Software
- Analysis with the AVL Vehicle Simulation Software
- ADAC (Germany) EcoTest Program. Vehicle simulations with the NEDC and WLTC

- BOSMAL Insitute Analysis

Ricardo DVT Analysis

Ricardo Inc. is an engineering company which developed a simulation model to simulate CO2 emissions for predefined driving cycles and vehicles. This software is used in [20] to simulate different cycles with different vehicles configurations from all types of car segments. The results are summarized in 31 and 32, where WNQ is the WLTC-NEDC-Quotient, calculated as:

$$WNQ = \frac{CO_2WLTC[\frac{g}{km}]}{CO_2NEDC[\frac{g}{km}]} \tag{3.1}$$

Segment	Fuel	Engine	DI	AT	SS+	ADV	HEV	WNQ
small (B)	petrol	1.5l, 82 kW		X				**0.95**
small (B)	petrol	1.5l, 82 kW		X	X			**1.04**
small (B)	petrol	0.7l, 72 kW	X	X	X	X		**1.14**
small (B)	petrol	0.6l, 59 kW	X	X		X	X	**1.16**
small (B)	diesel	1.2l, 59 kW	X	X				**0.95**
small (B)	diesel	1.2l, 59 kW	X	X	X			**1.04**
small (B)	diesel	1.1l, 69 kW	X	X	X	X		**1.04**
medium (C)	petrol	2.0l, 88 kW		X				**0.93**
medium (C)	petrol	2.0l, 86 kW		X	X			**0.96**
medium (C)	petrol	0.8l, 76 kW	X	X	X			**1.12**
medium (C)	petrol	0.6l, 62 kW	X	X		X	X	**1.12**
medium (C)	diesel	1.6l, 97 kW	X	X				**0.98**
medium (C)	diesel	1.6l, 75 kW	X	X	X			**1.01**
medium (C)	diesel	1.3l, 77 kW	X	X	X	X		**1.00**
large (D)	petrol	2.4l, 118 kW		X				**0.90**
large (D)	petrol	2.4l, 118 kW		X	X			**0.98**
large (D)	petrol	1.0l, 101 kW	X	X	X	X		**1.10**
large (D)	petrol	0.8l, 83 kW	X	X		X	X	**1.11**
large (D)	diesel	2.0l, 122 kW	X	X				**0.89**
large (D)	diesel	2.0l, 122 kW	X	X	X			**1.03**
large (D)	diesel	1.7l, 105 kW	X	X	X	X		**0.99**
SUV (J)	petrol	2.4l, 128 kW		X				**0.94**
SUV (J)	petrol	2.4l, 128 kW		X	X			**1.00**
SUV (J)	petrol	1.1l, 110 kW	X	X	X	X		**1.13**
SUV (J)	petrol	0.9l, 90 kW	X	X		X	X	**1.13**
SUV (J)	diesel	2.2l, 131 kW	X	X				**0.90**
SUV (J)	diesel	2.2l, 131 kW	X	X	X			**1.02**
SUV (J)	diesel	1.8l, 109 kW	X	X	X	X		**1.02**

DI = direct injection; SS+ = stop-start + improved alternator + regenerative braking; AT = automatic transmission; ADV = advanced 2020/2025 technology package; HEV = hybrid electric vehicle;

Figure 31 Different tests and results obtained in the NEDC-WLTC comparison with Ricardo DVT [20]

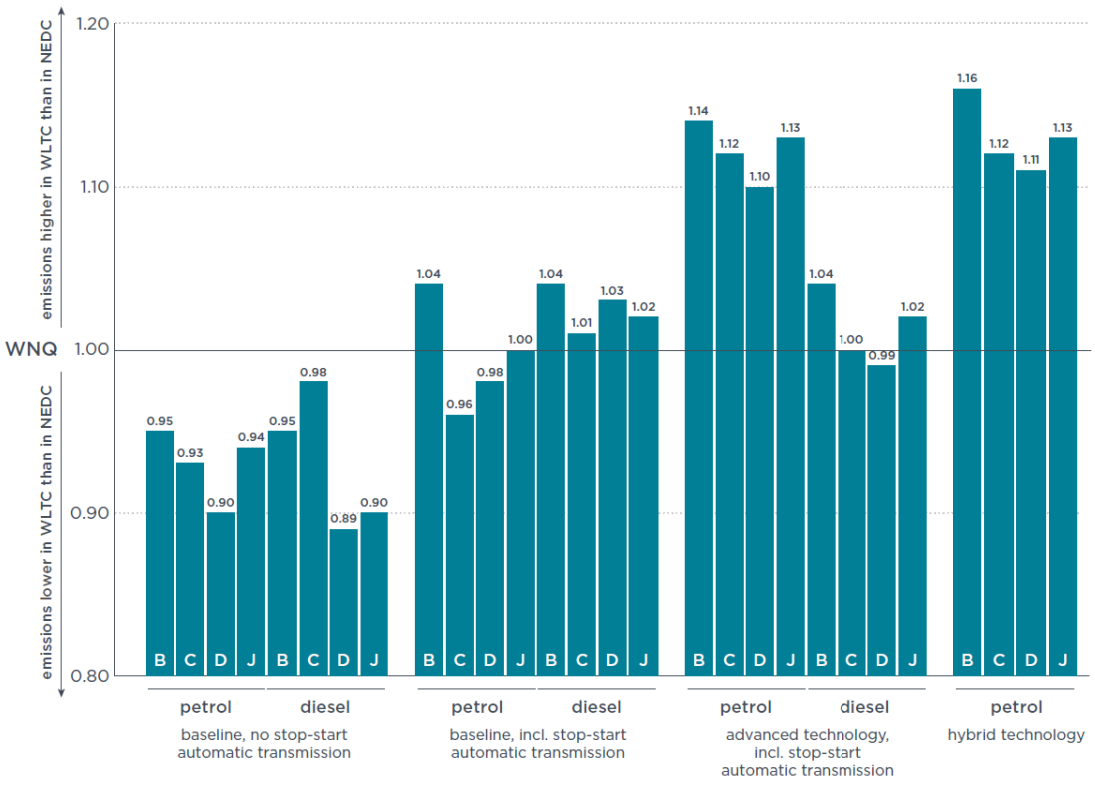

Figure 32 Different tests and results obtained in the NEDC-WLTC comparison with Ricardo DVT [20]

As it can be seen, the deviations are not really significant, around a $\pm 10\%$ in the worst cases. The main conclusions which Mock u. a. [20] deduct from these simulations are:

- The Non-hybrid vehicles with conventional technologies have lower CO2 emissions in the WLTC than in the NEDC, probably because of a higher stop phase rate
- Vehicles which make use of a start-stop system, a basic braking energy recuperation system and an advanced alternator show abut the same CO2 levels for both cycles
- More advanced engines, like the downsized or hybrid ones, show in general terms a 10% higher emissions in the WLTC than in the NEDC
- Cars with automatic transmissions tend to have a higher WNQ than manual transmission ones
- The worst case scenario, the type of car which is worstly affected by the WLTC are the downsized engines with automatic transmissions.

AVL Simulation Analysis

Using a similar program to the previous one, the paper analyzes the C-segment, which is the most popular in Europe. The results shown in figure 33 confirm the previous one obtained

with Ricardo.

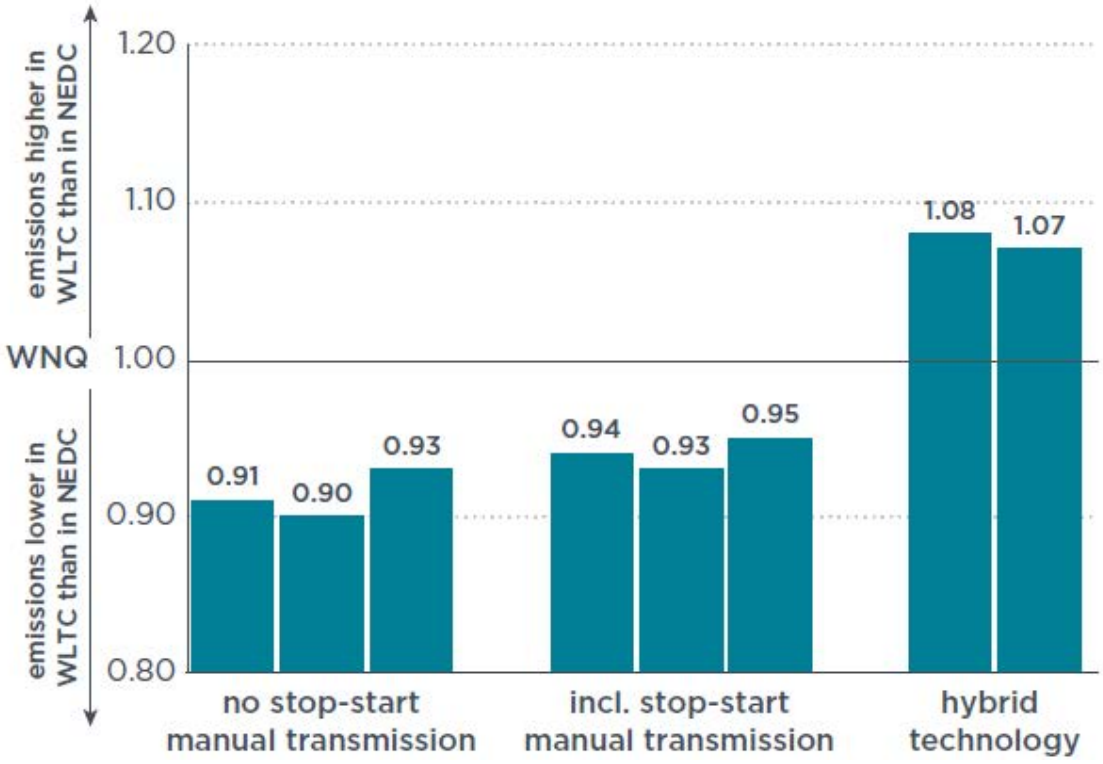

Figure 33 Different tests and results obtained in the NEDC-WLTC comparison with AVL carried out by Mock u. a. [20]

Manual transmissions have better results in WLTP than in NEDC, against automatic transmissions, as the new cycle fixes the shifting points, resulting in higher average engine speeds.

ADAC Tests

The german compay ADAC (Allgemeiner Deutscher Automobil Club), tested 378 passenger cars between October 2011 and July 2014 and figure 34 presents the results of this study. As the ADAC tests were carried out with todays cars, it represents a good result for todays standards but does not allow precise projections for the future. However, these results confirm the Ricardo and AVL simulation results.

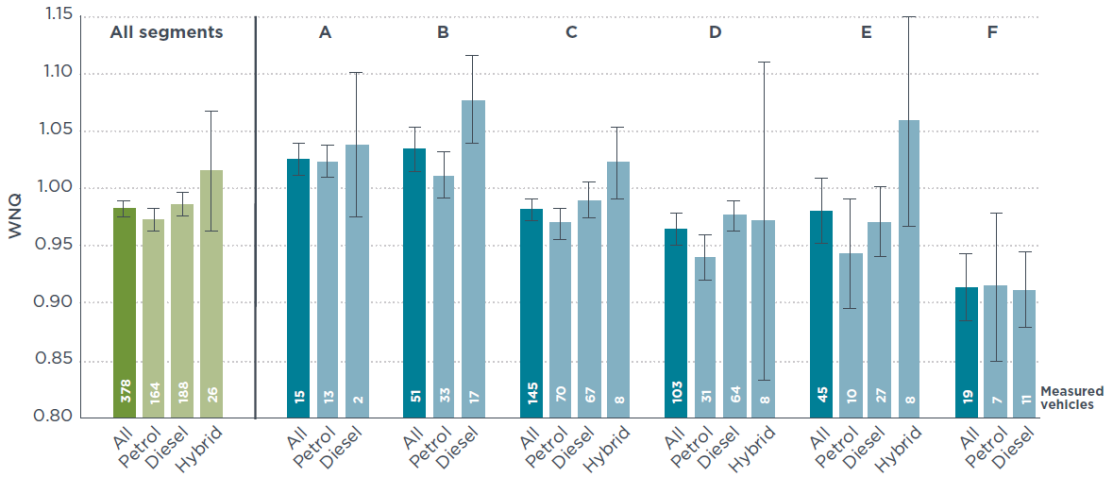

Figure 34 ADAC Test results averages where error bars represent 95% confidence intervals [20]

BOSMAL Institute Analysis

The BOSMAL Automotive Research and Development Institute, has compared both cycles, reaching the conclusion that with identical test conditions, the emission results from NEDC and WLTP were numerically similar, with a mean deviation of 1.6% for SI engines, and even there were vehicles which emitted more CO2 emissions in the NEDC [1].

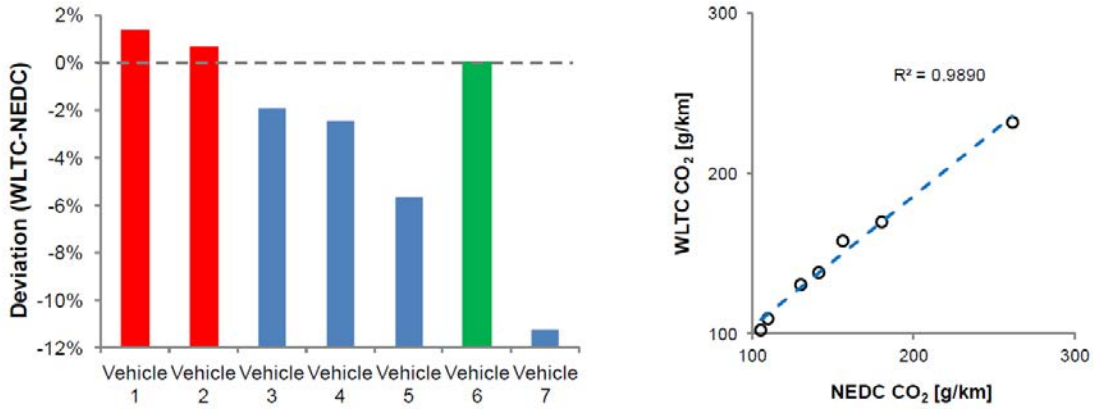

Figure 35 (1) Deviations in the CO2 emissions tests for 7 different cars between NEDC and WLTC. (2) Scatterplot NEDC-WLTC. [1]

The conclusions reached by BOSMAL according to the new cycle are:

- WLTC is well designed and a good tool to determine CO2 emissions
- WLTC shows a good test-to-test repeatability
- The greatest changes between tests are the test itself and the gear usage stipulations

- There is a slight tendency for the WLTC to produce lower CO2 emissions results, however, not in all cases.
- Interesting is the fact that in some cases the WLTC results show less CO2 emisssions when compared to the NEDC. This would mean that if the NEDC has a big difference with real world emissions, the WLTC would have a bigger gap which means that the test is less accurate.

4. Measurements and calculation methodology

4.1 The Mexa Measuring System

The Mexa 7170 is the system used at the test bench, in order to measure pollutant emissions. The measuring device is connected to the exhaust system through a magnetic valve, capable to switch between raw emissions (direct after the engine and before the pre-catalyst) or real emissions which would go into the atmosphere (after the main catalyst).

The MEXA-7170HEGR gives as a result the corresponding concentration of some pollutant in ppm or volume percentage, depending on the considered species. Table 6 shows the Mexa characteristics:

Component	Range	Model	Principle	Line
ECO2	0-0.5∼20 vol%	AIA-722	NDIR	EGR
CO(H)	0-0.5∼12 vol%	AIA-722	NDIR	DIRECT
CO2	0-0.5∼20 vol%	AIA-722	NDIR	DIRECT
CO(L)	0-50∼5000 ppm	AIA-721A	NDIR	DIRECT
O2	0-1∼25 ppm	MPA-720	Magnetic	DIRECT
NOx	0-1∼25 ppm	CLA-750A	Vac. CLD	DIRECT
THC	0-5∼200, 500∼15000 ppm	FIA-726D	H. FID	DIRECT

Table 6 MEXA-7170HEGR Characteristics [15]

The MEXA unit has three different systems to measure emissions: NDIR (Non-Dispersive Infra-Red Detector), Magnetic, Vac. CLD (Chemi-Luminiscence Detection) and H.FID (Flame Ionisation Detection).

4.1.1 The Non-Dispersive Infrared Detection method (NDIR)

The Non-Dispersive Infrared Detection is one of the most standarized methods to measure CO and CO2 concentrations. The method takes advantage from the fact that all gases which are in a sample will absorb some infra red emissions at a particular frequency. The system first shines an infra-red beam through a sample cell which would contain CO or CO2 from the calibration bottles, which have an already known concentration. Secondly, the sample of the engine's emissions will also be shined and the NDIR detector will be able to measure the

volumetric concentration [2].

Figure 4.6 shows an schema of the system and its components. The chopper wheel or spinning filter is disposed to correct the offset and gain of the analyser, allowing a single sampling head to measure the concentrations of two different gases without the necessity of two different measuring devices, this means that just one sensor measures both CO and CO2 emissions [2].

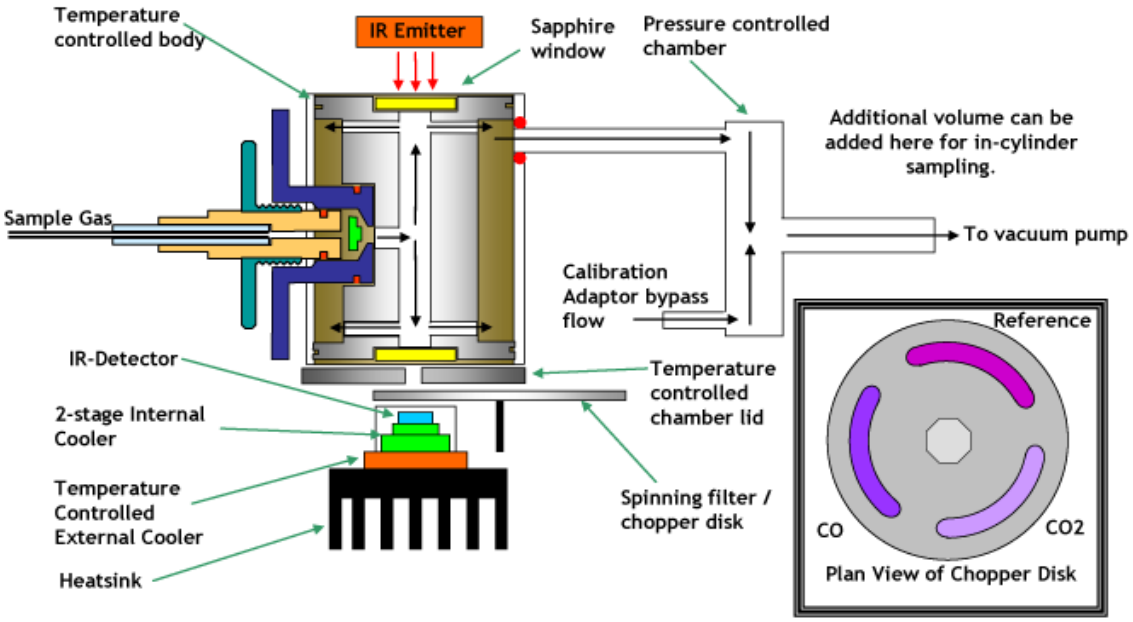

Figure 36 Basic schema of the NDIR Emissions measuring method [2]

4.1.2 The Flame Ionisation Detection Method (FID)

The flame ionisation detection method is standarized in the automotive industry to measure hydrocarbon concentration. It is interesting to denote that the MEXA result for hydrocarbon give a concentration of THC Total hydrocarbons, which is the sume of all the elements which contain hydrogen and carbon. However, it is not possible to know the real concentration of each element [2].

Some of the most known hydrocarbon compounds are, for example, Methane (CH4), Propane (C3H8) or Butane (C4H10). However, in petrol, the main hydrocarbons are the ones which have elements with eight carbon atoms. Some of the most common hydrocarbons and their uses are shown in table 7 [2].

Element	Number of Carbon Atoms	Uses
Methane	1	Fuel in electrical generation. Produces least about of carbon,dioxide.
Ethane	2	Used in the production of ethylene, which,is utilized in various chemical applications.
Propane	3	Generally used for heating and cooking
Butane	4	Generally used in lighters and in aerosol cans
Pentane	5	Can be used as solvents in the laboratory and in the production of,polystyrene.
Hexane	6	Used to produce in glue for shoes, leather,products, and in roofing
Heptane	7	The major component of gasoline
Octane	8	An additive to gasoline that reduces knock, particularly in its,branched forms
Nonane	9	The component of fuel, particularly diesel
Decane	10	A component of gasoline, but generally,more important in jet fuel and diesel

Table 7 Main common hydrocarbons and their uses [22]

In the FID, the sample gas is introduced into a hydrogen flame inside the FID. The burning of any hydrocarbons present in the sample will produce ions which will be proportional to the rate of ionisation, which depends on he concentration of HC in the gas. Normally, conventional FIDs have an small amount of lag in the measurements refreshing, which is due to sample handling as the ionisation process is, in fact, really quick [3]. Figure 4.7 shows an schema of the system, where the sample gas goes through the pipe at the bottom of the image and goes up by capillarity to the combustion chamber. Together with a fuel gas and air, the sample is burnt and the ion collectors measures the resulting ions.

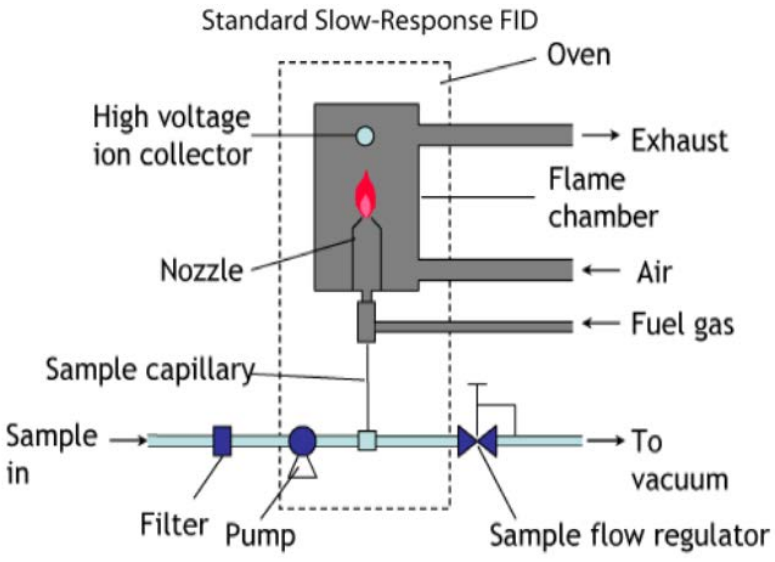

Figure 37 Basic schema of the FID Emissions measuring method [3]

4.1.3 The Chemi-luminiscence detector (CLD) Method

Regarding the NOx emissions, the industry's standard method is the chemi-luminescence, also known as CLD.

The procedure takes advantage of the chemiluminescence reaction which occurs between NO and O3 (Ozone) and which has the property of emitting light. This reaction is the basis for the CLD, where the photons which have been produced in the reaction are detected by a photo multiplier tube (PMT). The system will output a voltage which is proportional to the NO concentration.

As the chemiluminescence reaction is really fast, the sample handling has to be also really quick [4]. A schema of the device is shown in figure 38

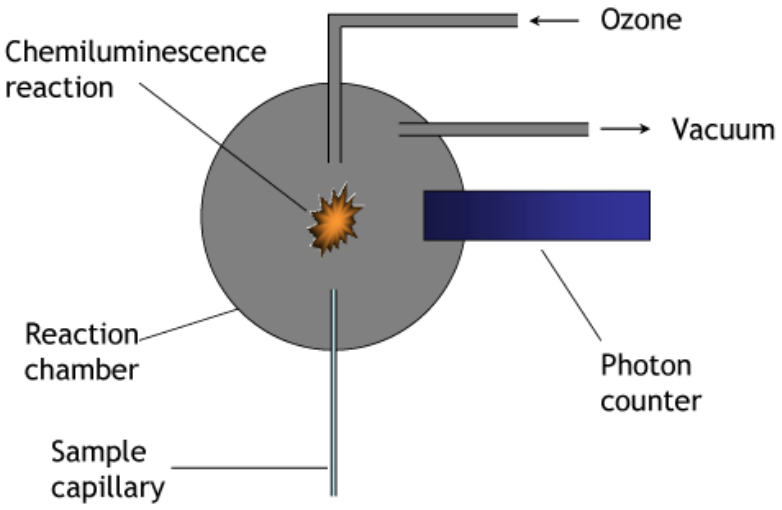

Figure 38 Basic schema of the CLD Emissions measuring method [4]

4.2 Humidity calculation and conversion

As it will later be shown, it is necessary to calculate the humidity present in the atmospherical air in grammes of vapor per kilogramme of air. The humidity sensor measures relative humidity, which is defined as the quotient of the water vapour pressure to the saturation water vapour pressure (over water) at the gas temperature [29]:

$$RH = \frac{P_w}{P_{ws}} \cdot 100\% \tag{4.1}$$

In order to determine the vapour pressure from the previous equation, it is necessary to calculate the water vapour saturation pressure. This can be done with accuracy with psychrometers, but for future simulations it is necessary to program an script forcing the use of an

	A	m	Tn	Max error	Temperature range
Water	6.116441	7.591386	240.7263	0.083%	-20...+50C
	6.004918	7.337936	229.3975	0.017%	+50...+100C
	5.856548	7.27731	225.1033	0.003%	+100...+150C
	6.002859	7.290361	227.1704	0.007%	+150...+200C
	9.980622	7.388931	263.1239	0.395%	+20...+350C
	6.089613	7.33502	230.3921	0.368%	0...+200C
Ice	6.114742	9.778707	273.1466	0.052%	-70...0C

Table 8 Constants for the water vapour saturation calculation [29]

equation. With a lower accuracy, the equation which represents the water vapour saturation pressure is [29]:

$$P_{ws} = A \cdot 10^{(\frac{m \cdot T}{T + T_n})} [hPa] \tag{4.2}$$

where A, m and T_n can be found in table 8 and T is the temperature in degrees centigrade.

It is possible to calculate the absolute humidity from the vapour pressure as Vaisala Oyj [29] shows:

$$A = C \cdot \frac{P_w}{T} [g/m^3] \tag{4.3}$$

where:

- C = Constant 2.16679 kg/J
- P_w = Vapour pressure in Pa
- T = Temperature in K

For the last step, it is needed to convert the concentration in g/m^3 to g/kg through the air density which can be calculated as:

$$\rho = \frac{p}{R \cdot T} \tag{4.4}$$

where:

- p = absolute pressure in Pa
- T = absolute temperature in K
- R = specific gas constant for dry air which is 287.058 $J/(kg \cdot K$

4.3 Dry-wet Emissions conversion

The Mexa system refers some of its results in volume percentage of dry air, when the reality is that there is a component of water vapor in the air. The emissions rate in kg/s of the different pollutants will be calculated as:

$$\dot{m}_{Pollutant} = \dot{m}_{ExhaustGases} \cdot w_{Pollutant} \tag{4.5}$$

Where w represents the mass fraction of the pollutant in dry base.

In order to trasform from dry to wet base, it is necessary to calculate the amount of water vapor in the exhaust gases. The humidity is only known for the intake air, as it is the same humidity as the environment. The water amount in the exhaust could be known by adding the water which results from the combustion and the water from the ambient air in the intake.

However, combustions are incredibly difficult reactions which consists in hundreds of small reactions which may occur fully or only partially. Because of this, estimating the water produced or consumed in the combustion chamber, without the used of GT-Suite or any other simulation programme is a difficult task. For this reason, the assumed procedure will be the explained at the Real Driving Emissions test regulation, published by the European Commission [12] in March 2016.

The "dry-wet correction" is carefully explained with a group of equations which include some other parameters, as the measured CO2 or CO concentrations. It is assumed that the disposed correction is effective and returns accurate results. Although it were inaccurate, it is still a simple and easy way to correct the mass flow and concentrations, as well as it is the same procedure and will have the same accuracy when running the RDE cycle.

The basic correction equation is 4.6, which shows:

$$c_{wet} = k_w \cdot c_{dry} \tag{4.6}$$

where:

- c_{wet} is the wet concentration of a pollutant in ppm or per cent volume
- c_{dry} is the dry concentration of a pollutant in ppm or per cent volume
- k_w is the dry-wet correction factor

In order to calculate k_w, it is necessary to use formula 4.7:

$$k_w = (\frac{1}{1 + a \times 0.005 \times (c_{CO_2} + c_{CO})}) \times 1.008 - k_{w1}) \tag{4.7}$$

where:

$$k_{w1} = (\frac{1.608 \times H_a}{1000 + (1.608 \times H_a)}) \tag{4.8}$$

where:

- H_a is the intake air humidity in grams of water per kilogramme of dry air
- c_{CO_2} is the dry CO2 concentration in volume percentage
- C_{CO} is the dry CO concentration in volume percentage
- a is the molar hydrogen ratio

European Commission [12] explain in the RDE legislation that the NO_x emissions shall not be corrected for ambient temperature and humidity.

4.4 Emissions rate calculation

After the emissions have been converted to wet basis from the dry one, it is important to calculate the mass flow of the exhaust gases.The exhaust mass flow will result from adding the intake air mass flow and the fuel mass flow as follows [12]:

$$q_{mew,i} = q_{maw,i} + q_{mf,i} \tag{4.9}$$

where each term corresponds to:

- $q_{mew,i}$ is the instant exhaust mass flow rate in [kg/s] or [kg/h]

- $q_{maw,i}$ is the instant intake air mass flow rate in [kg/s] or [kg/h]
- $q_{mf,i}$ is the instant fuel mass flow rate in [kg/s] o [kg/h]

However, it is also interesting the possibility that the European Comission presents at [12] as an alternative method to calculate the instantaneous exhaust mass flow rate from the air mass flow rate and the air-to-fuel ratio. It would be calculated as:

$$q_{mew,i} = q_{maw,i} \times (1 + \frac{1}{A/F_{st} \times \lambda_i}) \tag{4.10}$$

where:

$$A/F_{st} = \frac{138.0 \times (1 + \frac{\alpha}{4} - \frac{\epsilon}{2} + \gamma)}{12.011 + 1.008 \times \alpha + 15.9994 \times \epsilon + 14.0067 \times \sigma + 32.0675 \times \gamma} \tag{4.11}$$

and

$$\lambda_i = \frac{T \qquad + Q \times S}{4.764 \times (1 + \frac{\alpha}{4} - \frac{\epsilon}{2} + \gamma) \times (c_{CO_2} + c_{CO} \times 10^{-4} + c_{HC_w} \times 10^{-4})} \tag{4.12}$$

where:

$$T = (100 - \frac{c_{CO} \times 10^{-4}}{2} - c_{HC_w} \times 10^{-4}) \tag{4.13}$$

$$Q = (\frac{\alpha}{4} \times \frac{1 - \frac{2 \times c_{CO} \times 10^{-4}}{3.5 \times c_{CO_2}}}{1 + \frac{c_{CO} \times 10^{-4}}{3.5 \times c_{CO_2}}} - \frac{\epsilon}{2} - \frac{\sigma}{2}) \tag{4.14}$$

$$S = (c_{CO_2} + c_{CO} \times 10^{-4}) \tag{4.15}$$

and each of the terms corresponds to :

- $q_{maw,i}$: Instant intake air mass flow rate in [kg/s]
- A/F_{st}: The stoichiometric air-to-fuel ratio in [kg/kg]
- λ_i: The instantaneous excess air ratio

- c_{CO_2}: Dry CO_2 concentration in percentage
- c_{CO}: Dry CO concentration in [ppm]
- c_{HC_w}: Wet HC concentration in [ppm]
- α: Molar hydrogen ratio (H/C)
- β: Molar carbon ratio (C/C)
- γ: Molar sulphur ratio (S/C)
- σ: Molar nirogen ratio (N/C)
- ϵ: Molar oxygen ratio (O/C)

This coefficients refer to a fuel with the form $C_\beta H_\alpha O_\epsilon N_\sigma S_\gamma$ with $\beta = 1$ for carbon-based fuels. As the document ensures, the concentration of HC emissions is typically low and may be ommited for the calculation of λ_i [12] [12].

Once all the previous steps have been followed, it is time to determine the instantaneous mass emissions, also explained at [12]. The mass emissions in [g/s] will be calculated by multiplying the instantaneous concentration of the considered pollutant [ppm] and the instantaneous exhaust mass flow rate [kg/s]. So, the final equation will look like [12]:

$$m_{gas,i} = u_{gas} \cdot c_{gas,i} \cdot q_{mew,i} \tag{4.16}$$

where each term is defined as:

- $m_{gas,i}$ Mass flow of the studied gas species, for example CO, NO... in [g/s]
- u_{gas} Ratio between the studied gas species and the overall density of the exhaust gases. This parameter is tabulated and shown in 9.
- $c_{gas,i}$ Measured exhaust mass flow rate or calculated one as previously shown.
- $q_{mew,i}$ Mass flow of the exhaust gases

Attending to the low accuracy of the mass flow sensor in the inlet of the engine at the test bench, it has been preferred to calculate the exhaust mass flow from the fuel mass flow and air-to-fuel ratio. This equation is also displayed at the European Commission regulation [12] and can be used in the Real Driving Emissions tests.

$$q_{mew,i} = q_{mf,i} \times (1 + A/F_{st} \times \lambda_i) \tag{4.17}$$

where:

- $q_{mew,i}$ is the instantaneous exhaust mass flow rate in expressed [kg/s]
- $q_{mf,i}$ is the instantaneous fuel mass flow rate expressed in [kg/s]
- A/F_{st} is the stoichiometric air-to-fuel ratio expressed in [kg/kg]

Table 9 shows the values of the parameter u_gas which is the relationship between the density of a determined pollutant and the density of the exhaust gases for different fuels. This ratio converts the volume concentration of the pollutant in the previous equations to mass concentration and also has the corresponding units conversions to have units coherence [12].

Fuel	$\rho_e[kg/m^3]$	Component or pollutant i					
		NOx	CO	HC	CO2	O2	CH4
		$\rho_{gas}[kg/m^3]$					
		2,053	1,250	Depends on fuel	1,9636	1,4277	0,716
		u_{gas}					
Diesel (B7)	1,2943	0,001586	0,000966	0,000482	0,001517	0,001103	0,000553
Ethanol (ED95)	1,2768	0,001609	0,000980	0,000780	0,001539	0,001119	0,000561
CNG	1,2661	0,001621	0,000987	0,000528	0,001551	0,001128	0,000565
Propane	1,2805	0,001603	0,000976	0,000512	0,001533	0,001115	0,000559
Butane	1,2832	0,001600	0,000974	0,000505	0,001530	0,001113	0,000558
LPG	1,2811	0,001602	0,000976	0,000510	0,001533	0,001115	0,000559
Petrol (E10)	1,2931	0,001587	0,000966	0,000499	0,001518	0,001104	0,000553
Ethanol (E85)	1,2797	0,001604	0,000977	0,000730	0,001534	0,001116	0,000559

Table 9 Raw exhaust gas u values depicting the ratio between the densities of exhaust component or pollutant [km/m^3] and the density of the exhaust gas [kg/m^3]. Extracted from [12]

5. Emissions experimental analysis with the V1 Exhaust System of the SCE

5.1 The V1 Exhaust System

The V1 Exhaust System is the aftertreatment system configuration which was built for the tests. The system is composed mainly by two different catalysts: a precatalyst and a main catalyst. The first one is considerably smaller than the main one and located after the turbine. Being so near to the engine is benefitial for the warm-up periods. In this configuration, only the primary engine was tested. Figure 39 shows a CATIA model of the exhaust system at the test bench, where the precatalyst is marked with number 2 and the main catalyst with number 3.

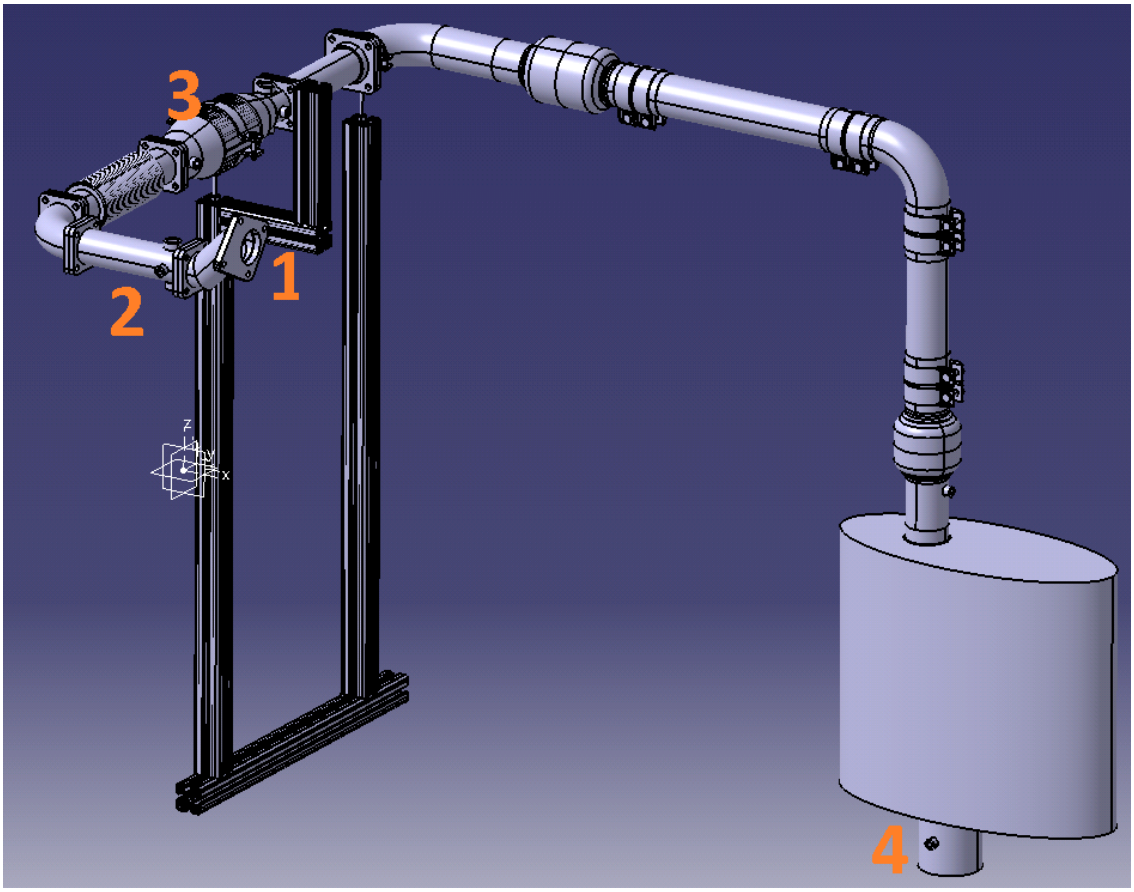

Figure 39 The V1 Exhaust System. 1) Inlet 2) Precatalyst 3) Main Catalyst 4) Outlet

Figure 40 is a photograph of the test bench with both catalysts being marked.

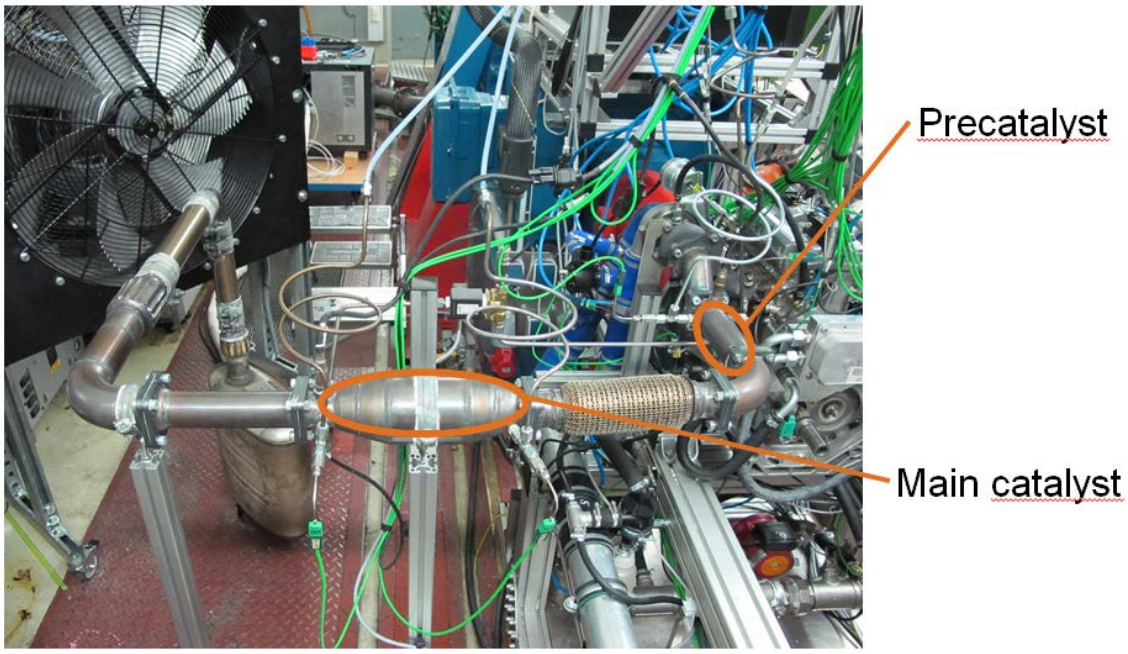

Figure 40 Photograph of the test bench

5.2 Application of the Primary Engine

Engine application refers to the different strategies which have to be decided in order to control the engine. In this concrete case, the application of many parameters, like the fuel injection which controlled that lambda = 1. However, in order to build the emissions maps of the primary engine it was necessary to decide how the torque would be controlled, as it can be regulated through the waste gate or the throttle valve. Also, it was necessary to decide how the working area of the engine was going to be grided in order to fully cover all the possible scenarios.

To begin with, it was necessary to decide how the torque would be regulated, as there are two different parameters: the throttle valve position and the waste gate opening. The decission taken was regulating the torque through the throttle valve until it no longer has an influence on the output torque and then opening it linearily until its maximum being reached at the maximum torque of the determined engine speed and closing the waste gate to obtain the desired torque.

In order the find the point where the throttle valve no longer has an influence on the torque, the motor was driven dragged, without firing nor injecting, in order to study the influence of the opening angle of the throttle valve in the aspirated air mass flow. The engine was driven from 1000 rpm to 6000 rpm in 1000 rpm steps and, in each of the cases, the throttle valve was opened from its minimum to its maximum. Figure 41 shows for each engine speed, the throttle valve position which results in the 80% and 90% of the maximum air flow for the

determined position.

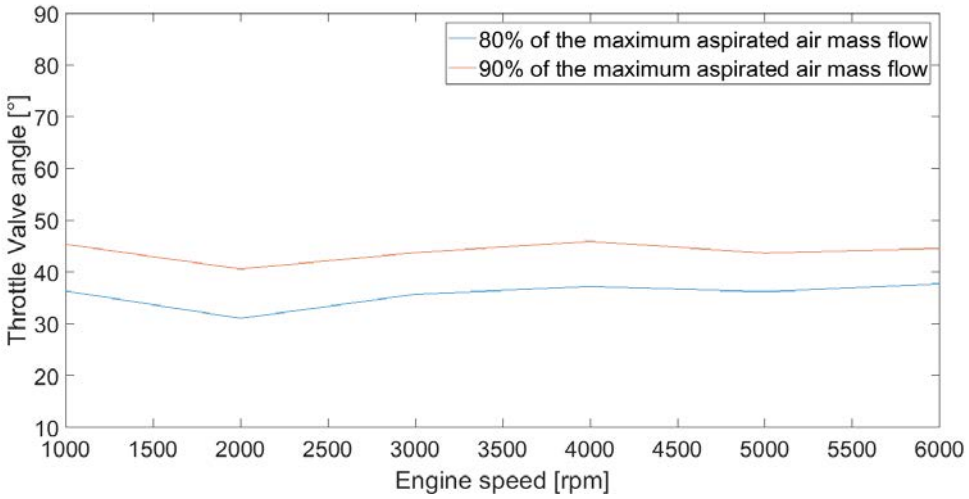

Figure 41 Influence of the throttle valve in the aspirated air mass flow

As it can be seen, the throttle valve has a little influence in the output torque after $45°$. For this reason, the decision meant regulating the torque with the throttle valve until it was opened $45°$ and then, opening it linearly and regulating the torque with the waste gate.

Regarding other parameters, the injection point was $0°$ BTDC in the region where the torque is regulated through the throttle valve and then, it was seen in the test bench, that the results were better with an injection point of $360°$ BTDC. The combustion peak was always set to $-12°$ and regulated by the ignition timing, as it produced the best results, lowering emissions, fuel consumption and resulting in a reasonable smooth running. However, when approaching to torques near 0 Nm, an ignition time of $-12°$ presents a poor smoothness, so it has to be manually adapted in these points. To end with, the lambda has to be theoretically equal to 1, in order to let the catalytic converters work in perfect conditions. However, it was manually adjusted for every measured point in order to improve global emissions, taking into account the relationships of the maximum allowed quantities of each pollutants, being the limit of CO emissions ten times greater for CO thand HC, and for HC around double than for NOx. Figure 42 shows an schema of the application strategy.

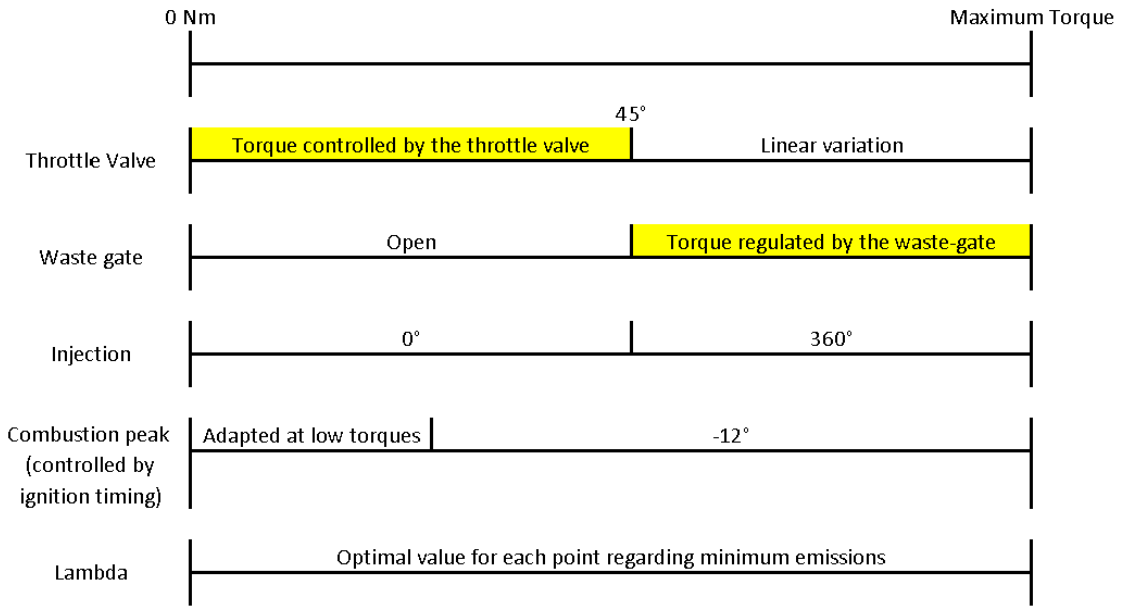

Figure 42 Application strategy for the primary engine

5.3 Measured Emission maps and torque grid

The emissions maps are depicted in 3D plots which show the emissions produced (raw emissions direct after the engine or after the catalytic converters) with respect to the engine speed and torque. This last variable, torque, can either be represented as effective torque in Nm or as a mean pressure like the mean indicated pressure (pmi) which is expresed in bar.

Theoretically, the engine can work in engine speeds up to 7000 rpm and torques around 110 Nm at its maximum torque point. However, the engine was tested from 1000 rpm to 6000 rpm.

In order to build the different emissions maps, it was necessary to measure different points and then interpolate the corresponding surface with MATLAB. A total of 66 points were measured, which corresponded to 11 different torques for each engine speed, with a total of 6 different engine speeds from 1000 rpm to 6000 rpm in steps of 1000 rpm. Although the engine may work at speeds lower than 1000rpm, it was assumed that the idle point was not that low and was considered at 1000 rpm.

For each engine speed, it was first measured the maximum torque which the engine could produce by regulating the boost pressure with the throttle valve fully open. It has to be taken into account that the lambda values had to be always around 1 in order to measure an emissions-optimum point, resulting in lambda values around 1.013 as setpoint in the test bench.

Figure 43 shows the 66 measured points, where the points with a coloured background are those where the torque is being regulated through the waste gate and those with a white background are being regulated by the throttle valve.

	Torque [Nm]					
100%	50	67	90	77	63	47
90%	45	60,3	81	69,3	56,7	42,3
80%	40	53,6	72	61,6	50,4	37,6
70%	35	46,9	63	53,9	44,1	32,9
60%	30	40,2	54	46,2	37,8	28,2
50%	25	33,5	45	38,5	31,5	23,5
40%	20	26,8	36	30,8	25,2	18,8
30%	15	20,1	27	23,1	18,9	14,1
20%	10	13,4	18	15,4	12,6	9,4
10%	5	6,7	9	7,7	6,3	4,7
Idle Speed	0	0	0	0	0	0
45° Throttle valve, WG Open	47	52	55	50	57,5	X
	1000	2000	3000	4000	5000	6000
	Engine speed in rpm					

Figure 43 Points measured to build the engine emissions maps

As it can be clearly seen, the maximum output torque is 90 Nm at 3000 rpm. The limitant factor of the highest torque is not the maximum boost pressure but the exhaust temperature when engine speeds are higher than 3000 rpm. As it has been previously explained, temperatures of the catalytic converter over 1050°C may lead to deactivation or, even worse, physical internal damages of the catalyst. In the case of the primary engine, the maximum temperature measured before the pre-catalytic converter was considered around 880°C, not increasing the boost pressure to obtain higher torques when these temperatures are reached. Having 880°C before the precatalyst when running at lambda = 1 values means that the temperature inside the precatalytic converter is increased due to the oxidizing reactions. However, having 880°C before the the precatalyst when running with rich mixtures would be no problem as the number of pollutants being oxidized would diminish.

Figure 44 shows how the precatalytic converter was damaged due to the high temperatures which lead it become completely incandescent when working at the highest torques and engine speeds.

Figure 44 Damages in the pre-catalytic converter due to the high temperatures

All the previously shown points were measured twice, for emissions before and after both catalytic converters as the system cannot measure both points at the same time. The emissions were converted to a wet basis as previously explained and then fitted in MATLAB with a thin plate interpolation, which is a spline-based interpolation method, producing smooth interpolations of the given data. It is a method analogous to cubic splines but in three dimensions.

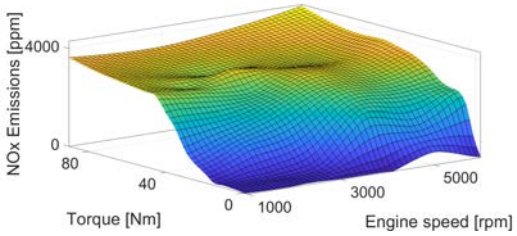

(a) NOx raw emissions map

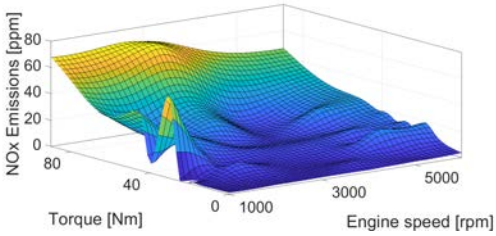

(b) NOx emissions map after both catalytic converters

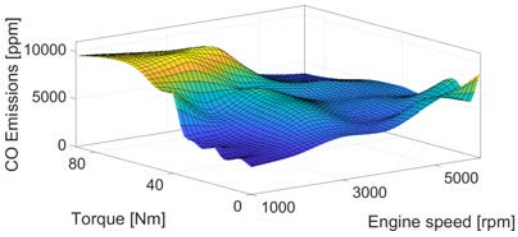

(c) CO raw emissions map

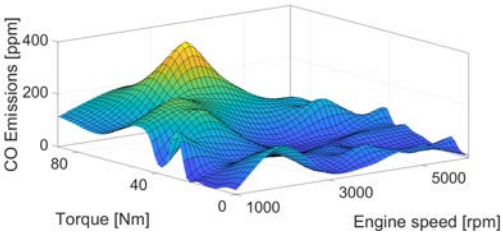

(d) CO emissions map after both catalytic converters

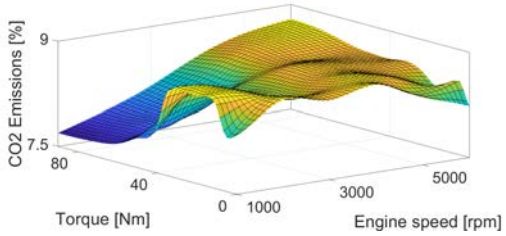

(e) CO2 raw emissions map

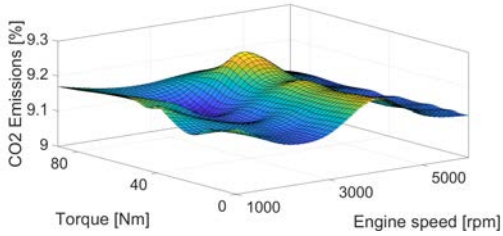

(f) CO2 emissions map after both catalytic converters

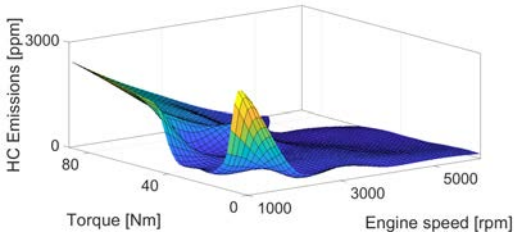

(g) HC raw emissions map

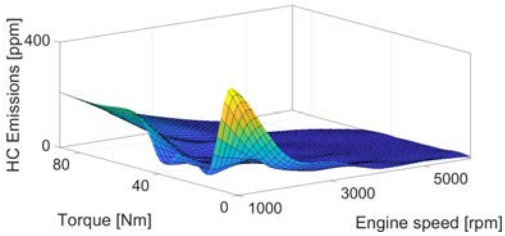

(h) HC emissions map after both catalytic converters

Figure 45 NOx Emissions in the different simulated cases

The 8 figures (45(a) to 45(h)) show the emissions maps for HC, CO, CO2 and NOx, both raw and after catalytic converters.

Figure 45(a) presents the NOx emissions raw, which correlates with the theoretical explaination which relates the increasing temperature in the exhaust gases produced by an increment of the torque, to a increment of the after reactions which increase the NOx emissions. In this case, for a constant torque, the primary engine does not seem to produce higher NOx amounts for higher engine speeds in a noticeable way. On the other hand, 45(b) shows the NOx emissions after being treated, showing much lower concentrations. It is interesting to

see how there is a peak around idle speed and torques of 30Nm, which is produced due to the high increase of the raw emissions in this point and the low temperatures of the catalytic converters which are not capable of converting emissions properly. When the torque is increased, the emissions decrease again as the working temperature of the catalytic converter is reached and the conversion rates are improved.

The CO raw emissions theoretically diminish as the torque and engine speeds are increased, due to the higher temperatures which produce the oxidation of the CO into CO2. In this case, figure 45(c) shows that at high torques, increasing the engine speed diminishes the emissions, as well as increasing the torque at constant high engine speeds. However, at low engine speeds, increasing the torque does not lead to a decrement of the emissions as would be theoretically expected. This is not a measuring error but an extrapolation failure of the fitting function. As previously shown in figure 43, the maximum torque produced at 1000 rpm is 50 Nm, point where the fitted map begins to increase but all those plotted points are extrapolated. At torques lower than 50 Nm, CO emissions for 1000 rpm are almost constant. On the other hand, figure 45(d) shows the CO emissions after being treated, showing much lower emission values. These values can be considered quite constant with the existance of two peaks in the whole map. The first peak can be found at low engine speeds and torques around 40 Nm, where the catalytic converter does not have enough temperature to oxidate the CO emissions and lower them enough. The second peak is shown at speeds around 3000 rpm and high torques, where the raw emissions of the system are the highest ones possible and the aftertreatment is not capable of oxidating all the amount of CO.

To end with, figures 45(g) and 45(h) show the HC emissions maps, having both similar curves but with clearly lower values the emissions which have been treated. If we look at the theoretical behaviour of the raw HC emissions, they diminish with an increasing torque as the temperature of the combustion is higher and more HCs are burned. This is clearly seen in figure 45(g), where the emissions are reduced when increasing the torque. Interesting is how big the difference is at low engine speeds, where there is an enourmous decrement of the emissions when running at 1000 rpm and going from 0 Nm to 30 Nm. This may be caused as the engine presents misfiring at low engine speeds together with low torques, which is observed in the bad running quietness of the engine, resulting in higher HC emissions due to the bad combustion. It is also interesting to remind that the points at low engine speeds with torques higher from 50 Nm are not measured points but extrapolated by the engine map. On the other hand, the catalytic converter seems to convert the emissions at all working points effectively, reducing equally the amount of pollutants and conserving a similar shape of the emissions map.

Appart from the presented emissions maps, it was also necessary to calculate an exhaust mass flow map for future simulations. This map will allow in the simulations the calculation of the emissions in g/km, as a mass flow is needed to be multiplied by the pollutants concentration.

Due to the inaccuracy of the mass flow sensor, the map was calculated from the measured lambda values and the amount of injected fuel.

The exhaust mass flow map is presented in figure 46 and shows a linear relationship with both torque and engine speed.

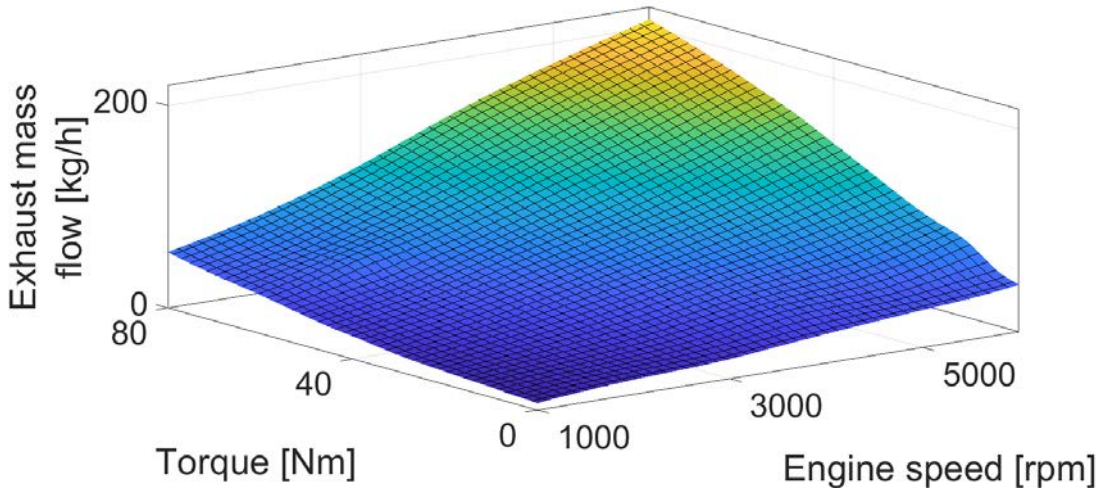

Figure 46 Exhaust mass flow map

5.4 Transient analysis of the catalytic conversion

5.4.1 The Light-Off and Light-Out Temperatures

The fact that many driving trips are so short that there is not enough time for the catalyst to reach working temperatures is so important, that new cycles have been designed to penalyze slow catalyst heating. The Light-On and Light-Off curves are the graphics which show how well the catalyst performs at low temperatures and how long does it take to the system to reach normal conversion rates. These curves are usually measured holding fixed the inlet gas concentrations, while the temperature of the reactor is slowly increased and then decreased [25]. The result is a plot of the conversion rate (or outlet concentration) versus the inlet gas temperature. It is important to notice that the X axis is the inlet gas temperature and not the catalyst temperature itself.

The light-off point occurs when the temperature is increased and is defined as the point in which the conversion rate reaches 50%. On the other hand, when the opposite occurs and the inlet gas temperature decreases, the light-out or extinction point occurs when the conversion rate drops below 50%. As figure 47 shows, it may occur that the light-off and light-out temperatures are not exactly the same, resulting, somehow, in some type of "hystheresis".

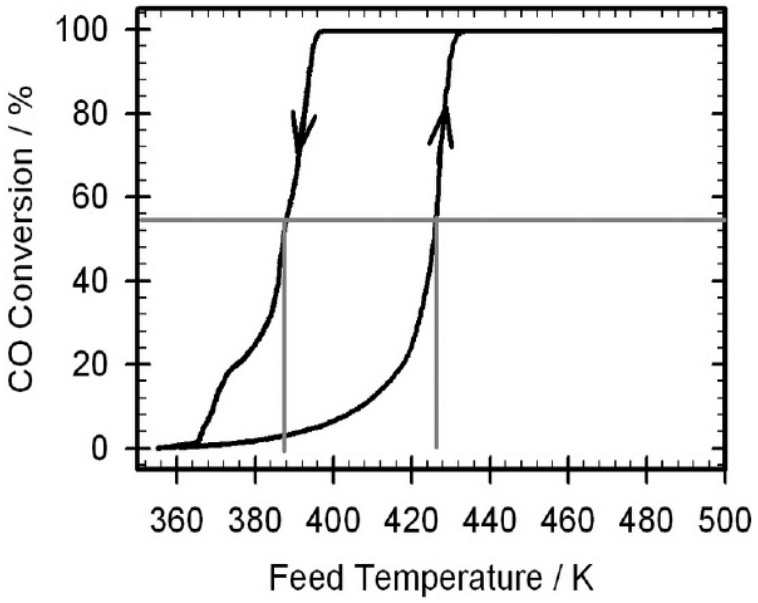

Figure 47 Complete light-off curve with both light-off and light-out points [25]

5.4.2 Experimental analysis of the transient behaviour of the aftertreatment system

The transient behaviour of the catalytic converters and the engine heating process have to be really take into consideration as a big amount of the total pollutants emitted in the testing cycles are produced in this stage. For this purpose, the system was studied in the test bench, running the engine from a cold starting point to a running point of 2000 rpm and 30 Nm. This experiment was carried out two times two different days with similar conditions to measure the raw emissions and the emissions after the main catalyst. In order to study and analyse the data, it was only necessary to shift the curves, matching the start of firing by matching the temperature curves in order to adapt both timelines.

Figures 48(a) to 48(d) show the temperatures measured before and after each catalytic converter for the two different tests carried out (measuring raw and treated emissions), in order to deduct if it is possible to compare emissions through this two different tests or there are disturbances which make the data unfavorable to be compared. As it can be seen in figure 48(a), the temperature before the first catalyst, point where the raw emissions are measured, is exactly equal for both tests during the transient period but there is a difference of about 15°C when the steady state is reached. This may be caused as the test was carried out in two different days, although the ambient conditions were not much different and the test bench is provided with a conditioning system which maintains constant the temperature of the aspirated air flow. The change of the emissions measuring point influences also the temperature measurements. However, figures 48(b) to 48(d) show the temperatures after the precatalyst and before and after the main catalyst, which are exactly equal for both tests. This is a first indication that both tests can be compared to analyse the conversion rates.

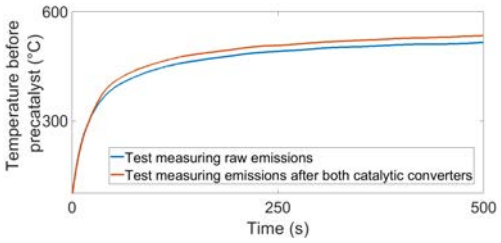

(a) Temperature before the precatalyst

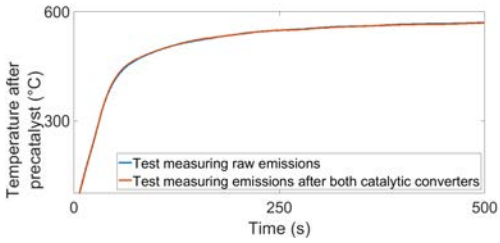

(b) Temperature after the precatalyst

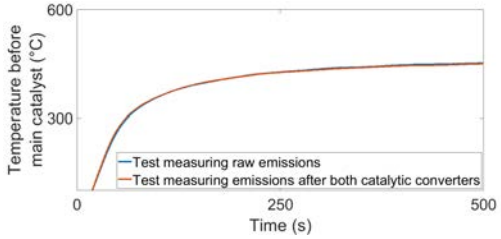

(c) Temperature before the main catalyst

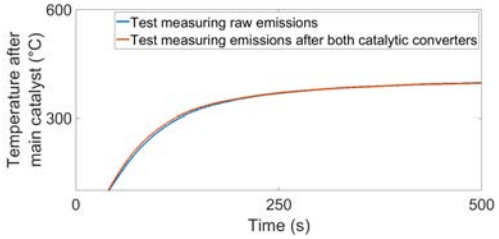

(d) Temperature after the main catalyst

Figure 48 Temperatures before and after each catalytic converter

Many other parameters were checked to find discrepancies between both tests to see it they were suitable to be compared, like lambda values or torque, shown in figures 49(a) and 49(b) respectively. The lambda value presents a perfect fitting between both tests with no major fluctuations or regulating issues. Regarding the torque, both tests present the sames values and transient curves. However, the tests where the emissions were measured after both catalytics converters shows somes points where the torque falls around 3 Nm and then increases again, issue which was not translated into a temperatures change. This issue was also observed in some other tests, where the torque felt down for some seconds and then was incremented again without variations in the mean indicated pressure. This was probably caused by variations in the torque measuring device and makes no difference in order to compare the emissions between both tests.

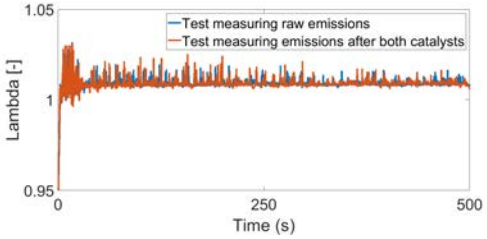

(a) Lambda value measured by the wide-band lambda sensor

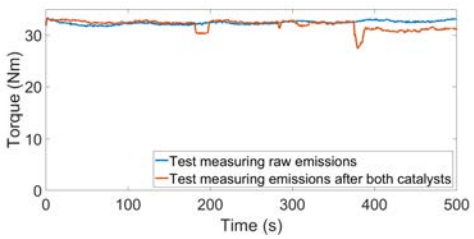

(b) Effective torque

Figure 49 Wide-Band lambda value and effective torque for both tests

The following figure (50) shows the HC emissions, where the blue curve are the raw emissions

measured directly after the engine and the red one are the treated emissions. Both curves are shifted to fit their timelines. During the first 40 seconds there is no conversion carried out by the catalysts and both curves are exactly equal. Then, there is sudden jump in the raw emissions at the same time that the catalyst begins to convert and the emissions after being treated being to fall. There are no changes in torque, engine speed, lambda, injected fuel mass or combustion which can explain this instant increment (less than 1 second) of the raw emissions. Interesting is that the catalytic converter begins to reduce the emissions at the exact same point, which corresponds to a temperature of 371°C measured before the precatalyst. In the steady state, the raw emissions are around 280 ppm while the pollutants which are being emitted to the ambient air are around 18 ppm.

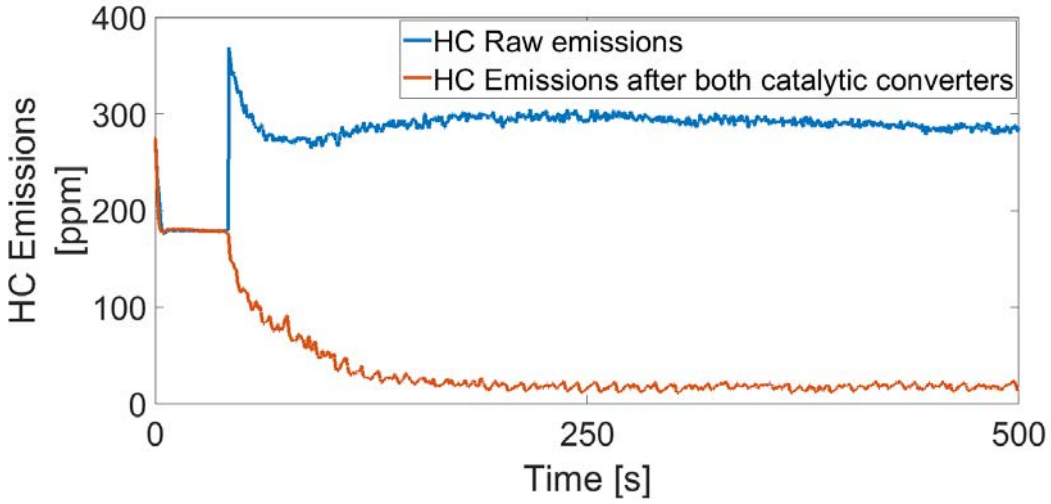

Figure 50 HC Emissions raw and after both catalytic converters

The NOx emissions are presented in figure 51. The raw emissions present a big peak in the first moments of the transient curve and which cannot be converted due to the low temperatures of the exhaust system. The maximum peak of 2500 ppm is reached after 13 seconds and is present in both curves. However, when raw emissions begin to decrease, the catalysts are hot enough to begin to react and emissions after the main catalyst decrease faster. It is not possible to find the light-off temperature as defined because the system is not tested with a constant pollutants concentration with an increasing gases temperature. However, it can be clearly seen that with the tested configuration, the system needs from about 40 seconds to reach a proper conversion rate of values of the 10% of the maximum peak. In the steady state, the NOx emissions are almost inexistend and amount just 1 to 2 ppm.

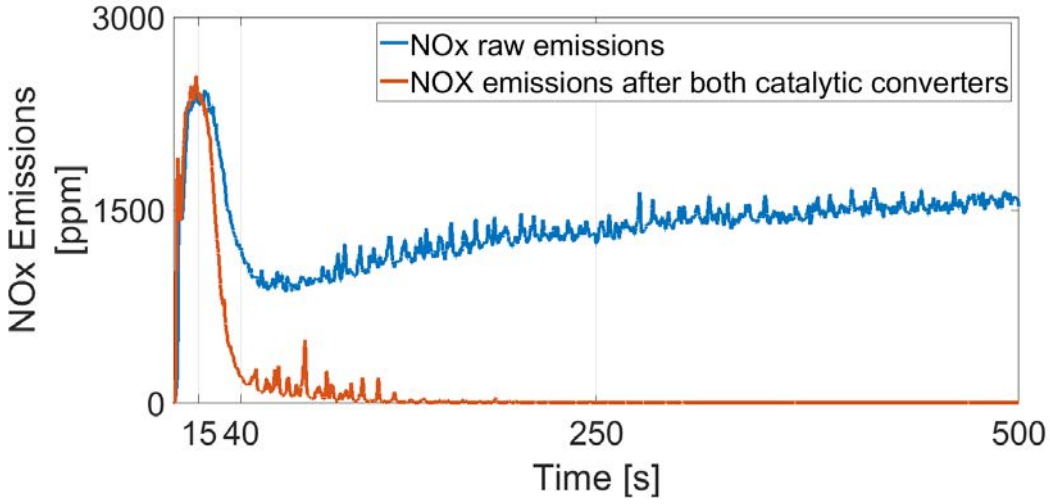

Figure 51 NOx Emissions raw and after both catalytic converters

The CO behaviour is somehow similar to the NOx. The raw emissions present a sudden high increment at the begining of the test with a peak of 1.5Vol-% after 10 seconds. Then the raw emissions begin to decrease but for the first 15 seconds the catalytics converters do not convert any of the emissions and both curves are exactly equal. After this moment, the system begins to oxidize the CO particles and a full conversion is reached after about 40 seconds like in the case of the NOx emissions.

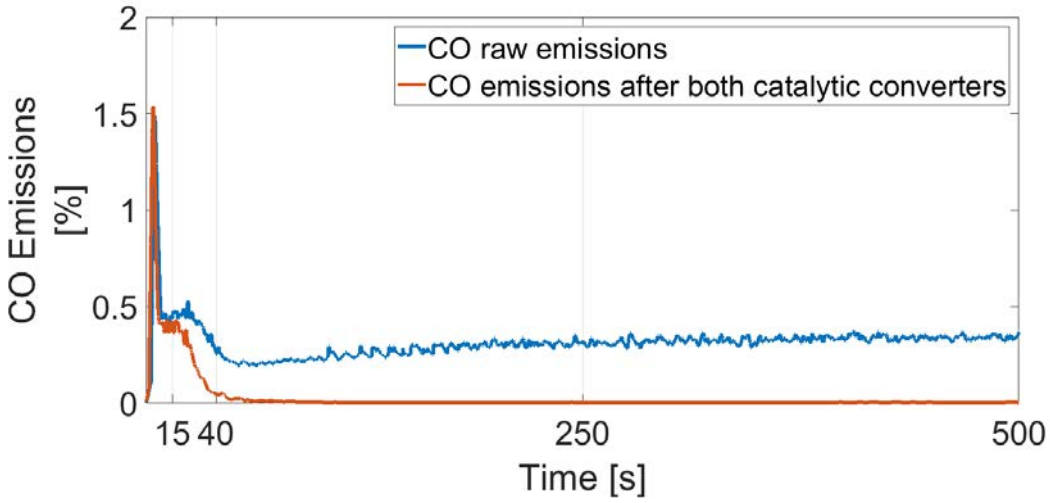

Figure 52 CO Emissions raw and after both catalytic converters

Finally, the CO2 emissions are presented in figure 53. The raw CO2 curve also matches the treated CO2 curve in the first 15 seconds of the test, meaning that no conversion is produced for this pollutant in this period of time. After this moment, the CO particles shown in 52 begin to be oxidized in the catalytics converters and the amount of CO2 after the exhaust system begins to be greater than directly after the engine.

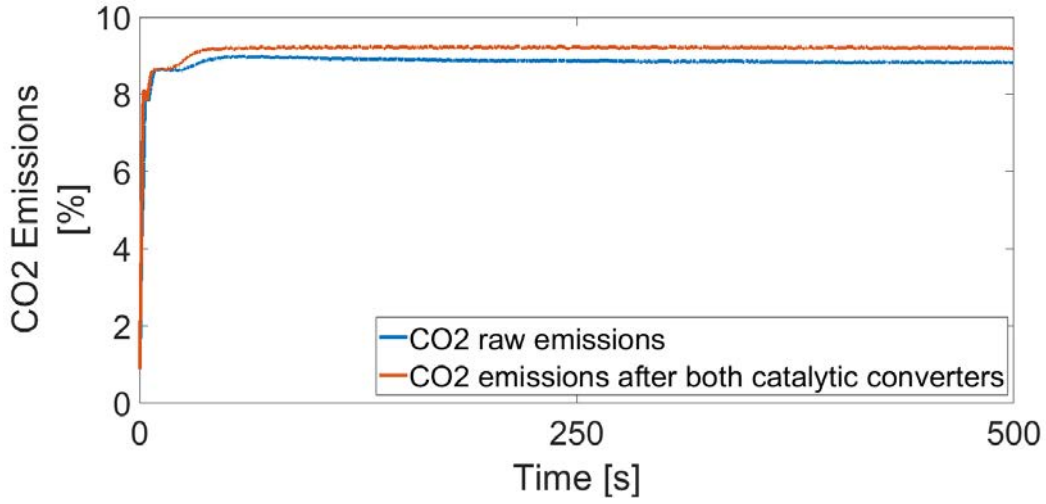

Figure 53 CO2 Emissions raw and after both catalytic converters

From the previous presented figures it can be deducted that the tested exhaust system does not make any conversion for the first 15 seconds of the test, meaning that no reactions are produced for temperatures lower to 270°C (referred to the air mass flow before the precatalyst). It is not possible to determine the light-off temperature of the system as the necessary test to calculate it as it is defined cannot be carried out in the test bench and would be necessary a device which can introduce in the system a constant amount of pollutants with an increasing temperature, something that is completely impossible to do with an engine. However, the system needs from 40 seconds to fully convert the emissions and reach the steady state.

5.4.3 Experimental analysis of the conversion rate of the precatalyst

After the previous tests in the test bench, a third heating curve was measured to analyse the amount of pollutants which react in the precatalyst. The same curve as before was used in this experiment but measuring emissions after the precatalytic converter. In this cases, the pollutants present inbetween both catalytic converters will be compared to the emissions after the main catalyst to see how fast the precatalyst becomes hot and how many pollutants are converted, which can give us a first approach to see if an exhaust system with just a catalyst is enough or two are necessary.

Figures 54(a) to 54(d) show the temperature measured before and after each catalyst for the tests where raw emissions and emissions after the precatalyst were measured. As previously done, this will give information from whether both tests are suitable to be compared. As it can be seen, the temperatures show a difference between both tests which was not present in the previous comparison although the engine speeds and torque curves present no variation. It has to be noticed that between the measurement of the raw emissions and the test measuring emissions after the precatalyst there is a delay of a month, while the raw emissions and after main catalyst measurements were carried out in consecutive days.

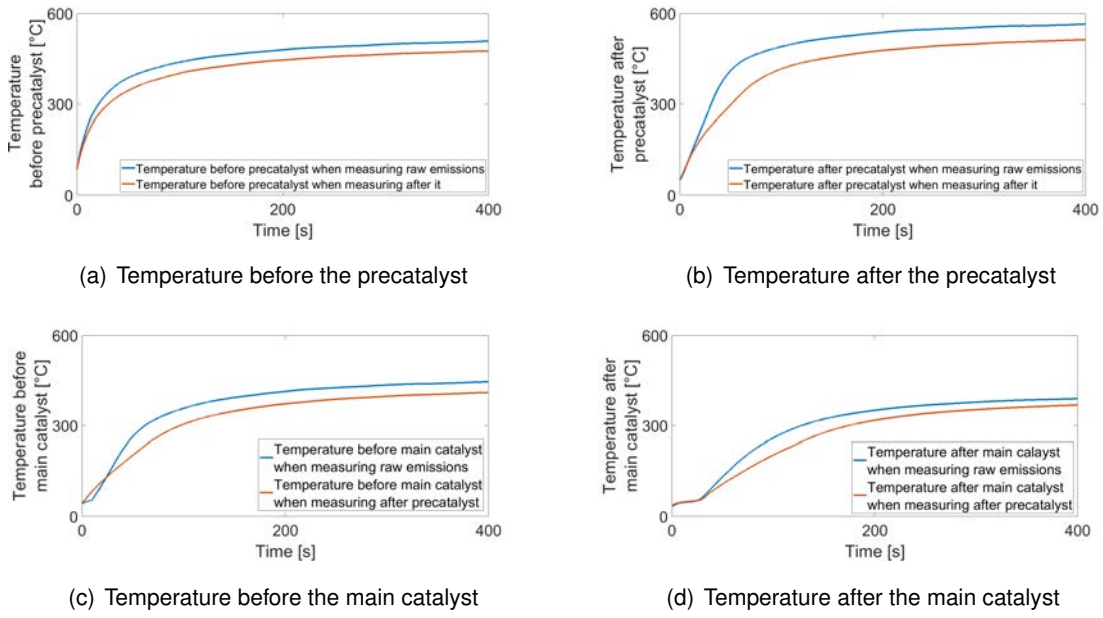

(a) Temperature before the precatalyst

(b) Temperature after the precatalyst

(c) Temperature before the main catalyst

(d) Temperature after the main catalyst

Figure 54 Temperatures before and after each catalytic converter when measuring raw emissions and after the precatalyst

Regarding the ambient factors which may influence the measured temperatures, the most noticeable difference is the relative humidity, shown in figure 55, where the relative humidity presents a high increment when testing emissions after the precatalyst regarding the measurement of raw emissions.

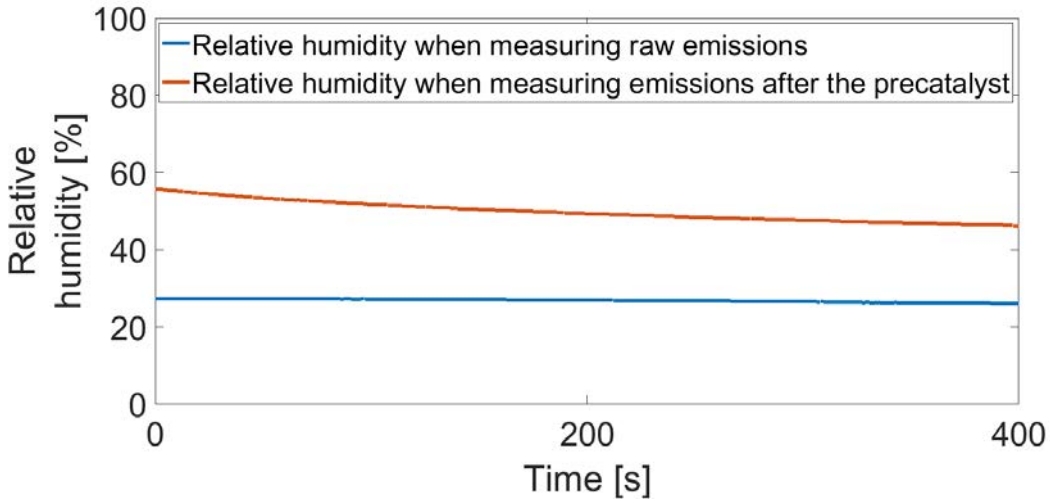

Figure 55 Relative humidity in the tests measuring raw emissions and after the precatalyst

The following figure (56) shows the angle at which the 50% of the combustion is completed for both cases. This parameter indicates how fast the combustion is taking places and is normally limited at high loads by engine knocking, also having a big influence in combustion efficiency and fuel expense. Figure 56 shows a later ignition timing of about 2° or 3° when measuring

emissions after the precatalyst. According to Konrad [18], a later ignition timing increases the exhaust gases temperature and makes the catalytic converter reach the working temperature faster. However, in this case the opposite occurs and the temperature in the test which measures emissions between both catalytics converters presents lower temperatures.

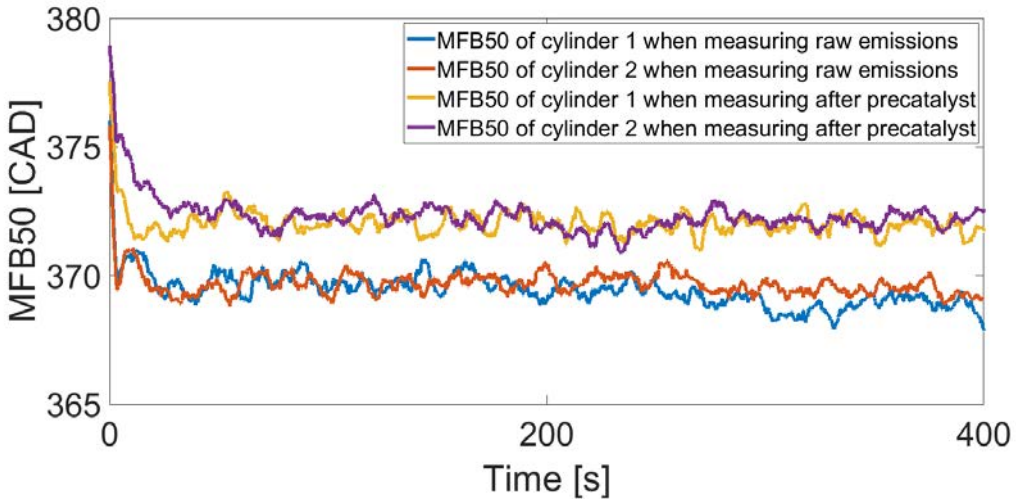

Figure 56 MFB 50%

It is possible that the difference on the MFB 50% was caused because the ignition controller may have not been activated. Figures 57 and 58 show the difference of the pmi and torque between both tests. This difference is caused by the ignition delay which results in a difference of 1 bar in the sum of the pmi of both cylinders and 1.5 Nm difference in the output torque.

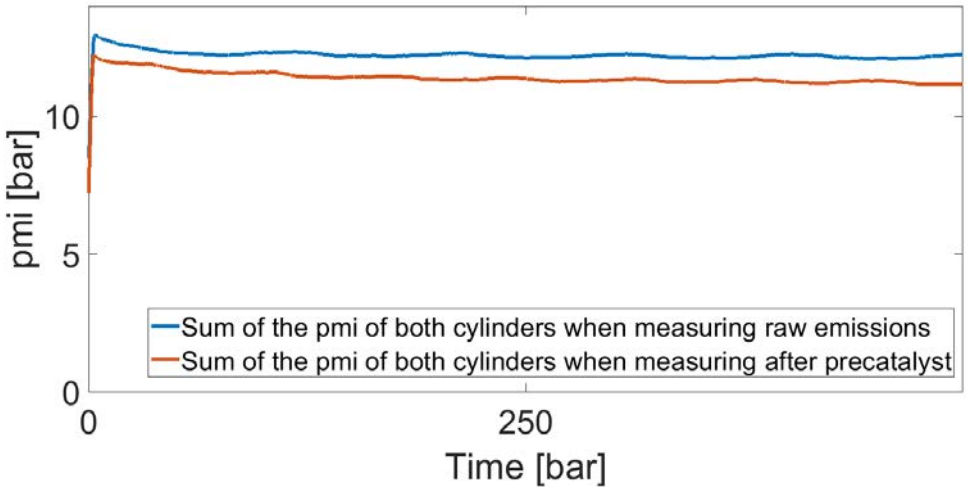

Figure 57 Sum of the pmi of both cylinders

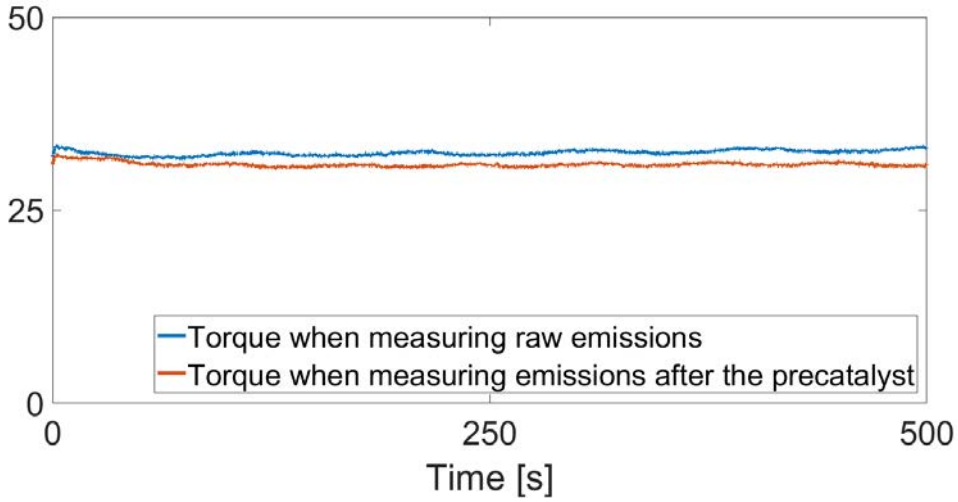

Figure 58 Effective torque

With all this difference between both tests, it may not be completely accurate to compare the emissions results between them in terms of exact values. However, as engine speed presents no difference and the torque only a 1.5 Nm difference, both tests are suitable to be compared in terms of magnitude orders and tendence in the emissions.

The following figure shows the HC emissions in the three possible measuring points: after the engine, after the precatalyst and after the main catalyst.

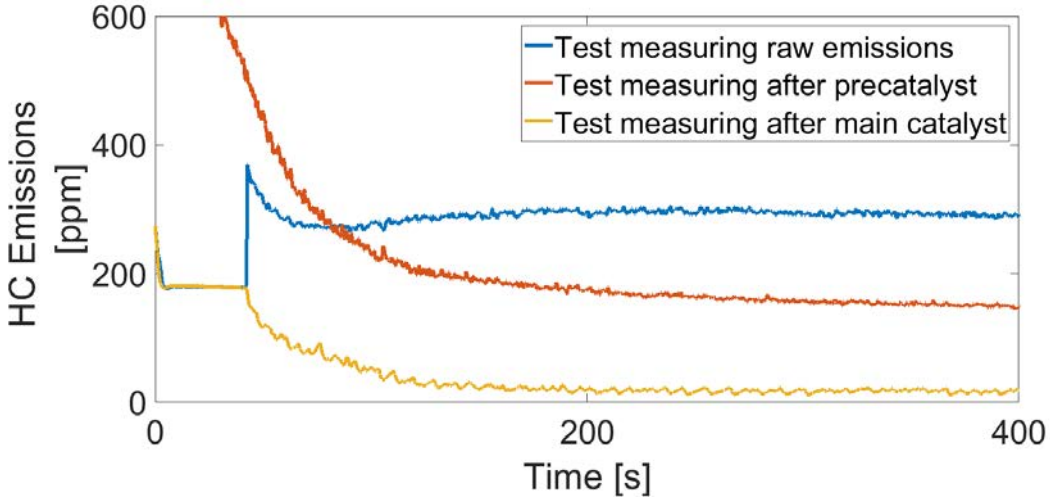

Figure 59 HC emissions in the three points

In the case of the emissions after the precatalyst, it can be seen that the transient curve is clearly slower than the other two cases and even has more emissions in some point than the raw emissions, which is obviously nonsense. Furthermore, it can be seen at the beginning of figure 57 that the pmi of both tests are properly alligned.

In the steady state, the values present coherence and the emissions after the precatalyst (150 ppm) are smaller than the raw emissions (290 ppm) but greater than the emissions after the whole exhaust system (15 ppm). Taking into consideration that the tested point is only at 2000 rpm and 30 Nm, it looks clear that the precatalyst is not capable of reducing all the HCs present in the exhaust gases and the system needs from both catalytic converters or a greater one.

The NOx emissions in the three measuring points are presented in figure 60. In the steady state, again, the emissions after the precatalyst are greater than the emissions after the main catalyst, which indicates that there were some issues in the first moments of the test. The transient curve of the emissions after the precatalyst shows also a slower response to conversion which is the opposite as would be expected as the precatalyst is built to improve the cold-start behaviour and increase the conversion rate of the system during the first seconds of the tests. However, this slower answer is probably caused by the temperature differences previously shown in this section which make the transient period not be suitable for comparison.

Regarding the steady state, the raw emissions are around 1500 ppm, while after the precatalyst are 366 ppm and 1 ppm after the main catalyst. Once again, the main catalyst seems to be completely necessary for the system as, with the so low limits in the NOx emissions, values of 300 ppm make impossible to pass the current tests.

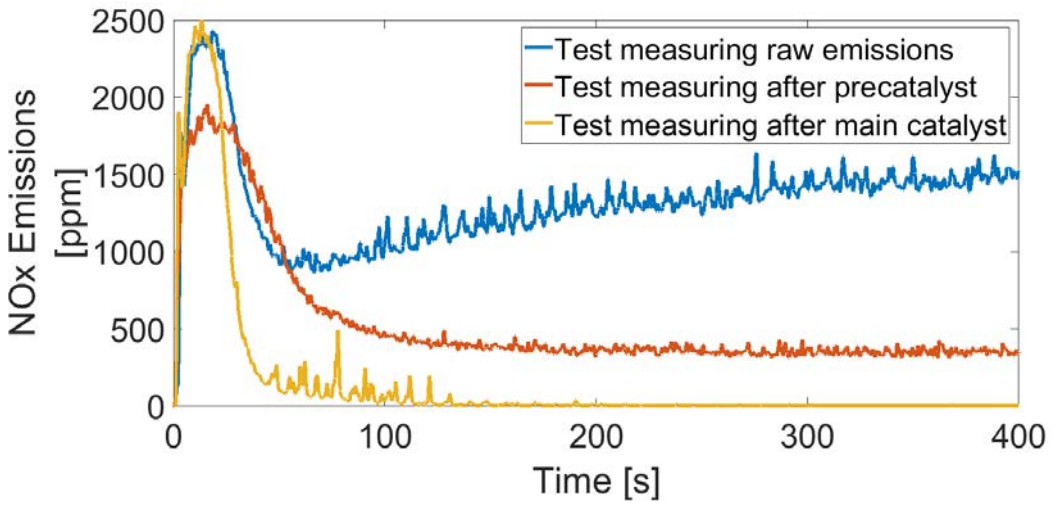

Figure 60 NOx emissions in the three points

The CO emissions are plotted in figure 61 and, in this case, shows a good fitting between the three curves in the first moments of the transient period but then the curve of the emissions after the precatalyst again react slower. Once again, in the steady state the raw emissions (0.3%) are greater than the emissions after the precatalyst (0.16%) and the main catalyst (0.002%). The main catalyst presents, as in the case of the NOx and HCs, a great improve-

ment to the system with regard to the precatalyst.

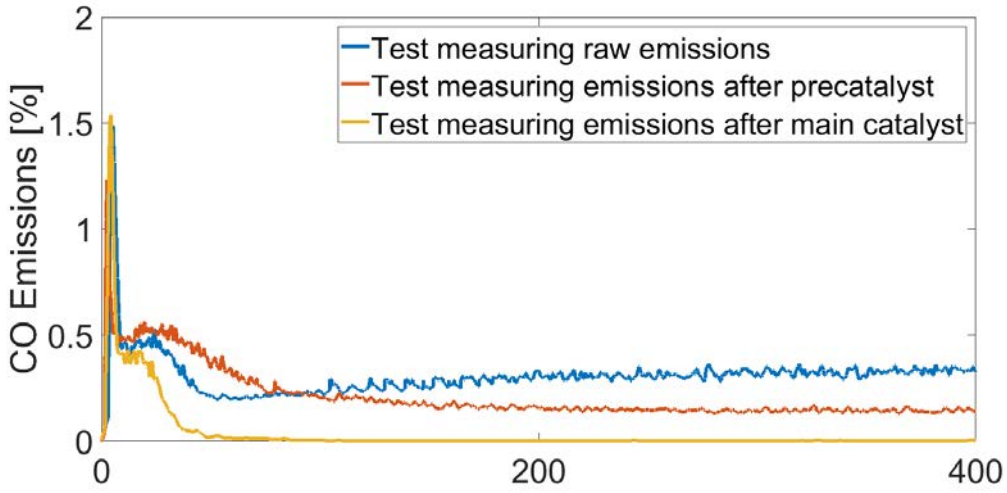

Figure 61 CO emissions measured in the three points

To end with, CO2 emissions are presented in figure 62 and match the CO curves as they are both related, being CO2 the result of oxidating CO. In the transient curve, the CO2 emissions after the precatalyst are lower than after main catalyst as the CO curve in 61 shows a slower response and thus the oxidation of the CO into CO2 is also slower. In the long run, the results are according to what is expected and precatalyst presents less CO2 after it than after the main catalytic converter, as it is not capable of oxidating so much CO.

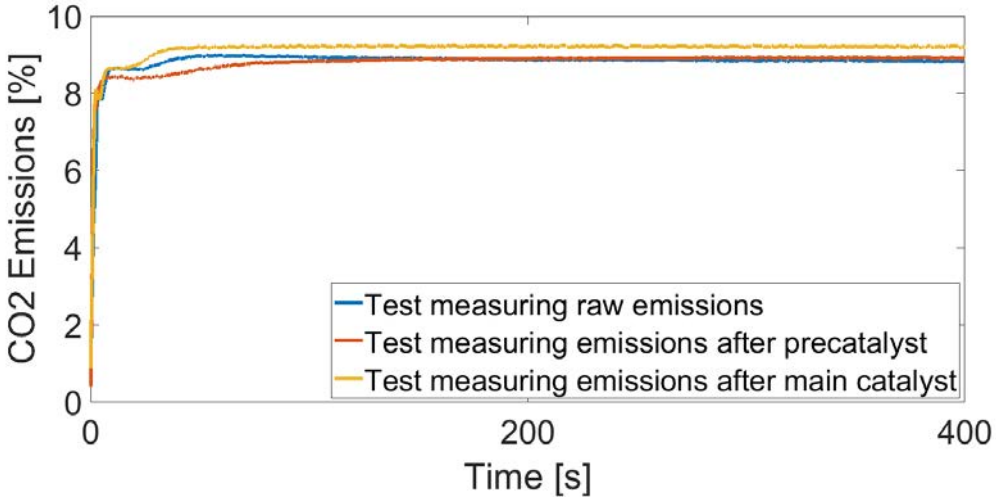

Figure 62 CO2 emissions measured in the three points

This analysis of the conversion rates of the precatalytic converter cannot make statements regarding the transient behaviour. However, it can be confirmed that with the used precatalyst, the system needs from another catalytic converter as it has not enough converting capacity.

5.5 Experimental analysis of the stationary conversion rates of the system without the precatalytic converter

After the transient analysis, a last set of points were measured to compare the stationary conversion rates of the precatalyst for different working point. Three different points were measured before and after each catalytic converter as follows:

	Engine speed [rpm]	**Torque [Nm]**
Point 1	2000	33.5
Point 2	3000	45
Point 3	4000	38.5

Table 10 Points measured to analyse the steady state conversion rate of the precatalyst

For each of the previous points, the emissions were measured before the precatalyst, after it and after the main catalyst. The results as a mean value for ten seconds are presented in table 11:

	Pollutant	Emissions after engine	Emissions after precatalyst	Emissions after main catalyst
Point 1	**NOx [ppm]**	1906.3	543.27	307
	HC [ppm]	491.87	215.49	34
	CO [%]	0.7416	0.2218	9.97E-4
	CO2 [%]	13.84	14.42	14.64
Point 2	**NOx [ppm]**	2596	577.33	15.01
	HC [ppm]	285.84	103.78	30.09
	CO [%]	1.2005	0.333	0.03
	CO2 [%]	13.46	14.38	14.67
Point 3	**NOx [ppm]**	2805	560.24	277.88
	HC [ppm]	268.09	100.03	21.39
	CO [%]	0.9549	0.2347	3.44E-4
	CO2 [%]	13.69	14.46	14.67

Table 11 Emissions for the analysis of the precatalyst's conversion rate

The emissions between both catalysts are clearly higher than after the main catalytic converter. A clearly example of the need from both converters is the second measured point, where precatalyst can convert the 2596 ppm raw emissions to 577 ppm which is still a high value, while the main catalyst can reduce the amount of NOx present to just 15 ppm.

It can be concluded by this analysis and the transient one that the system needs from both catalytic converters with the configuration which is being used. It should be analyzed whether the main catalyst is enough for the whole system but being built nearer the engine so its temperature can be higher and increased the number of pollutants converted.

6. Simulation of a real test cycle considering a complete vehicle simulation and the tested engines

6.1 Objective of the simulation

After all, one of the main purposes of the study is the analysis of the improvement which the SCE represents and whether it would suit the emission limits which are imposed nowadays. The only way to find the answer to all these questions is by carrying out a simulation where a whole cycle, like the WLTC for example, can be recreated and returns an estimation of the emissions produced by the whole vehicle.

Sylvain Garnier [26] developed a model in GT-Suite and Simulink (MATLAB) where the whole vehicle was included like it would happen in the test bench. Previously to this model, Sylvain Garnier [26] had to develop a costs function which would determine when was it worth to start the secondary engine and when was it more efficient to run in partial mode due to low speed or small accelerations for example. As a result of this study, the engine speed and pmi curves for both engines of the SCE were obtained for the whole WLTC cycle. This can be joined with the engine emissions maps to estimate the total pollutants emitted and, therefore, fulfilling the first objective of this section of calculating the total emissions.

The second objective of this sections is the evaluation of the improvement that the SCE represents with regard to a not downsized engine. The way purposed by Sylvain Garnier [26] was to compare the SCE with two fictional engines: a Cylinder Deactivation Engine (CDA) and a Complete Engine (CE). Both engines only exist in the simulation but allow a comparison with the SCE as they are both composed by the same primary and secondary engines. For example, in the case of the complete engine, it is simulated having the PE and SE joined together through the crankshaft and running it like a normal 4-Cylinders engine, while the CDA runs always all the cylinders but only fires 2 or 4 of them, depending of the needs of the vehicle.

According to Sylvain Garnier [26], *"in the CDA model, the SE can be deactivated, but it still runs at the same speed than the PE. When deactivated, the valves of the SE are closed, and the air/fuel ratio is set to 1000 (Maximal possible value in GT-Power), to represent the cut of the fuel injection. The SCU has been removed, and the SE is activated within a cycle after a switch request. In the current stage of development, the operating strategy is the same as for the SCE. It includes the optimal load distribution between the engines, the activation/deactivation strategy and the shift strategy. The comparison between this model and the SCE's model represents the friction losses of the dragged SE and the energy of coolant and*

oil flow when it is activated. It is the gain through the mechanical cylinder decoupling. In the CE model, the two engines are always activated. The load is optimally distributed between the two engines. The operating strategy has to determine the best gear. This model is a basis to estimate the consumption reduction through the cylinder deactivation."

6.2 Methodology, approximations and assumptions

The simulation of the test cycle emissions begins with the data from Sylvain Garnier [26] which consists of a time profile of the mean indicated pressure (pmi) and engine speed (rpm) for the primary and secondary engines of the three different simulated motors: SCE, CDA and CE. Figures 63 and 64 show, as a an example, the pmi and engine speed profiles for the SCE in the case of the WLTC. It can be seen how the red curve, which corresponds in both figures to the secondary engine, only appears partially, meaning that the engine is connected and disconnected depending on the needs.

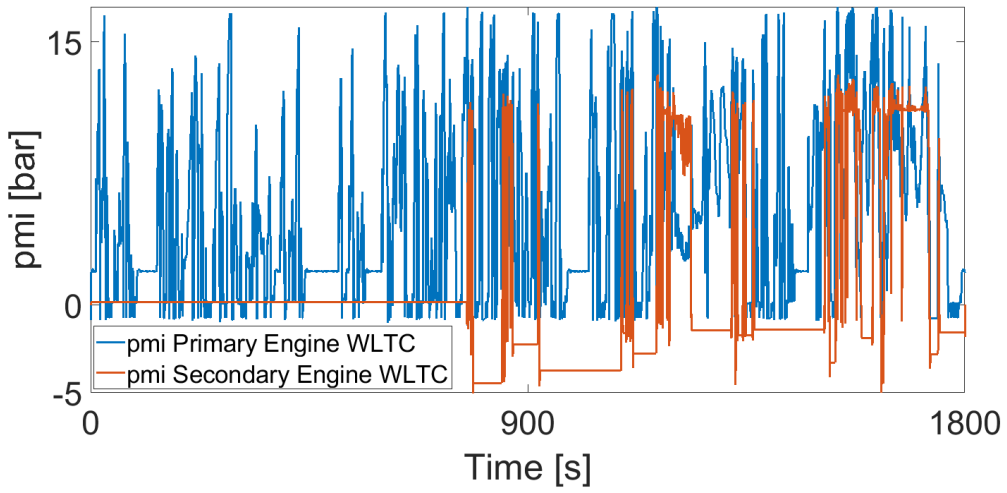

Figure 63 pmi-Time profile for the simulation carried out by Sylvain Garnier [26] in the case of the SCE running the WLTC

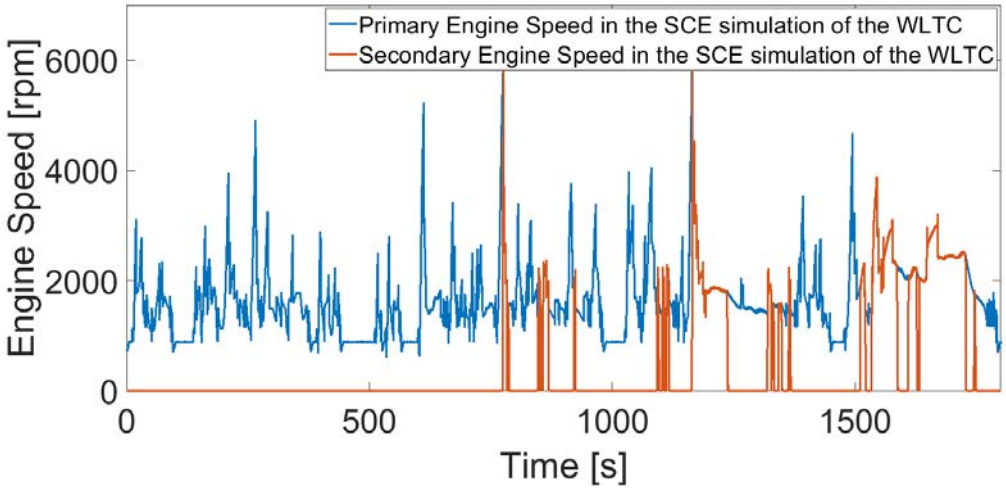

Figure 64 Engine speed-Time profile for the simulation carried out by Sylvain Garnier [26] in the case of the SCE running the WLTC

Both profiles were exported to MATLAB and a script for the simulation was developed. The emissions were calculated with the maps previosly shown, together with a map which returns the exhaust gases mass flow, allowing the calculation of the pollutants in [g/s]. The main assumptions considered are:

- The cold start was simplified and assumed that the catalytic converters made no conversion of the pollutants at all, a worse case scenario, which was simply calculated by considering that during the first seconds of the test the final emissions were equal to the raw emissions after the engine.
- The simulation presented in Sylvain Garnier [26] considered that the PE is a turbocharged engine and the SE is aspirated. Due to this difference, the secondary engine is more efficient. However, as there was not enough time to measure both engines in the test bench, it will be considered that both engines have the same emissions maps.
- Due to the temperature limits that the engine present due to the lambda = 1 requirement, the real torque produced by the engine is lower than the manufacturer's certification and the values in the simulation. The points in the simulation where the pmi values are higher than real ones will be extrapolated in the emissions maps and exhaust flow map.

Emissions are only calculated for engine speeds higher than 1000 rpm and pmi values higher than 0 bar. Although it may happen that pmi values greater than 0 produce no effective torque due to the power used by auxiliary system but the engine is being fired. The emissions are calculated by using the formulas presented in chapter 4.

6.3 World Harmonized Light-vehicles Test Cycle Simulation

6.3.1 Analysis of the emissions

For the three different engines, the SCE and the fictive CDA an CE, the World Harmonized Test Cycle was simulated considering three different cases, where the cold start phases lasts 20, 30 or 40 seconds respectively. With the exhaust configuration which is built at the moment, the SCE real result would be somewhere near the simulation with the 40 secons cold start phase.

The following table (12) shows the emissions in grammes pro kilometer of the total cycle and the maximum limit allowed by the Euro 6b normative. The emissions are calculated by integrating through the whole cycle the instantaneous emissions and then dividing the total amount in grammes by the length driven in the cycle which is 23.307 km.

	SCE			**CDA**			**CE**			**Euro 6b limit**
Cold start phase duration [s]	**20**	**30**	**40**	**20**	**30**	**40**	**20**	**30**	**40**	-
NOx [g/km]	0.0843	0.114	0.1214	0.074	0.1127	0.1250	0.0578	0.08	0.0884	0.06
HC [g/km]	0.0524	0.0555	0.0563	0.04715	0.0511	0.0525	0.0634	0.0654	0.0671	0.1
CO [g/km]	0.2171	0.2636	0.2754	0.2287	0.2844	0.3096	0.211	0.2595	0.278	1
CO2 [g/km]	150.04	149.95	149.91	159.90	159.8	160.4	166.17	166.04	166.04	-
Fuel [l/100km]	9.022			9.559			9.84			-

Table 12 Emissions and fuel consumption from the simulation of the WLTC

The first analysis of the results shows:

- The SCE produces a 10% reduce in fuel consumption with respect to the complete engine and a 5% saving with the cylinder deactivation engine.
- All the engines have emissions values lower than the maximum limits except for the NOx. The only case which presents all the emissions inside the limits is the complete engine when the cold start is shorter than 20 seconds.
- NOx: the SCE and the cylinder deactivation engine present similar NOx values, while the complete engine clearly has lower emissions. It would be expected a reducion in the NOx from the SCE, however, this results will explained later.
- HC, CO and CO2: the three different engines present really similar values, being always inside the maximum limits with a reasonable margin, which may indicate that the limitant

design pollutant is the NOx.

The reason to the higher NOx emissions from the SCE is the assumption that the primary and secondary engines have the same emissions maps, while the simulations carried out by Sylvain Garnier [26] had into consideration the better efficiency of the secondary engine and the high pmi values that the primary engine of the SCE suffers when the secondary engine is not running. The following table shows the the average pmi and engine speed values of each engine when considering a 30 seconds cold start:

	SCE PE/SE	**CDA PE/SE**	**CE PE/SE**
Average pmi in Cold Start	5.87/0	6.39/0.5	2.37/4.4
Average pmi total cycle	5.2/0.718	4.47/3.2	2.8/4.8
Average engine speed in Cold Start	1499/0	1438	1432
Average engine speed total cycle	1691/403	1612	1560

Table 13 Average pmi and engine speed during the cold start or the total WLTC

The cylinder deactivation engine and the complete engine have during the cold start an average pmi of 6.89 and 6.77 bar of both cylinders together respectively, while the SCE has only 5.87 bar, as the losses of two of the four cylinders are equal to 0. The same happens in the average values of the complete cycle. Notice that the difference of the pmi between the primary and secondary engine of the complete engines are due to the fact that the secondary engine is modelled as more efficient by Sylvain Garnier [26].

This lower total pmi of the SCE results in a fuel saving with respect to the other two engines as the fuel consumption shows a linear behaviour when increasing torque and engine speed. This means that having one engine at 3000 rpm and 6 bar pmi consumes as much fuel as having two engines at 3000 rpm and 3 bar pmi. However, the absence of the friction losses of two of the cylinders produces this decrement of the total average pmi which results in a fuel saving. Figure 65 shows the empirical fuel consumption map measured in the test bench:

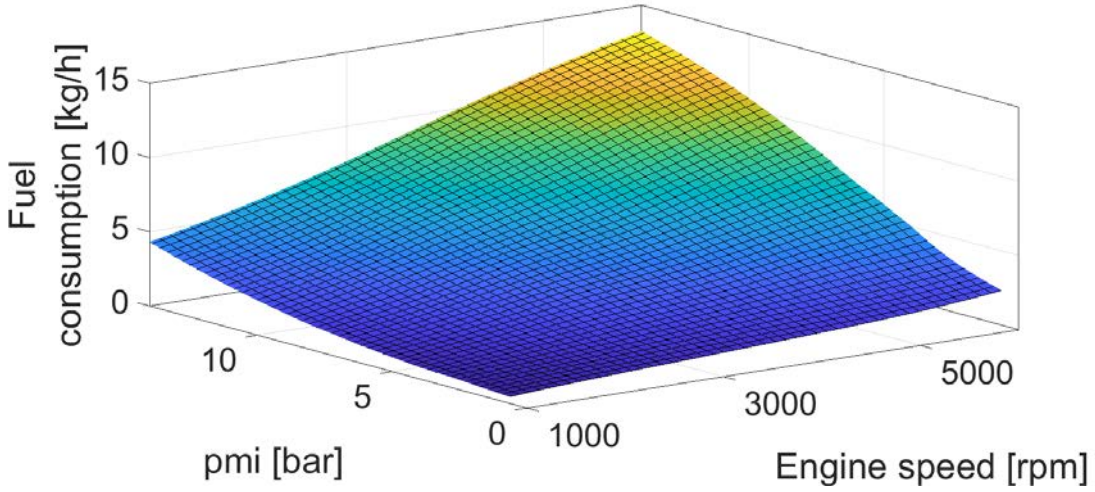

Figure 65 Fuel consumption map measured in the test bench

However, this linear soft behaviour cannot be found in the case of the NOx emissions, where there is a huge gradient which rapidly increases the emissions when going from 0 bar pmi to higher torques. The result of this big increment is the unefficiency of one engine alone regarding NOx emissions, being more favourable having in the complete engine the four cylinders with a lower mean pressure than just the primary engine in the case of the SCE with a high pmi, although the combined pressure of the four cylinders is lower in the case of the SCE. Figure 66 shows the raw emissions map, directly measured after the engine, which is the map being used during the cold start simulation where the catalytic converter is not working. It can be observed that, for example, in the range from 1000 rpm to 3000 rpm, where the cold start takes place, there is a sudden increment from almost no emissions to really high ones. This makes more efficient, in terms of NOx emissions, having a complete engine than a SCE, for the measured emissions maps.

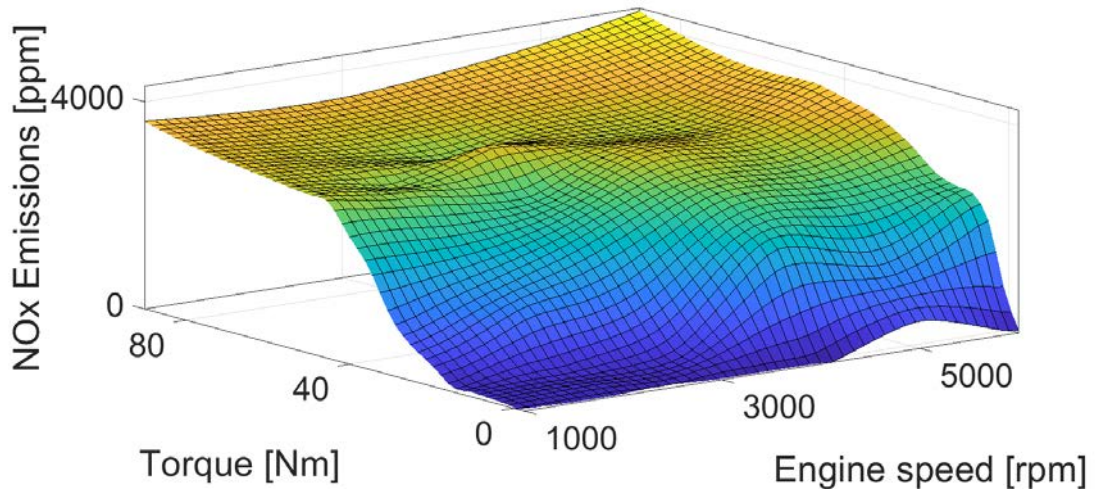

Figure 66 NOx raw emissions map

Simplfying the calculations, the emissions considering the average values of the cold start can be calculated, using the same equation as in the simulation, to confirm the first indications seen in the previous figure:

$$\begin{aligned} SCE_{NOx} &= 0.001587 \cdot EmissionsPrimaryEngine = \\ &= 0.001587 \cdot MassFlow_{Exhaust}(1499rpm, 5.87bar) \cdot NOx(1499rpm, 5.87bar) = \\ &= 79.48g/h \end{aligned} \tag{6.1}$$

$$\begin{aligned} CE_{NOx} &= 0.001587 \cdot (EmissionsPrimaryEngine + EmissionsSecondaryEngine) = \\ &= 0.001587 \cdot (MassFlow_{Exhaust}(1432rpm, 2.37bar) \cdot NOx(1432rpm, 2.37bar) + \\ &+ MassFlow_{Exhaust}(1432rpm, 4.4bar) \cdot NOx(1432rpm, 4.4bar)) = \\ &= 33.31g/h \end{aligned} \tag{6.2}$$

where 0.001587 is the coefficient which converts the volume ppm into mass ppm and also includes a units transformation to have the results in g/s.

This simplification shows a big difference in emissions during the cold start between both engines due to the shape of the NOx emissions map.

Regarding the CDA engine, although it has higher mean values during the cold start than the SCE, the lower average values of the total cycle compensate the higher emissions of the first moments, resulting in similar emissions to the SCE.

6.3.2 Analysis of the influence of the cold start for each pollutant

The following table (14) shows the percentage that the cold start emissions represent from the total amount during the whole vehicle simulation. NOx presents the highest ratio NOx emitted during cold start/Total NOx emitted and is the most sensitive pollutant to the cycle start. Reducing the time of the cold start will have an enormous impact on the NOx emissions and would probably make them be below the Euro 6b limits. However, with the tested exhaust system, cold starts should last less than 10 seconds to pass the limits, a time which is not feacible at this moment.

The CO2 emissions are not included in the table as they are almost constant at any time and suffer small variatios.

	SCE			CDA			CE		
Cold Start Duration [s]	**20**	**30**	**40**	**20**	**30**	**40**	**20**	**30**	**40**
NOx	31.05	49.48	52.57	35.1	57.9	62.16	30.16	49.72	54.57
HC	8.55	14.11	15.5	8.33	15.99	18.65	7.53	10.7	13.33
CO	23.79	37.62	40.45	23.06	38.5	43.76	21.15	36.21	40.66

Table 14 Percentage of emissions which correspond to the cold start with regard to the total cycle

NOx presents the highest percentage of emissions procedent from the cold start, while HC are the when which are less affected. Being the NOx the limitant pollutant and the only one out of the allowed range, the cold start plays a really important role in the SCE to be in the accepted limits.

6.3.3 Conclusions of the WLTC simulation

The simulation of the WLTC considering the whole vehicle model together with the engine emissions maps measured in the test bench have returned valuable results, being the most interesting conclusion here summarized:

- The SCE's limitant pollutant are the NOx. As the measured points were measured for a lambda value which resulted in a global emissions optimum, HC and CO emissions can be sacrifized in order to improve NOx emissions and fulfill all the requirements.
- Running the primary engine of the SCE may not be beneficial in terms of emissions when compared to running both engines together although there are higher friction losses. This is caused because for the tested engine working at high pmi points results in much more emissions than working with two engines and low pmi values.
- The SCE presents a 10% fuel consumption reduction compared to a four-cylinders engine composed by the same primary and secondary engines.
- NOx is the most influenced pollutant by the cold start. As it is the only pollutant out of the legal limits, the cold start plays a really important role in the SCE and should be improved with some other measurements.

7. Building a model and simulation of the aftertreatment system to optimize and develop the concept

7.1 Objective of the GT-Simulation

In engineering, when trying to design a system or components, it is common the use of simulation models, being no exception the SCE. Once that the test bench has been built, building a model which can foresee the conversion rates and behaviour of the catalytic converters will help when trying to improve the system. What would happen if it is installed a catalytic converter which is double the size of the one we are using at the moment? How would the system behave if the catalytic converters had a different precious metals concentration? Is it favourable to use a bigger precatalyst?

The following figure shows an schema of the optimization process followed in the SCE project. A model of the engines is built in GT-Suite (a simulation software specifically for engines and automotive applications) and is improved through iterations with the test bench. The simulation model is improved by the tests carried out with the real engines while the aftertreatment system is improved with the simulations with GT.

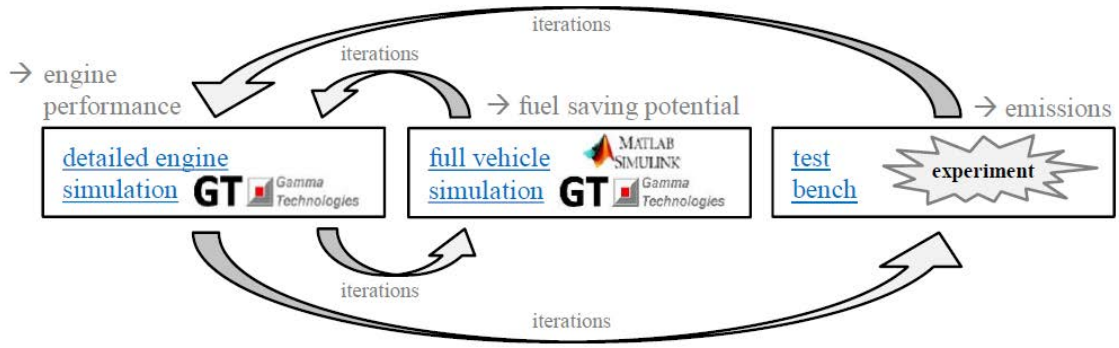

Figure 67 Optimization process of the SCE [24]

In the middle of the schema, a full vehicle model is disposed. This full model is the same one developed by Sylvain Garnier [26] which provided the data for the WLTC simulation presented in the previous chapter. The full vehicle model will be joined with the catalyst model and the engine emissions maps to simulate testing cycles.

7.2 Simulation models of catalytic converters

For the last decades, the automotive industry has improved the simulation of the catalyst reactions which occur inside the system. Understanding what happens inside the reactor is crucial for a correct design and sizing of the required components. The simulation of the light-on/light-off is also important as it is the only way to ensure that the transients are well simulated. Furthermore, transients may be the prevailing working point of catalysts. In Ramanathan u. Shekhar Sharma [23], the authors distinguish among different types of simulation models:

- The one-dimensional two-phase (gas-solid) model distinguishes between the gas and solid phase concentrations and seems to present quite satisfactory results.
- Simpler models such as the look-up tables consist on a database of conversions for different species as a function of temperature and space velocity. Then, from the actual working point of the system, the conversion rate can be estimated by interpolation. These models present really fast results but penalize the lack of understanding the reactions and processes inside the catalyst.
- Mikrokinetic models are capable of accounting all the intermediate reactions and present all the rate expressions. However, these models present high computational costs.
- As mikrokinetic models are difficult to develop and even present difficulties in exhaustively measuring all the different species, one popular alternative are the models with Langmuir-Hinshelwood expressions. These models present the capability of determining the reactions rates, have a good predictive capability and help in quick design evaluations and control algorithms. This type of models is semiempirical, which means that not all the phenomena inside the catalyst is explicitly accounted.

As kinetic parameters are very sensitive to washcoat and also catalysts suffer from ageing, the estimation of kinetic parameters cannot be directly translated to the engine scale data. Furthermore, the ageing of the catalyst also depends and varies along the different channels. Also, the reaction path is dependant on the possible presence of species in real exhaust gases which are not present in the controlled experimental studies. To end with, the amount of H_2O and CO_2 will also affect the conversion rate.

The work carried out by Ramanathan u. Shekhar Sharma [23] was then used by the GT-Suite developers to build a generical Three-Way-Catalyst model which can be taken as a starting point for simulations. In the GT Simulation software, the "Catalyst block" is joined with a "Surface Reactions block". The first one, the catalyst block, contains the thermal and physical properties of the element, such as length, diameter, cell density, washcoat or temperature walls. On the other side, the surface reactions block includes information about the reactions and their pre-exponent multiplier, the activation temperature or energy, site elements and coverages or the different solver options. The main reactions in a three way catalyst are

displayed in table 15 with the corresponding heat of reaction. This data corresponds to the reactions used in the surface reactions block.

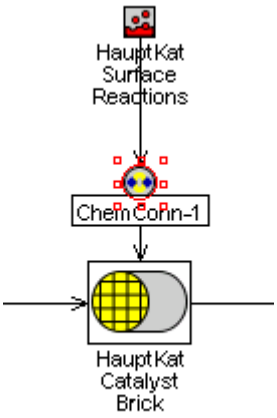

Figure 68 View of the catalyst block together with the surface reactions one in the GT-Suite simulation software

Equation number	Reactions	heat of reaction in J/mol
	Oxidation Reactions	
1	$CO + 0.5O_2 \rightarrow CO_2$	-2.83×10^5
2	$C_3H_6 + 4.5O_2 \rightarrow 3CO_2 + 3H_2O$	-1.93×10^6
3	$C_3H_8 + 5O_2 \rightarrow 3CO_2 + 4H_2O$	-2.04×10^6
4	$H_2 + 0.5O_2 \rightarrow H_2O$	h
	NO Reduction Reactions	
5	$CO + NO \rightarrow CO_2 + 0.5N_2$	-3.73×10^5
6	$C_3H_6 + 9NO \rightarrow 3CO_2 + 3H_2O + 4.5N_2$	-2.74×10^6
7	$H_2 + NO \rightarrow H_2O + 0.5N_2$	-3.32×10^5
	Water-Gas and Steam Reforming Reactions	
8	$CO + H_2O \leftrightarrow CO_2 + H_2$	-4.12×10^4
9	$C_3H_6 + 3H_2O \rightarrow 3CO + 6H_2$	$+3.74 \times 10^5$
	Ceria Reactions (Oxygen Storage)	

Table 15 continued from previous page

10	$2Ce_2O_3 + O_2 \rightarrow 4CeO_2$	-2×10^5
11	$Ce_2O_3 + NO \rightarrow 2CeO_2 + 0.5N_2$	-1.90×10^5
12	$CO + 2CeO_2 \rightarrow Ce_2O_3 + CO_2$	-1.83×10^5
13	$C_3H_6 + 12CeO_2 \rightarrow 6Ce_2O_3 + 3CO + 3H_2O$	-4.77×10^5
14	$C_3H_8 + 14CeO_2 \rightarrow 7Ce_2O_3 + 3CO + 4H_2O$	-4.95×10^5
15	$H_2 + 2CeO_2 \times Ce_2O_3 + H_2O$	-1.42×10^5

Table 15 Main reactions in Three Way Catalysts [23]

The pre-exponential factor is a constant for each chemical reaction which, according to collision theory, is the frequency of collisions in the correct orientation. Thus, the pre exponent multiplier represents the number of collisions (leading to a reaction or not) per second occurring with the proper orientation to react, while the activation energy is the probability that any given collision will result in a reaction.

7.3 Model overview

This study is not the first one carried out in the SCE project which takes advantage of GT-Suite software for its simulations. Furthermore, there is already a background previous to this model which was taken into account when building this simulations and adapting the software to the previous existing files.

The most important previous GT-Studies were:

- A complete vehicle simulation developed by Sylvain Garnier [26] and other previous studies. This model did not simulate the aftertreatment system nor emissions. It was composed by a complete vehicle simulation with a detailed engine models which simulated the primary and secondary engines. This detailed model calculated the internal pressure of the engine, combustion and injection but did not simulate the produced emissions. Furthermore, there was no aftertreatment system built in this model. The main objective in the near future is joining the aftertreatment model built in this study with the complete vehicle simulation developed by Sylvain Garnier [26].
- A study of the aftertreatment system by Christoph Eger [5] which studied different constructive options of the exhaust system. This model was not built from the emissions

measured in the test bench, but the test bench was built after the simulations developed by Christoph Eger [5]. The study concluded with an interesting design of the catalyst which had two concentrical catalytics converter, one for the primary engine and the other for the secondary engine, which were only thermically coupled. This concept allowed the use of only one catalytic converter when running in partial mode but maintaining the temperature of the secondary catalyst.

In this study, two different models have been developed. The first one is an isolated exhaust system model with both catalytic converters and an inlet flow which is specified by the different components and mass flow. This inlet conditions have to be manually given in the model and came from the measurements in the test bench. The following figure 69 is an screenshot from the actual GT model, where some of the parts are highlighted. Number 1 contains the first part of the model, where the inlet conditions are specified. It is connected to the second block, which contains the precatalyst and its dimensions and reactions are defined. Between the first and second parts of the model, there are no connection pipes as the inlet conditions are measured in the test bench directly infron of the precatalytic converter and, therefore, the measured temperatures are considered as the inlet temperatures. On the third part, the connection between the precatalytic converter and the main catalyst is simulated, having a straight pipe and an elbow as built in the test bench. To end with, number four includes the main catalyst.

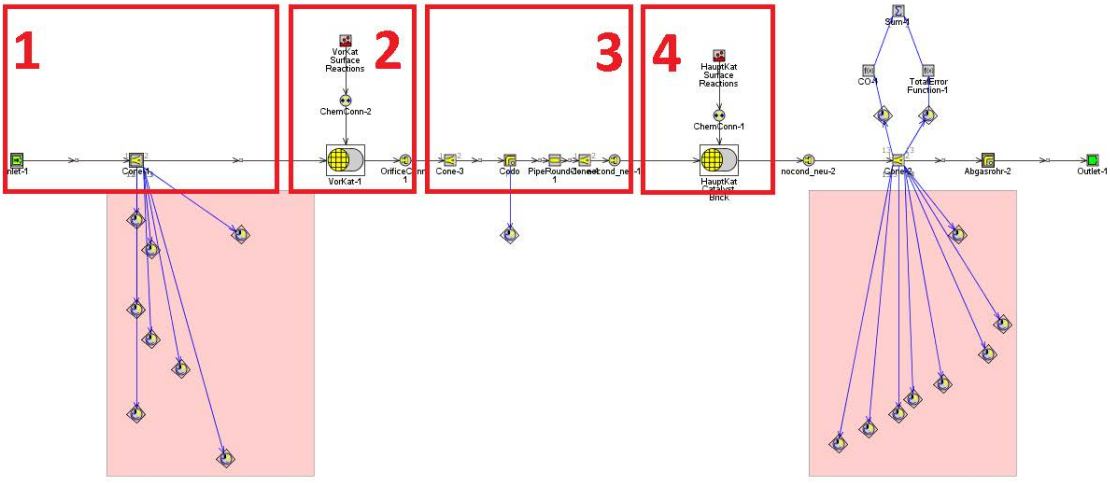

Figure 69 Screenshot from the exhaust system model

The second model is an evolution of the first one but including an engine state model, which is one of the alternatives offered by GT-Suite to simulate an engine. This is a really simplified version of an engine, which has torque and engine speed as inlet variables and, from the previously measured emissions maps which have also been implemented in GT-Suite, can calculate the emissions which enter the catalytic converters and estimate emissions. Figure 70 shows an screenshot of both, the engine state and exhaust system models joined, where inside number 1 box is located the engine state and in number 2 the previously shown exhaust system model.

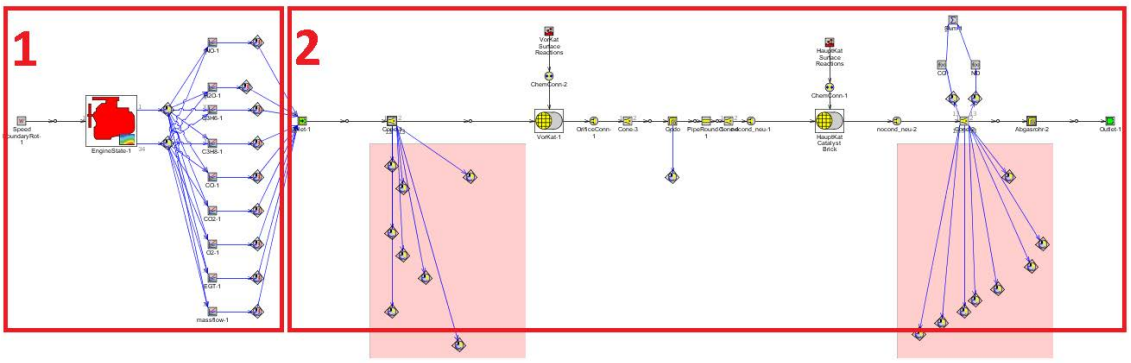

Figure 70 Screenshot engine state model plus the exhaust system

The engine state model has 9 different look-up tables, which can calculate different parameters of the engine looking by engine speed and torque. These parameters are measured in the different screenshots which compose the previously shown emissions maps. The implemented look-up tables (depending on torque and engine speed) are:

- NO emissions map
- H2O: this is not an emissions map itself but a map which represents the humidity in the test bench when each of the different points was measured
- C3H6: emissions map which is calculated as the 85% of the HC emissions map
- C3H8: emissions map which is calculated as the 15% of the HC emissions map
- CO emissions map
- O2 emissions map
- Exhaust Gas Temperature: this map returns the temperature of the exhaust gases for each of the different measured points
- Mass flow: map which returns the exhaust gases mass flow calculated from the lambda value and the injected fuel mass flow

Between all the considered emissions, the HC or total Hydro-Carbons, have an unknown composition in species and proportion. This means that when measured, it is possible to know the amount of molecules which are composed by carbon and hydrogen atoms but it is not possible to know the exact amount of each one. For example, it is not possible to know the exact amount of CH3, CH4, C3H6, C3H8...

However, some guidelines are shown in the GT-Suite library tutorials, help and literature [13]. In this files, the software developers recommend making certaing assumptions about the HC's present in the system. As they affirm, the aftertreatment modeling community tends to agree that using 1 HC is not enought, but using more than 3 HC elements is impractical and

inefficient. Thus, typically 2 HC species are enough in order to model the system. Generally, one fast, partially oxidized HC, like C3H6 (propylene) for both gasoline and diesel, and one slow, or large HC, like C3H8 (propane) for gasoline and C10H22 (propylene) or unburned diesel fuel for diesel. They also declare, that multiple literature sources use between 80 and 85% of fast HC and 15-20% of slow HC for gasoline, and 30-50% fast C and 50-70% slow HC for diesel, on a molar basis.

7.3.1 Tests, modelling theory and strategy

The GT-Suite manual shows a catalyst's calibration procedure which needs from a steady mixture of inlet gases with various known fractions of trace reactants (O2, CO, H2, C3H6, C3H8, NO, NO2) with a steady inlet mass flow rate and a slow transient linear temperature ramp of the inlet gas. It is impossible to achieve all these conditions with an engine.

To analyse the behaviour of the model, two tests were simulated. The first test was simulated with only the aftertreatment model (without the engine state model) and is the same heating curve as analysed in previous chapters, when running the engine from a cold start to 2000 rpm and 30 Nm. The second test is a simulation of all the points which were measured to create the emissions maps with the complete model composed by the engine state model plus the aftertreatment system.

The emissions of the model were calibrated by using a total error function which compared the emissions produced by the model to the known amount of pollutants measured in the test bench. The pre-exponent multipliers of the equations of the pollutants which show a worse behaviour in the first simulations were chosen as optimization variables to reduce the total error function of the determined pollutant. However, as it will be detailled, the model showed a poor behaviour with the transient curve when being optimized with steady state points and, the other way round, when optimizing the parameters from the transient curve, the model shows a really bad behaviour with the steady state simulations. Thus, as it will be explained, it was chosen to keep the model calibration with the transient curve.

In the following sections, the different simulations and calibration procedure will be presented. The behaviour of the model will be analysed and possible future tests are discussed.

7.3.2 Thermal model

Before simulating the model with the catalytic converters reacting, it is necessary to check that the model can simulate properly the different heat transfers between elements. When the application strategy of the primary engine had to be decided, a transient curve of the engine was ran, without firing nor injection, just blowing air with the engine being dragged. The engine was moved by an electric motor and the throttle valve was opened linearly, increasing the flow through the exhaust system. This same curve was simulated to check that the temperatures differences between the temperatures measuring points is according to reality when no reactions in the catalytic converters occur because no pollutants are being emitted

and is pure ambient air what flows through the system.

The fluid-pipe interference is simulated using the Colburn-Correlation, which estimates the heat transfer coefficient depending on the mass flow and is the recommended method by GT when the transfer coefficient is unknown. On the other hand, the heat transfer coefficient of the system with the ambient is already known as it was calculated by Christoph Eger [5].

Figure 71 shows the temperature measured before the main catalytic converter measured at the test bench (red) and simulated (blue). The simulation presents in the long run a 2°C higher temperature and also a higher thermal inertia which leads to a slower transient curve. This was the best possible adaptation achieved of the thermal model which is not as good as would be expected.

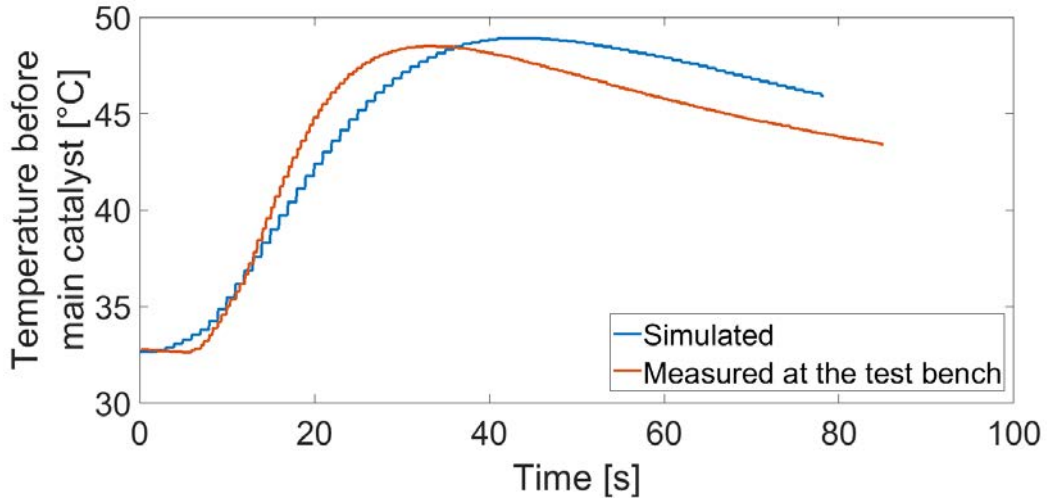

Figure 71 Temperature before main catalytic converter when simulating a point where the engine is running aspiratedly

7.3.3 Transient curve simulation

The first model, the one consisting of both catalytic converters, was then tested with a transient curve with pollutants producing reactions in the catalyst converters. At first, the model showed a poor behaviour in the conversion of NO and CO emissions. Thus, two total error functions were set, which calculated the accumulated error for NO and CO emissions which were then summed. This sum was the parameter to be minimized in the calibration by altering the pre-exponent multiplier as the activation energy was found not to produce noticeable changes in the reactions.

The following curves show the temperatures after the precatalyst and before and after the main catalyst, simulated in GT and measured in the test bench. The temperature before the precatalyst is not plotted as it is the inlet condition and, therefore, is equally imposed for the model as measured at the test bench.

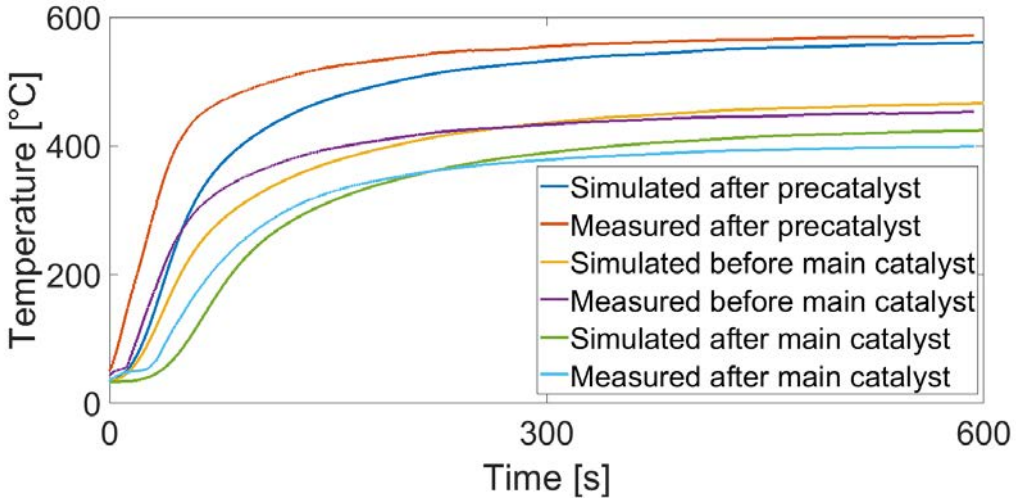

Figure 72 Temperatures of the simulation and at the test bench when simulating a transient curve

It can be observed that in all the points, the model presents a slower transient curve while the temperatures in the steady state are quite similar, with a difference to the measured values of around 10°C. The adaption of the thermal behaviour of the model is difficult to be improved as the heat transfer coefficient between pipe and the fluid (gas) is hard to be estimated and also changes with the temperature. The Colburn-Correlation used, which is a quite common analogy to calculate the heat transfer coefficient, shows a slow transient response but a reasonable good steady state behaviour. The catalytic converts show also a good thermal modelling of the reality with no more than 10°C difference at the outlet from reality. It is also noticeable how the precatalyst increases the temperature of the gases while the main catalyst does not have such a high conversion rate and decreases the temperature of the exhaust flow.

Regarding the NOx emissions, the simulation shows a good transient behaviour at the beginning but then presents a quicker conversion and the curve begins earlier to decrease. In the steady state, both curves, the simulated and measured present similar values with really low emissions.

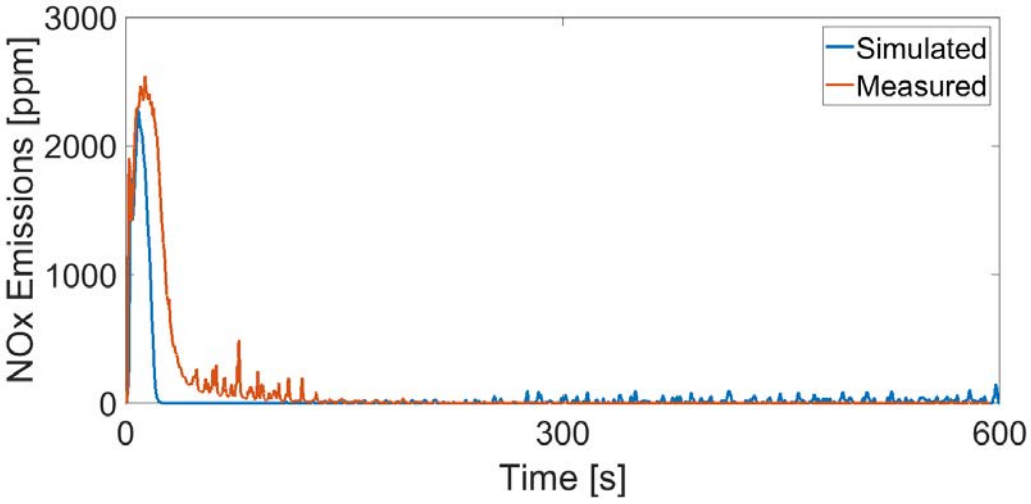

Figure 73 NOx emissions simulation and measurement at the test bench

A similiar situation occurs with the CO emissions, where the model during the transient phase estimates the emissions according to reality but then shows a quicker conversion rate as measured.

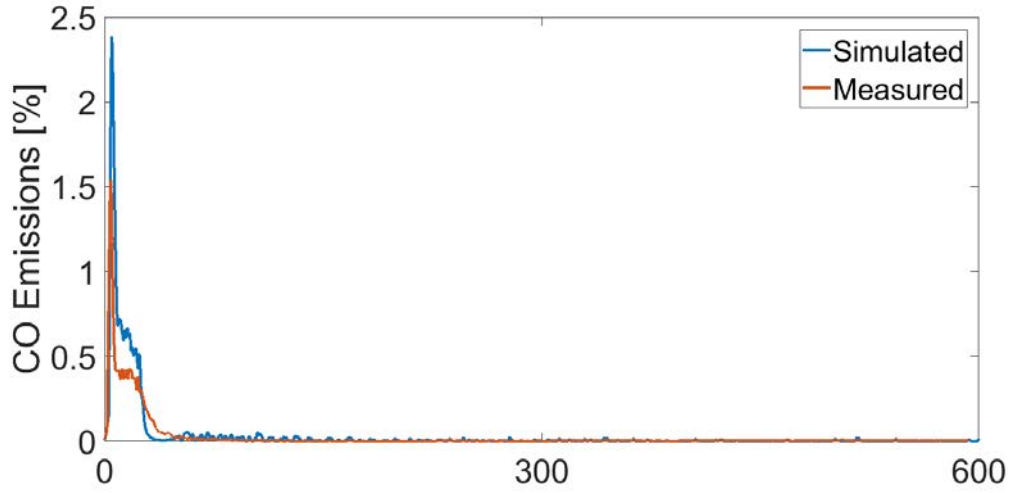

Figure 74 CO emissions simulation and measurement at the test bench

Related to the CO emissions, the CO2 as a result of the simulation shows a similar curve to the measured emissions. However, the simulation presents a deviation in the steady state which is maintained constant. It has to be noticed that the Mexa O2 measurement device may have some deviations as it returns negative values when measuring after the main catalyst. These negative values are obviously non-sense but suggest that probably all the O2 present in the inlet is consumed in the oxidation reactions of both converters. Therefore, if the system also presents this discrepancy when measuring O2 at the inlet, the amount of O2 which is introduced in the simulation may be altered.

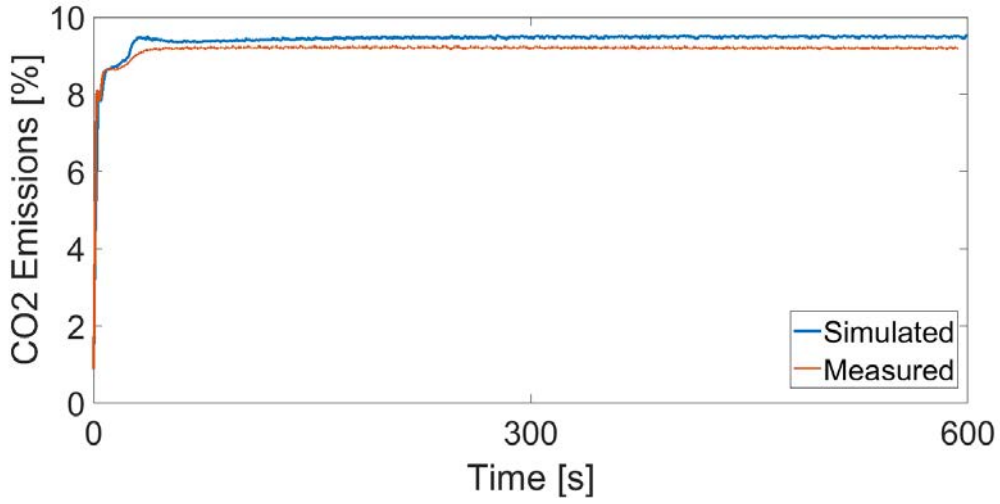

Figure 75 CO2 emissions simulation and measurement at the test bench

To end with, the HC emissions are presented in figure 76. In the steady state, the model shows big fluctuations, probably due to a bad simulation of storaging periods which are produced in reality. Once again, the model begins earlier a full conversion as in reality.

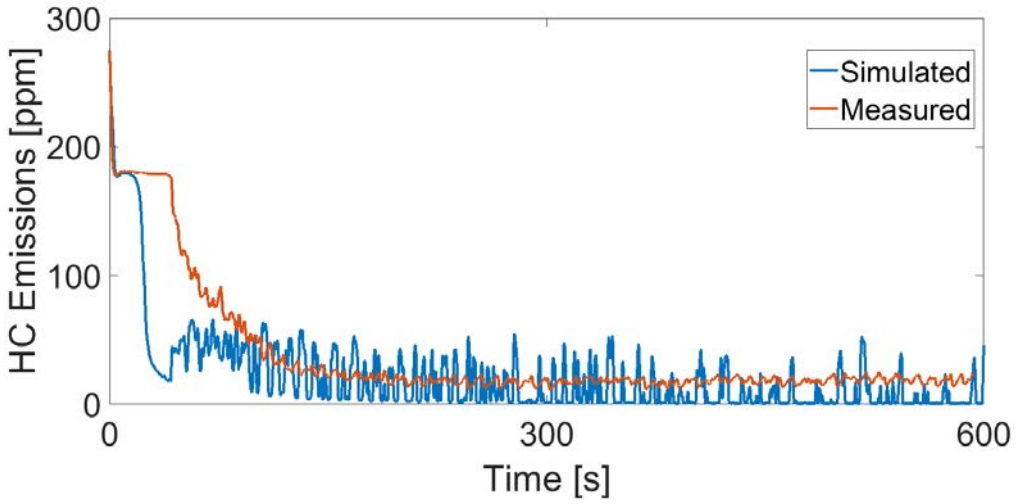

Figure 76 HC emissions simulation and measurement at the test bench

The previous graphics show the thermal and emissions behaviour of the aftertreatment model. As it can be seen, the thermal simulation is relatively good for the studied transient curve but may fit better or worse other emissions profiles. Regarding emissions, the system seems to present a quicker conversion rate as the real test bench does. This model is the best optimization achieved by calibrating different pre-exponent multipliers to minimize the total error function, while changes in the activation energy produce almost no differences in the optimization process.

7.3.4 Snapshot simulation

The second simulation was carried out with the complete model (engine state model plus aftertreatment system) and consists in simulating all the 66 points which were measured in the test bench to build the emissions maps. These points were measured from 1000 to 6000 rpm in 1000 rpm steps (6 points), with 11 different torques for each engine speed (66 points in total). The measurements are a 10 seconds average.

The simulated profile consists of an engine speed and torque curves which compose the different points of the emissions maps. That means, the engine starts at 1000 rpm and goes up to 6000 rpm while maintained 30 seconds through each different torque. The simulation was then compared to the measured points. However, these points were not measured together but independently. This would show how the model would behave when trying to simulate a speed profile together with the engine. The following figure shows the engine speed and torque profile which were simulated:

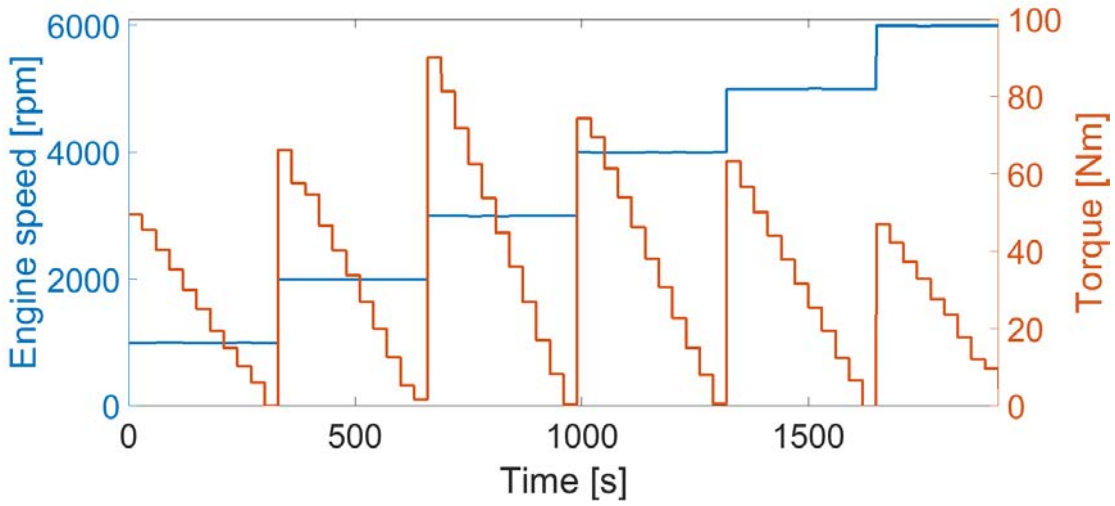

Figure 77 Engine speed and torque when simulating the points which composed the emissions maps

The results of the simulations were not anywhere near the measurements from the test bench in terms of emissions, while the model seems to correlate the temperatures properly. Figures 78, 79 and 80 show the simulated and measured temperatures. It has to be remembered that the measured temperatures is a "fictive profile". This means that the snapshots were taken separately and thus, the temperatures measured have no thermal inertia. However, the model correlates properly the temperatures and is quite accurate to reality. Obviously, the thermal inertia of the model makes that the temperatures curves react slower than in the snapshots but the correlation is good. This indicates that thermally, the engine state model together with the aftertreatment model are suitable for simulations.

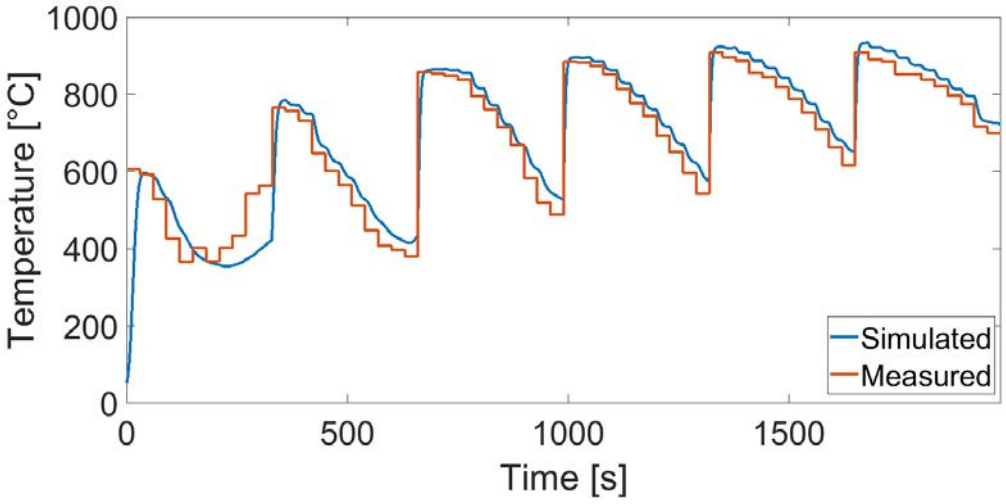

Figure 78 Temperature after the precatalyst

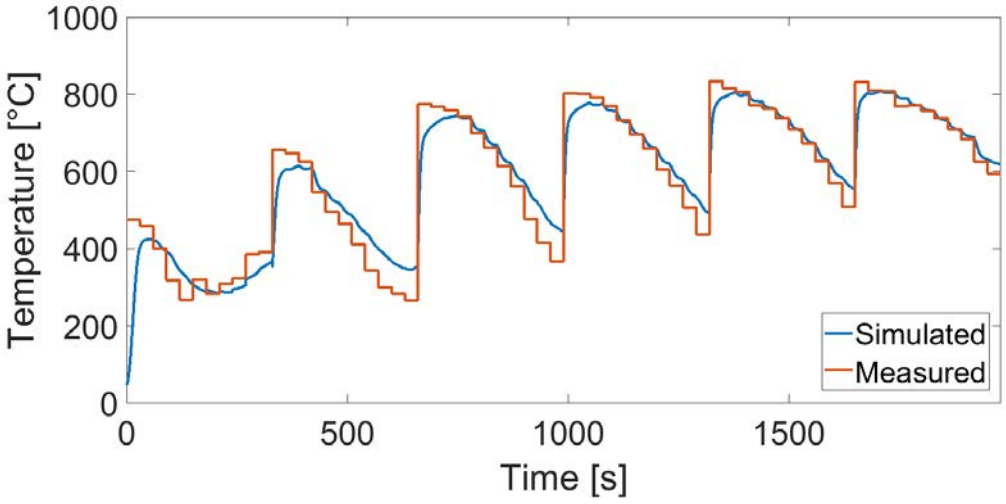

Figure 79 Temperature before the main catalyst

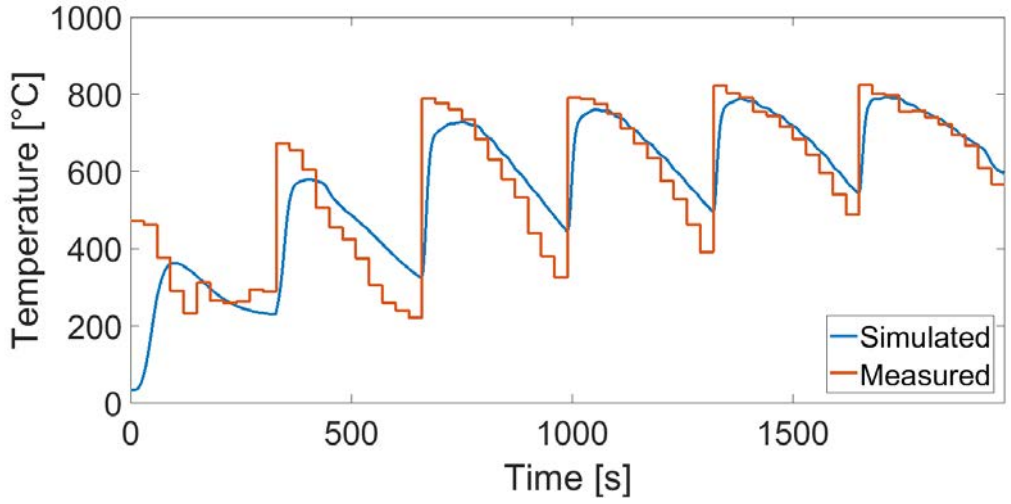

Figure 80 Temperature after the main catalyst

However, the simulation of the different emissions was nothing near reality with the same aftertreatment model used in the transient curve section. When calibrating the model with this curve, the behaviour of the model with the transient curve showed then a poor behaviour. Figures 81(a) and 81(b) show the enormous difference between simulation and the snapshots.

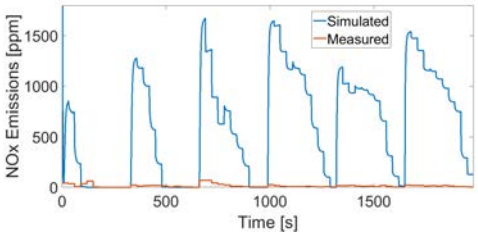

(a) NOx emissions simulation

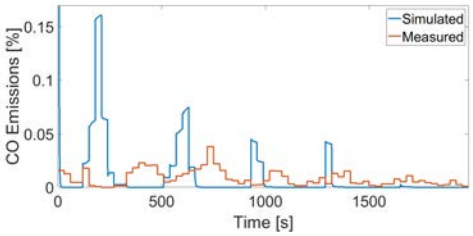

(b) CO emissions simulation

Figure 81 NOx and CO emissions after main catalyst

After observing such a big difference in this simulation, a question appers: which is then the proper calibration method for the model? It was chosen as better method the transient calibration as it is a real transient curve measured in the test bench while this curve is a sum of different snapshots which are a 10 seconds average of all the measurements in the test bench.

This snapshots may also be part of the cause of the failure of the simulation as its the only new part introduced in the model with respect to the previous one is the engine state model. The simulation runs with a high frequency calculation while the inlet data comming from the engine state model is purely constant when maintaining a speed and torque. In reality, in the

test bench some fluctuations in the different species would have been measured. A difference in the composition of one of the emissions affects also other reactions present in the catalytic converters. This means, that probably it is not the same to calculate the conversion rates with the average values of 10 seconds than having for every houndred of a second the exact relationship between each of the pollutants. The following figure shows the amount of O2 and CO present in the simulation. Both components are highly related as when there is enough O2, the whole amount of CO is oxidated, producing CO2 and no CO final emissions.

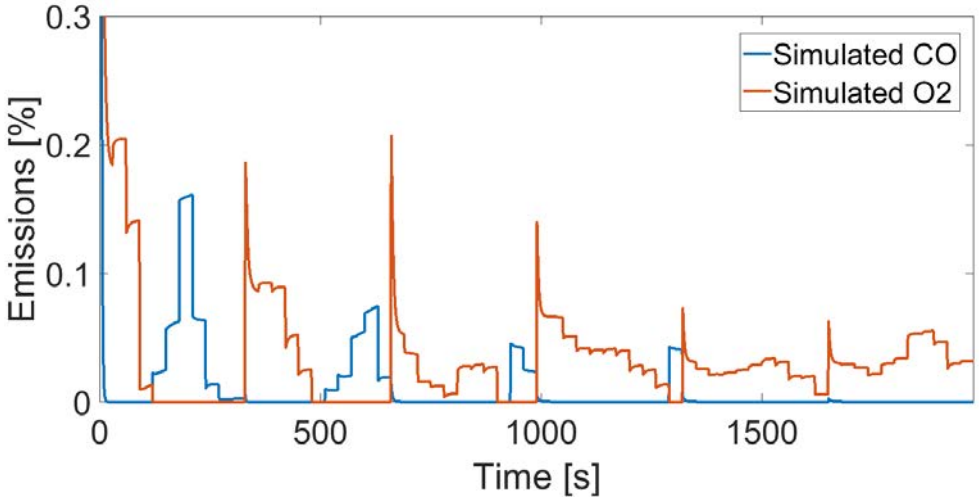

Figure 82 CO and O2 emissions

Theoretically, the amount of O2 present in the simulation should always be equal to zero but, as it can be seen, some times there are O2 particles. The only explaination found for this, assumming that all the measurements were properly done and the Mexa system measuring error of the O2 is not big enough to produce such discrepancies, is the necessity to have an exact relationship between all the components with a high frequency.

7.4 Conclusions and optimization potential of the model

From the previous data shown, it can be seen that the model is not so accurate as would be expected from a good model to improve the system. The aftertreatment model, when used alone, shows earlier conversion rates than reality altough shows a slower temperature response. However, in the steady state, temperature differences are low.

On the other hand, when coupling the aftertreatment model with the engine state model, the simulations return emissions with values which differ highly from reality.

In order to improve the model in the future, it would be interesting to run other transient curves or different engine speeds and torque profiles in the test bench to simulate then them in the model. It has to be checked that the model also presents a good thermal behaviour with

different inlet profiles. It would also be interesting to have as inlet an emissions profile which does not end in a constant value but is constantly changing to see how the emissions are modelled after the catalyst reaches its optimum temperature.

Regarding the simulation of the engine plus the aftertreatment system, it is interesting the study through a detailled engine model which properly correlates the instant variations of the pmi with the emissions maps.

8. Conclusions, summary and outlook

After many years of development, the SCE has shown to be an interesting technology to be implemented in the future. The simulations and tests carried out for this study have shown interesting results. The most remarkable issues are:

- The industry has been generally implementing precatalysts as closed to the engine as possible to reduce the time needed to reach the light-off temperature. This concept was implemented in the SCE exhaust system but has presented advantages as well as disadvantages. It improves the heating of the precatalyst but suffers from the high temperatures of the exhaust system due to the need of running at lambda = 1 values. The new emissions legislations are so restrictive that it is impossible to run short periods of time with rich lambda values to cool down the exhaust system.
- The new WLTC cycle together with the RDE will now substitute the old NEDC. This new legislation will reflect better the real behaviour of the emissions in the real world. It will also be more restrictive and the RDE means that for the first time tests will be measured while running in real open traffic. This means that the tests will now be influenced by many uncontrolled variables and the routes will have to be highly optimized.
- The full vehicle simulation of the SCE has shown a 10% fuel consumption reduction when compared to a normal engine. From all the emissions, NOx are the only ones out of the legal range. Furthermore, the SCE presents higher NOx emissions than the CDA and CE due to the higher pmi values that the PE suffers when running alone. However, it is possible to run with a different lambda value which increases HC and CO emissions while reducing NOx as there is a high margin until the limits are reached. It would be interesting in the future to run the same simulation but with the real emissions maps of the secondary engine and not considering it to be the same one as the primary engine.
- The exhaust system simulation in the GT-Suite has shown a poor behaviour. The aftertreatment alone model presents a shorter light-off time than the real one measured. When joining the model with an engine state model and simulating steady state points, the system presents a good thermal response but emissions are far away from reality. It would be interesting in the future to test the aftertreatment alone model with a different engine speed and torque profile to see how the model estimates emissions after the light-off temperature is reached. It would also be interesting to simulate the engine through an engine detailled model which uses the same emissions maps but calculates the pmi with a high frequency as would be measured in the test bench.

Bibliography

[1] BIELACZYC, Piotr ; WOODBURN, Joseph ; SZCZOTKA, Andrzej: The WLTP as a new tool for the evaluation of CO2 emissions. In: *BOSMAL Automotive Research and Development Institute Ltd, Poland* 2014

[2] CAMBUSTION: *The CLD Principles*. `https://www.cambustion.com/products/cld500/cld-principles`

[3] CAMBUSTION: *The FID Operating Principle*. `https://www.cambustion.com/products/hfr500/fast-fid-principles`

[4] CAMBUSTION ; CAMBUSTION (Hrsg.): *The NDIR Principle*. `https://www.cambustion.com/products/ndir500/operating-principle`

[5] CHRISTOPH EGER: *Entwicklung einer Splitkurbelwellenmotorspezifischen Abgasanlage: Masterarbeit (simulativ und konstruktiv)*. Munich, Technische Universität München, Diss.

[6] DOLZA, John: *Economy Engine and Method of Operation. United States Patent Number 2875742.* 1959

[7] DONATEO, Teresa (Hrsg.) ; GIOVINAZZI, Mattia (Hrsg.): *Building a cycle for Real Driving Emissions*. Lecce : Science Direct, September 2017

[8] DR.-ING FORTNAGEL, Manfred ; DIPL.-ING NÖLL, Roland ; DR.-ING SCHOMMERS, Joachim ; DIPL.-ING RECKZÜGEL, Christoph ; DIPL.-ING CLAUSS, Roland ; DIPL.-ING TREYZ, Willy ; DIPL.-ING GLÜCK, Roland: Der neue Mercedes-Benz-Zwölfzylindermotor mit Zylinderabschaltung. In: *MTZ Motortechnische Zeitschrift* 61 (2000), S. 280–291

[9] DR.-ING MIKULIC, Leopold ; DIPL.-ING HEIL, Bernhard ; IND. MÜRWALD, Mario ; DR.-ING BRUCHNER, Klaus ; DIPL.-ING PIETSCH, Albert ; DIPL.-ING KLEIN, Rudolf: Neue Vierzylinder-Ottomotoren von Mercedes Benz mit Kompressoraufladung. Teil 1: M 271 KE - dre Leistungsvarianten mit Kanaleinspritzung. In: *MTZ Motortechnische Zeitschrift* (2002), Nr. 6, S. 436–447

[10] EUROPEAN AUTOMOBILE MANUFACTURERS ASSOCIATION: *What is the Real Driving Emissions (RDE) test?* `http://www.caremissionstestingfacts.eu`

[11] EUROPEAN AUTOMOBILE MANUFACTURERS ASSOCIATION: *WLTP Facts*. `http://wltpfacts.eu`

[12] EUROPEAN COMMISSION: *Comission Regulation (EU) 2016/427*

[13] GT-SUITE - GAMMA TECHNOLOGIES: *Exhaust Aftertreatment Application Manul*. v7.5. GT-Suite Help Files, 2016

[14] HARUHIKO IIZUKA, Yokosuka ; FUKASHI SUGASAWA, Yokohama: *Split engine control system*. 1984

[15] HORIBA ; HORIBA (Hrsg.): *Mexa Test Report: Calibration document by Horiba when installing the Mexa analyzer*. 18 Nov 2004

[16] IIT KANPUR ; NPTEL (Hrsg.): *Module 4: Vehicle Emission Standards and Measurement. Lecture 18: Emission Measurement*. http://nptel.ac.in/courses/112104033/18. Version: 2012

[17] ISENSTADT, Aaron ; GERMAN, John ; DOROBANTU, Mihai: Naturally aspirated gasoline engines and cylinder deactivation. In: *The Internal Council on Clean Transportation (ICCT)* (2016), Nr. 12

[18] KONRAD, Reif: *Ottomotor-Management im Überblick: Series: Bosch Fachinformation Automobil*. Springer : Springer, 2015. – ISBN 978–3–658–09523–9

[19] LEE, Seokhwan ; BAE, Choongsik ; LEE, Yongpyo ; HAN, Taesik: Effects of Engine Operating Conditions on Catalytic Converter Temperature in an SI Engine. In: *SAE International* (2002-01-1677)

[20] MOCK, Peter ; KÜHLWEIN, Jörg ; TIETGE, Uwe ; FRANCO, Vicente ; BANDIVADEKAR, Anup ; GERMAN, John: The WLTP: How a new test procedure for cars will affect fuel consumption values in the EU. In: *ICCT (Internationl Council on Clean Transportation)* 2014-9 (2014)

[21] ODENDALL, Bodo: *Ein vereinfachtes Modell des Lambda-geregelten Dreiwegekatalysatoren zum Einsatz in Motor-Steuergeräaten und zur On-Board-Diagnose: Von der Fakultäat 4, Energie-, Verfahrens- und Biotechnik der Universitäat Stuttgart zur Erlangung der Würde eines Doktors der Ingenieurwissenschaften (Dr. -Ing) genehmigte Abhandlung*. Stuttgart, Universität Stuttgart, Doktor Thesis, 19.04.2017

[22] PETROLEUM.CO.UK: *Common Hydrocarbons and Their Uses*. http://www.petroleum.co.uk/hydrocarbons

[23] RAMANATHAN, Karthik ; SHEKHAR SHARMA, Chander: Kinetic Parameters Estimation for Three Way Catalyst Modeling. In: *I&EC - Industrial & Engineering Chemistry Research* (2011)

[24] RÖSLER, Sebastian ; FISCHER, Patrick ; PFLAUM, Herman ; WACHTMEISTER, Georg ; STAHL, Karsten: *Experimental implementation of an internal combustion engine with a disengageable crankshaft - The Split-Crankshaft Engine*. Munich, Technische Universität München, Diss.

[25] SALOMONS, Stephen J.: *Kinetic Models for a Diesel Oxidation Catalyst*. Alberta, Canada, University of Alberta, PhD Thesis, Spring, 2008

[26] SYLVAIN GARNIER: *Fuel Saving Potential Determination and Optimization of the Split-Crankshaft Engine via Full Vehicle Simulation: Master Thesis (Simulative)*. Munich, Technische Universität München, Masterarbeit

[27] TSOKOLIS, Dimitris ; DIMARATOS, Athanasios ; SAMARAS, Zissis ; TSIAKMAKIS, Stefanos ; FONTARAS, Georgios ; CIUFFO, Biagio: Quantification of the effect of WLTP introduction on passenger cars CO2 emissions. In: *Journal of Earth and Geotechnical Engineering* 7 (2017), Nr. 1, S. 191–214

[28] TUTUIANU, Monica ; BONNEL, Pierre ; CIUFFO, Biagio ; HANIU, Takahiro ; ICHIKAWA, Noriyuki ; MAROTTA, Alessandro ; PAVLOVIC, Jelica ; STEVEN, Heinz: Development of the World-wide harmonized Light duty Test Cycle (WLTC) and a possible pathway for its introduction in the European legislation. In: *Elsevier* (2015), Nr. Transportation Research Part D 40(2015), 61–75. www.elsevier.com/locate/trd

[29] VAISALA OYJ ; VAISALA OYJ (Hrsg.): *Humidity Conversion Formulas: Calculation formulas for humidity*. www.vaisala.com. Version: 2013

[30] WACHTMEISTER, Georg: *Methoden der Motorapplikation. Folien. Thema 2: Anforderungen an Verbrennungsmooren*. 2016

A. Annex A

A.1 DVD Content

Description of the files in the DVD:

- Folder 01_Literature: all the literature which has been found during this study whether it has been used in this document or not
- Folder 02_Emissions Maps
  - Columns Explaination: Document which explains what is each column in the other two .mat files
  - SnapshotsExcelCompleteRoh: results of the 66 measured points to build the emissions maps of the engine raw emissions
  - SnapshotsExcelCompleteNachHK: results of the 66 measured points to build the emissions maps of the emissions after the main catalytic converter
- 03_Matlab Scripts
  - ContilogEmissionsDry2Wet: Script which converts the emissions in the Contilog files from dry to wet base
  - EmissionsIntegrationPME: Script which runs the emissions integration of the full vehicle simulation using the pme
  - EmissionsIntegrationPMI: Script which runs the emissions integration of the full vehicle simulation using the pmi. The missing data needed in the script is inside the folder 04_Full Vehicle Simulation
  - fcn_convertTDMS: Script which converts the Snapshots as they come direct from the test bench to Matlab files
  - fcn_convertTDMS_list: Script which uses fcn_convertTDMS and converts a list of Snapshots without having to call the function individually for each file
  - Kenfelder: Script which creates the the emissions maps. The inlet data is inside folder 02_Emissions maps
  - KennfelderPlot: Script to plot the different Emissions Maps
- 04_Full Vehicle Simulation: Results of the full vehicle simulated run with the script inside 03_Matlab Scripts.
  - Files beginning with 01: results of the simulation of Sylvain Garnier which are used for

the full vehicle simulation

- Files beginning with 02: emissions maps as Matlab objects
- Files beginning with 03: results

- 05_GT-Simulation